

X4

Copy 283
RM E50J26

NACA RM E50J26

E 50 J 26



TECH LIBRARY KAFB, NM

8C99

RESEARCH MEMORANDUM

FORCE AND PRESSURE CHARACTERISTICS FOR A SERIES OF NOSE
INLETS AT MACH NUMBERS FROM 1.59 TO 1.99

I - CONICAL SPIKE ALL-EXTERNAL COMPRESSION INLET
WITH SUBSONIC COWL LIP

By Fred T. Esenwein and Alfred S. Valerino

Lewis Flight Propulsion Laboratory
Cleveland, Ohio

THIS DOCUMENT CONTAINS CLASSIFIED INFORMATION BELONGING TO THE NATIONAL ADVISORY COMMITTEE FOR AERONAUTICS OR THE UNITED STATES GOVERNMENT. IT IS THE PROPERTY OF THE UNITED STATES GOVERNMENT AND IS LOANED TO AN AUTHORIZED PERSON. ITS TRANSMISSION, DISSEMINATION, OR RETENTION IN ANY FORM OTHER THAN THAT AUTHORIZED BY LAW IS UNLAWFUL.

Information contained in this document was derived from sources which are not necessarily classified or which have been determined to be unclassified by reason of age, source, or other factors. It is the property of the United States Government and is loaned to an authorized person. Its transmission, dissemination, or retention in any form other than that authorized by law is unlawful.

NATIONAL ADVISORY COMMITTEE
FOR AERONAUTICS

WASHINGTON
January 19, 1951

Classification cancelled (or changed to UNCLASSIFIED)

By authority of WASA, Det. 1, Pub. Admin. & Maint. #129
(OFFICER AUTHORIZED TO CHANGE)

By 11 Aug 58
NAME / NO.

[Signature]

GRADE OF OFFICER MAKING CHANGE

23 Mar 61
DATE



0143212

NACA RM E50J26

~~CONFIDENTIAL~~

NATIONAL ADVISORY COMMITTEE FOR AERONAUTICS

RESEARCH MEMORANDUMFORCE AND PRESSURE CHARACTERISTICS FOR A SERIES OF
NOSE INLETS AT MACH NUMBERS
FROM 1.59 TO 1.99I - CONICAL SPIKE ALL-EXTERNAL COMPRESSION INLET
WITH SUBSONIC COWL LIP

By Fred T. Esenwein and Alfred S. Valerino

SUMMARY

An experimental investigation to determine the force and pressure characteristics of a typical nose-inlet ram-jet configuration was conducted in the NACA Lewis 8- by 6-foot supersonic tunnel. The model consisted of a conical spike all-external compression inlet attached to an annular subsonic diffuser. Internal-and external-pressure distributions, pressure recovery, and lift, drag, and pitching moment were measured for a range of mass flows at angles of attack from 0° to 10° for free-stream Mach numbers of 1.59, 1.79, and 1.99. The investigation was conducted at a Reynolds number of approximately 2.13×10^6 based on model inlet diameter.

Results of the investigation indicate that a rapid increase in total drag with decreasing mass flow was associated with the large increase in additive drag. The increment of external drag due to angle of attack was found to be essentially independent of mass flow and free-stream Mach number.

At critical mass flow, the external-lift-curve slope increased slightly with angle of attack and Mach number, whereas the pitching moment increased almost linearly with angle of attack and was independent of Mach number. At low angles of attack, the lift and pitching moment remained nearly independent of mass-flow spillage. At 10° angle of attack, however, the lift decreased with decreasing mass flow but the pitching moment remained nearly constant.

~~CONFIDENTIAL~~~~3737~~

In general, the decrease in pressure recovery with angles of attack up to 10° was of the order of 1 percent and no shock instability was noted except for very low mass flows at 6° and 10° angles of attack for Mach number 1.99.

Comparison of the experimental results with available theories revealed that the additive-drag and friction-drag coefficients were predicted satisfactorily at zero angle of attack for the range of mass flows and free-stream Mach numbers investigated. Prediction of the pressure drag, however, was limited to the condition of zero mass spillage.

INTRODUCTION

As part of a program to determine the aerodynamic characteristics of ram-jet engines, an investigation of four axially symmetric spike-type supersonic nose-inlets was conducted in the NACA Lewis 8- by 6-foot supersonic tunnel. In order to simulate a portion of a complete ram-jet engine, each inlet was attached to a fixed afterbody that formed the subsonic diffuser.

The purposes of this investigation were: (1) to obtain pressure, force, and moment data; and (2) to compare the experimental results with theory where possible.

Results obtained from the investigation of a conical-spike all-external compression inlet with a subsonic cowl lip are presented. The investigation was conducted through a range of mass flows and angles of attack from 0° to 10° at Mach numbers of 1.59, 1.79, and 1.99. The Reynolds number based on the inlet diameter varied from 2.11 to 2.15×10^6 for the range of the investigation.

SYMBOLS

The following symbols are used in this report:

C_D drag coefficient, $D/q_0 S_m$

C_f friction-drag coefficient based on wetted area

C_L lift coefficient, $L/q_0 S_m$

C_M pitching-moment coefficient about base of model, $G/q_0 S_m l$

C_p pressure coefficient, $p-p_0/q_0$

2034

D drag
d diameter at area of maximum cross section, 8.125 inches
G pitching moment about base of model
L lift
l length of model, 58.76 inches
M Mach number
m mass flow
P total pressure
p static pressure
q dynamic pressure, $\gamma p M^2 / 2$
Re Reynolds number
S area
 S_c inlet capture area defined by cowl lip, 0.1750 square foot
 S_m maximum cross-sectional area, 0.3601 square foot
U velocity
u velocity in boundary layer
 v_x axial perturbation velocity
 x, r, θ cylindrical coordinates
y distance from model surface
alpha angle of attack
 γ ratio of specific heats, 1.40
 δ boundary-layer thickness

Subscripts :

- a additive drag
- f friction
- l local condition in boundary layer
- p pressure
- s conditions at outer edge of boundary layer
- 0 free stream
- 1 cowl lip
- 2 station at $x = 7.558$ inches
- 3 entrance to combustion chamber
- 5 minimum area at plug

APPARATUS AND PROCEDURE

Two identical models of the ram-jet configuration were investigated; one was used for force measurements, the other was used to obtain pressure data. The instrumentation conduits and the boundary-layer rake shown in figure 1 were not present on the force model.

The main components of the ram-jet configuration shown in figure 2(a) consisted of a conical-spike all-external compression inlet (fig. 2(b)) followed by an annular subsonic diffuser formed by the outer shell and the central inner body. Four support struts located 45° from the vertical center line were used to attach the outer shell to the center body. The over-all length of the model was 58.76 inches and the maximum body diameter was 8.125 inches.

The inlet was so designed that the angle formed between the center line of the model and a line joining the tip of the spike and the cowl lip was equal to the angle of the oblique shock generated by the 50° cone at a Mach number of 1.79. The cowl, which was designed for operation with the normal shock located slightly ahead of the cowl lip, had a rounded subsonic leading edge (fig. 2(b)). Coordinates for the center body and outer shell are presented in table I.

The mean geometric flow-area ratio (fig. 3) represents the ratio of the area based on the average normal to the surfaces of the annulus to the maximum cross-sectional area in the combustion chamber. The region of nearly constant area at the inlet was provided to permit stabilization of the boundary layer behind the normal shock prior to deceleration of the flow in the subsonic diffuser. The small decrease in flow area from $x/d = 0$ to 0.25 resulted from the design of the subsonic cowl lip.

The force model was rigidly connected to a three-component strain-gage balance located inside the center body and the balance was attached to the tunnel sting-strut combination.

Instrumentation of the pressure model included static orifices as indicated in table II and a $\frac{1}{2}$ -inch boundary-layer rake located on the outer surface of the model ($\theta = 0^\circ$) at station 51 (fig. 2(a)). For one of the runs at a Mach number of 1.79, two total-head rakes were located inside the model immediately in front of the support struts at $\theta = 135^\circ$ and 315° .

Six similar radial static and total-pressure rakes, equally spaced with respect to the vertical center line, were attached to the sting at the entrance of the combustion chamber for both the force and pressure models. A sting-mounted, hydraulically actuated plug was provided at the exit of the model to vary the flow conditions through the engine and a pendulum-type angle-of-attitude indicator with an accuracy of 0.1° was located inside the center body to measure the angle of attack.

All pressures were measured on multiple-tube manometer boards and were photographically recorded. The total pressures in the boundary layer were measured using mercury as the working fluid; all other pressures were measured using tetrabromethylene.

Both models were investigated through a range of mass flows at angles of attack from 0° to 10° for the free-stream Mach numbers of 1.59, 1.79, and 1.99. An additional run was made with the pressure model rotated 180° to obtain a more complete survey of the pressure distributions at Mach number 1.79.

For presentation of the data herein, the mass flow is expressed in terms of m_2/m_0 , defined as the ratio of the flow passing through the engine to the flow in a free-stream tube of cross-sectional area S_c (fig. 4). The mass flow passing through the engine was computed for choking at the minimum geometric area of the plug using the measured total pressure at the combustion-chamber inlet and was corrected by the factor 0.97, which was determined for the shock-swallowed condition.

RESULTS AND DISCUSSION

The presentation and the discussion of results are divided into two major sections covering the external and internal-flow characteristics. Evaluation of the effects produced by variations in mass flow, angle of attack, and free-stream Mach number are made in terms of the flow characteristics of the model.

External-Flow Characteristics

Zero angle of attack. - The total drag, which includes the pressure and the friction drag over the outer shell and the additive drag along the entering streamline, is presented in coefficient form in figure 5. At a constant mass-flow ratio, the mass-flow spillage had an increasingly adverse effect on the total drag as the free-stream Mach number varied from 1.59 to 1.99. At critical mass flow, the increase in drag with decreasing free-stream Mach number, as shown in figure 6, resulted from the increase in mass-flow spillage due to choking internally near the leading edge of the support struts.

Representative pressure distributions over the external surface of the model at zero angle of attack are shown in figure 7 for the three Mach numbers. These data indicate that the external static pressure over the cowl decreased with increasing mass spillage due to the rapid expansion produced by the increased curvature of the entering streamline. Additional pressure data are tabulated in table III.

The large variations in the external pressures over the cowl did not extend to more than approximately 1 diameter downstream of the cowl lip. For maximum mass flow at each free-stream Mach number, external pressures equal to or less than the stream static pressure were approached at approximately $x/d = 0.5$. Consequently, a greater part of the surface pressure drag occurred over the forward portion of the cowl.

The decrease in the external-pressure coefficient at $x/d = 4.31$ resulted from expansion of the flow produced by the change in contour of the outer shell. Variations in the pressure distributions at $x/d = 1.5$ at Mach number 1.79 and $x/d = 3.25$ at Mach number 1.99 have been determined to result from weak tunnel disturbances.

Comparison of the experimental pressure distributions at Mach number 1.99 with linearized potential theory ($C_p = -2 v_x/U_0$) shows excellent agreement at a mass-flow ratio of 1.00 (fig. 7(c)). Although

no valid comparison can be made at Mach numbers 1.59 and 1.79, the theoretical pressure distributions are included on figures 7(a) and 7(b) to represent the limiting pressures that would be attained at a mass-flow ratio of 1.00.

Typical schlieren photographs of the shock configuration at the inlet are presented in figure 8 for zero angle of attack. Enlargements of these photographs showed a small region of separated flow at the cowl lip with large mass spillage. Although the flow separation is not apparent in figure 8, the region of expansion and the compression shock subsequent to the separation of the flow can be readily identified.

The pressure-drag coefficient $C_{D,p}$ evaluated from a graphical integration of the pressures measured over the external surface of the model, decreased linearly with decreasing mass-flow ratio, as shown in figure 9. At mass-flow ratios below approximately 0.7, the pressure drag became negative due to the negative pressures over the cowl.

Reasonably good agreement is obtained between the theoretical pressure-drag coefficient and the experimental results for the shock-swallowed condition at Mach number 1.99. Extrapolation of the data for Mach numbers 1.59 and 1.79 to a mass-flow ratio of 1.00 would indicate that good agreement with theory could be expected at these conditions.

Typical boundary-layer profiles measured adjacent to the surface of the model at station 51 are presented in figure 10 in terms of the local Mach number. The Rayleigh equation was used to evaluate the boundary-layer data at zero angle of attack by assuming that the static pressure in the flow field was equal to the value measured at the model surface and that the total temperature was constant throughout the flow field.

The variations in the profiles with mass-flow spillage and free-stream Mach number were found to be associated with the detached bow wave ahead of the cowl lip and the data were analyzed using the method presented in reference 1. As a result of this analysis, the boundary-layer thickness δ was determined to extend to the point at which the slope of the profile rapidly increased, as indicated in figure 10.

The nondimensional-velocity profiles were calculated using the boundary-layer thickness δ , which was determined by the method in reference 1, and are presented in figure 11. For the range of mass flows and free-stream Mach numbers of this investigation, the velocity profiles are in agreement with the $1/7$ power law, which is usually applied to flat-plate data without pressure gradients. Calculations of the effect of the pressure gradient on the boundary layer indicated that

inasmuch as the gradient occurred only over the cowl in the region of thin boundary layer the effect would be of the order of 1.5 percent of the experimental friction-drag coefficient.

The experimental values of friction-drag coefficients, evaluated from a graphical integration of the decrement of momentum in the boundary layer, are presented in figure 12. Examination of the schlieren photographs indicated that the transition point in the boundary layer occurred at approximately $x/d = 0.6$ and that small variations in the friction-drag coefficient probably resulted from the movement of the transition point along the model.

A comparison of the average values of the experimental friction-drag coefficients with the theoretical values, obtained from the equations given by von Kármán (reference 2) for turbulent compressible flow over a smooth flat plate, is presented in figure 13. Although the small region of laminar boundary layer over the cowl and possible three-dimensional effects have been neglected in this comparison, good agreement is obtained.

The experimental additive-drag coefficients were evaluated at zero angle of attack from a momentum balance between the free-stream flow station 0 and flow station 2. The results presented in figure 14 indicate a very rapid increase in additive drag with decreasing mass flow with the rate of change being essentially independent of free-stream Mach number.

Good agreement is obtained between the theory based on one-dimensional flow considerations as presented in reference 3 and the experimental results for the three free-stream Mach numbers. Inasmuch as the oblique shock fell slightly ahead of the cowl lip at Mach number 1.59, the ordinate of the theoretical curve at a mass-flow ratio of 0.93 represents the supersonic additive drag at the maximum mass flow as determined from conical-flow theory for the shock-swallowed condition.

The drag components are summarized and compared with the total drag measured with the force model in figure 15. For this comparison, the friction drag was modified to include the increment of drag due to friction over the surface of the model from station 51 to 56 using the average friction coefficient obtained from the boundary-layer measurements. Good agreement was obtained at Mach numbers 1.79 and 1.99. At Mach number 1.59, however, the force-model drag was approximately 15 percent higher at critical mass flow than that obtained from the pressure model.

For critical mass flow, the additive drag at Mach number 1.59 was greater than the sum of the pressure and friction drags, whereas at Mach numbers 1.79 and 1.99 the friction drag was the largest component.

The decrease in pressure drag with decreasing mass flow was relatively unimportant because the increase in additive drag was much greater and the net effect was a rapid increase in total drag. For a mass-flow ratio of 1.0 at a Mach number of 1.99, the additive drag was zero and the pressure drag became a significant part of the total drag.

Angle of attack. - The effect of angle of attack on the total-drag coefficient is presented in figure 16. For a constant mass flow, the axial force due to the external flow was found to be nearly independent of angle of attack; the increase in drag with angle of attack therefore resulted from the component of the normal force. All increments of drag were essentially independent of mass flow except at 10° angle of attack for Mach number 1.99 where slight shock instability occurred.

Included in the external lift presented in figure 17 is the component of the force along the entering stream tube, which is inherent in the definition of the external forces. At low angles of attack for the three Mach numbers, the lift did not vary greatly with mass-flow spillage. At 10° angle of attack, however, the lift decreased with decreasing mass flow. The external pitching moment, evaluated by assuming that the turning of the flow occurred at the cowl lip, was almost independent of mass-flow spillage at all angles of attack, as shown in figure 18. For the complete range of the investigation, the center of pressure location presented in figure 19 varied from 5.4 to 4.4 diameters ahead of the base.

The variation of the drag increment, the lift, and the pitching moment with angle of attack for critical mass flow is presented in figure 20. The increase in drag increment was essentially independent of free-stream Mach number. The lift-curve slope increased slightly with angle of attack and Mach number whereas the pitching moment increased almost linearly with angle of attack and was independent of Mach number.

In order to provide a simple comparison, theoretical curves were calculated by the semiempirical method of reference 4, modified to apply to an open-nosed body, and are included in figure 20. End effects were neglected for the calculations. Comparison of the experimental results with the modified semiempirical method indicates that the increment of drag and the external lift are underestimated but that the pitching moment is in agreement with experimental values for low angles of attack. Inasmuch as the decrease in critical mass flow at 10° angle of attack resulted in an increase in drag, the discrepancy between the experimental increment of drag and the theoretical value at this condition is somewhat exaggerated.

Variation of the external-pressure distribution with angle of attack for a constant mass-flow ratio at Mach number 1.79 is shown in figure 21. As the angle of attack increased, the loading increased in the region of the cowl. It is of interest to note that the major contribution to the lift resulted from the increase in static pressure over the lower surface of the model ($\theta = 0^\circ$). Beyond 2 diameters downstream of the cowl lip, the external pressures over the upper surface ($\theta = 180^\circ$), which were practically unaffected by increasing angles of attack up to 10° , may indicate separation of the cross flow (reference 5).

Comparison of the angle-of-attack contribution to the circumferential pressure distribution with three-dimensional linearized potential theory at Mach number 1.79 indicated progressively better agreement as the distance downstream of the cowl lip was increased. For zero mass spillage at Mach number 1.99, better agreement was obtained between the experimental results obtained near the cowl lip and two-dimensional theory.

Variations of the total pressure in the boundary layer over the bottom ($\theta = 0^\circ$) and the top ($\theta = 180^\circ$) surfaces of the model at station 51 are presented in figure 22 for Mach number 1.79 in terms of the ratio of the local measured total pressure to the free-stream total pressure. With increasing angle of attack, a thinning of the boundary layer occurred over the bottom surface of the model. Over the top surface, however, a slight increase in boundary-layer thickness was noted for small angles of attack. At higher angles of attack, the boundary-layer thickness decreased appreciably and it is presumed that the boundary-layer air shifted to form a pair of lobes along the sides of the model similar to the boundary-layer shift reported for the RM-10 model in reference 5.

Internal-Flow Characteristics

Zero angle of attack. - The variation of total-pressure recovery and combustion-chamber Mach number with mass-flow ratio is presented in figure 23. The total pressure P_3 was determined from the corrected mass flow and the measured static pressure in the combustion chamber. The combustion-chamber Mach number was calculated based on isentropic expansion of the flow from the annular area at the rake to the cross-sectional area of the combustion chamber with the sting removed.

At Mach number 1.59, the total-pressure recovery remained nearly independent of mass flow in the subcritical region and the shock configuration was stable throughout the range of mass flow. Although the total-pressure recovery decreased with decreasing mass flow at Mach numbers 1.79 and 1.99, no shock instability occurred at zero angle of attack.

2024
A breakdown of total-pressure losses into inlet and subsonic diffuser losses, as shown in figure 24, indicates a decrease in subsonic diffuser losses and an increase in inlet losses for decreasing mass flow. The decrease in total-pressure recovery with decreasing mass flow for Mach numbers 1.79 and 1.99 resulted from a more rapid increase in inlet losses than the corresponding decrease in subsonic diffuser losses. At maximum pressure recovery near the critical mass flow for the three free-stream Mach numbers, the subsonic diffuser losses were approximately equal to the inlet losses.

Comparison of the experimental inlet recovery with a calculated shock recovery is presented in figure 25. In order to provide an independent method of estimating the shock recovery, the location of the normal shock ahead of the cowl lip for mass-flow ratios less than 1 was predicted by the method presented in reference 6. An over-all total-pressure recovery was then computed by weighing the separate recoveries of the flow passing through both the oblique and normal shocks and the flow passing through only the normal shock. Inasmuch as the friction effects over the internal surfaces were neglected, the agreement between the calculated values and the experimental results is fair and within the accuracy of the computations.

The subsonic diffuser characteristics shown in figure 26 indicate that the increase in total-pressure recovery P_3/P_2 with decreasing mass flow was independent of Mach number except in the region of critical mass flow. At maximum total-pressure recovery for Mach number 1.79, subsequent investigation revealed that approximately 4 percent of the loss in total pressure in the subsonic diffuser resulted from wake effects produced by the support struts.

The diffuser performance has also been expressed in terms of a loss coefficient $\Delta P/q_2$ and an effectiveness parameter ($\Delta p/\Delta p_{ideal}$). Although no Mach number effect was indicated in terms of the pressure recovery, the total-pressure loss expressed in terms of the available dynamic pressure showed an increase with Mach number as well as with mass flow. Attempts to correlate these data as a function of either Reynolds number or Mach number at the entrance to the subsonic diffuser were unsuccessful, and it is believed that the variation with Mach number may result from differences in the initial boundary layer (reference 7).

Typical Mach number profiles at the entrance to the combustion chamber for several mass flows at Mach number 1.79 are presented in figure 27. The largest variations in Mach number across the annular passage occurred at mass flows near maximum pressure recovery. The variations in the profiles measured by the various rakes were found to result from the wake effects produced by the support struts.

Angle of attack. - The effect of angle of attack on the total-pressure recovery is shown in figure 28. A decrease of approximately 1 percent in total-pressure recovery was measured as the angle of attack was increased to 10° . These results indicate a somewhat smaller decrement in pressure recovery with angle of attack than reported in reference 8.

The critical mass flow was essentially unaffected by changes in angle of attack up to and including 6° . At 10° angle of attack, however, a decrease in the critical mass-flow ratio from 0.915 at zero angle of attack to 0.865 was measured for Mach number 1.79. A similar decrease occurred at Mach numbers 1.59 and 1.99.

The abrupt decrease in pressure recovery for low mass flows ($m_3/m_0 \approx 0.46$) at Mach number 1.99 for 6° and 10° angles of attack resulted from boundary-layer separation over the upper surface of the spike and slight instability of the shock configuration. No appreciable decrease in pressure recovery resulted from the separation at high angles of attack for Mach numbers 1.79 and 1.99 when no instability occurred in the shock configuration (fig. 29).

The effect of angle of attack on the inlet and subsonic diffuser losses is presented for Mach number 1.79 in figure 30. These data indicate that the components of the total-pressure loss are essentially independent of angle of attack.

The basic cause of the reduction in critical mass flow at 10° angle of attack can be found from a study of the variation in internal pressure distribution with angle of attack at Mach number 1.79 presented in figure 31. For a constant mass flow, a slight decrease in pressure occurs over the bottom surface of the spike ($\theta = 0^\circ$) near the cowl lip at 10° angle of attack but the remainder of the static pressures show no significant trend. Over the top surface ($\theta = 180^\circ$), however, the decrease in static pressure in the region of $x/d = 1.0$ at 10° angle of attack indicates that the flow tends to choke between the upper support struts. It is believed that the cross-flow effects over the spike may result in increased mass flow in the upper portion of the annulus and consequently produces premature choking between the struts. Additional internal pressure data are tabulated in table III.

The variation of total-pressure distributions at the entrance to the combustion chamber was very pronounced with angle of attack (fig. 32). As the angle of attack was varied from 0° to 10° , the peak of the profile shifted toward the upper surface of the annulus, indicating an increase in mass flow in this region. In the lower portion of the combustion chamber, the profile tended to become flat with a reversal in curvature

near the wall. Comparison of the total-pressure ratio in this region with the pressure ratio at the wall indicates separation of the flow along this surface of the combustion chamber.

SUMMARY OF RESULTS

The force and pressure characteristics of a typical ram-jet configuration utilizing a conical spike all-external compression inlet were investigated in the NACA Lewis 8-by 6-foot supersonic tunnel at a Reynolds number of approximately 2.13×10^6 based on the inlet diameter. For the range of mass flows and angles of attack investigated at Mach numbers 1.59, 1.79, and 1.99, the following results were obtained:

1. At zero angle of attack, the external-pressure distribution for zero mass spillage was adequately predicted by linearized potential theory.
2. The boundary-layer velocity profiles measured over the external surface at the rear of the model were in good agreement with the $1/7$ power law. The skin-friction coefficients were essentially independent of mass flow and were predicted by two-dimensional compressible turbulent-flow theory.
3. The rapid increase in total drag with decreasing mass flow resulted from the large increase in additive drag. The variation of additive drag with mass flow was predicted at zero angle of attack from one-dimensional-flow considerations.
4. For a constant mass flow, the axial force due to the external flow was nearly independent of angle of attack indicating that the increase in drag with angle of attack resulted from the component of the normal force.
5. The external lift was essentially independent of mass flow at low angles of attack. At critical mass flow, the lift-curve slope increased with Mach number and was linear at angles of attack below 6° . The pitching moment was independent of mass flow and Mach number and increased almost linearly with angle of attack. The resulting center of pressure, which was located approximately 2 diameters downstream of the cowl lip, moved slightly rearward with angle of attack and Mach number.

6. At critical mass flow, the increment of drag and the lift were underestimated but the pitching moment was predicted with reasonable accuracy by a semiempirical method, which was modified to apply to an open-nosed body.

2054
2

Lewis Flight Propulsion Laboratory,
National Advisory Committee for Aeronautics,
Cleveland, Ohio.

REFERENCES

1. Luidens, Roger W., and Madden, Robert T.: Interpretation of Boundary-Layer Pressure-Rake Data in Flow with a Detached Shock. NACA RM E50I29a, 1950.
2. de Kármán, Th.: The Problem of Resistance in Compressible Fluids. Quinto Convegno "Volta", Reale Accademia d'Italia (Roma), Sett. 30-Ott. 6, 1935, pp. 3-57.
3. Dailey, C. L., and McFarland, H. W.: Development of Ramjet Components. Prog. Rep. 9961-8, Univ. Southern Calif. Aero. Lab., USC, Feb. 7, 1950. (Bi-Monthly Prog. Rep. Dec. 1949 - Jan. 1950 under Navy Contract NOa(s) 9961.)
4. Allen, H. Julian: Estimation of the Forces and Moments Acting on Inclined Bodies of Revolution of High Fineness Ratio. NACA RM A9I26, 1949.
5. Luidens, Roger W., and Simon, Paul C.: Aerodynamic Characteristics of NACA RM-10 Missile in 8- by 6-Foot Supersonic Wind Tunnel at Mach Numbers from 1.49 to 1.98. I - Presentation and Analysis of Pressure Measurements (Stabilizing Fins Removed). NACA RM E50D10, 1950.
6. Moeckel, W. E.: Approximate Method for Predicting Form and Location of Detached Shock Waves Ahead of Plane or Axially Symmetric Bodies. NACA TN 1921, 1949.
7. Copp, Martin R., and Klevatt, Paul L.: Investigation of High-Subsonic Performance Characteristics of a 12° 21-Inch Conical Diffuser, Including the Effects of Change in Inlet-Boundary-Layer Thickness. NACA RM L9H10, 1950.
8. Moeckel, W. E., Connors, J. F., and Schroeder, A. H.: Investigation of Shock Diffusers at Mach Number 1.85. I - Projecting Single-Shock Cones. NACA RM E6K27, 1947.

~~CONFIDENTIAL~~

2034

TABLE I - TABLE OF COORDINATES FOR NACA 8-INCH
RAM-JET CONFIGURATION

(a) Center-body coordinates.

Station	Diameter (in.)
0.500	3.000
1.000	3.330
1.500	3.600
2.000	3.820
2.500	3.983
3.000	4.1125
3.500	4.220
4.000	4.303
4.500	4.371
5.000	4.430
6.000	4.524
7.000	4.580
7.750	4.600
7.875	4.600
10.000	4.585
12.000	4.545
14.000	4.486
16.000	4.415
18.000	4.327
20.000	4.220
22.000	4.084
24.000	3.922
26.000	3.715
30.031	3.343

(b) Outer-shell coordinates.

Station	Diameter (in.)	
	External	Internal
0.100	5.730	5.598
.200	5.791	5.604
.300	5.844	5.622
.400	5.887	5.648
.500	5.927	5.678
1.000	6.100	5.845
2.000	6.360	6.110
3.000	6.550	6.300
4.000	6.666	6.416
5.000	6.750	6.500
9.875	6.998	6.748
22.000	7.616	7.366
30.000	8.024	7.774
32.000	8.125	7.875
56.000	8.125	7.875



TABLE II - LOCATION OF STATIC-PRESSURE ORIFICES FOR PRESSURE MODEL

2034

(a) Location of static tubes along shell contour.

Station		
	External ^a	Internal ^b
0.50	11.00	0.50
1.00	12.00	1.00
1.50	14.00	1.50
2.00	16.00	2.00
2.50	18.00	2.50
3.00	21.00	3.00
4.00	24.00	4.00
5.00	27.00	5.00
6.00	31.00	6.00
7.00	35.00	7.00
8.00	40.00	8.00
9.00	45.00	9.00
10.00		

(b) Location of static tubes ($\theta = 0^\circ$).

Station		
	Spike	Island
	-1.50	8.00
	-1.00	9.00
	-0.50	10.00
	0	11.00
	0.50	12.00
	1.00	14.00
	1.50	16.00
	2.00	18.00
	2.50	21.00
	3.00	24.00
	4.00	27.00
	5.00	31.00
	6.00	37.00
	7.00	

^aTwo rows of orifices, one at $\theta = 180^\circ$ and one at $\theta = 270^\circ$ ^b $\theta = 0^\circ$ 



TABLE III - EXTERNAL AND INTERNAL PRESSURE COEFFICIENTS OF NACA 8-INCH RAM-JET CONFIGURATION
FOR FOUR ANGLES OF ATTACK
(a) Free-stream Mach number of 1.59.

Station	$\alpha = 0^\circ; m_3/m_0 = 0.805$				$\alpha = 0^\circ; m_3/m_0 = 0.735$				$\alpha = 0^\circ; m_3/m_0 = 0.663$				$\alpha = 0^\circ; m_3/m_0 = 0.601$				$\alpha = 0^\circ; m_3/m_0 = 0.484$								
	Longitudinal distribution of C_p												Longitudinal distribution of C_p												
	Outer shell		Center body	Outer shell		Center body	Outer shell		Center body	Outer shell		Center body	Outer shell		Center body	Outer shell		Center body	Outer shell		Center body				
	External	Internal		External	Internal		External	Internal		External	Internal		External	Internal		External	Internal		External	Internal					
$\theta \rightarrow$	180°	270°	0°	180°	270°	0°	180°	270°	0°	180°	270°	0°	180°	270°	0°	180°	270°	0°	180°	270°	0°				
-1.5			0.515			0.514			0.635			0.987			1.091			1.091			1.091				
-1.0			.582			.901			1.013			1.075			1.151			1.151			1.151				
-.5			.890			.989			1.071			1.127			1.206			1.206			1.206				
0			.932			1.021			1.105			1.166			1.261			1.261			1.261				
.5	0.164	0.155	0.882	.690	0.092	0.079	1.058	1.012	0.014	-0.005	1.190	1.118	-0.047	-0.079	1.277	1.196	-0.156	-0.207	1.398	1.308					
1.0	.182	.121	.865	.818	.074	.071	1.053	.995	.021	.018	1.183	1.187	-.028	-.025	1.268	1.215	-.104	-.112	1.381	1.336					
1.5	.076	.078	.856	.788	.044	.054	1.055	.994	.006	.015	1.183	1.183	-.028	-.022	1.268	1.225	-.084	-.084	1.380	1.361					
2.0	.043	.052	.858	.753	.020	.033	1.056	.977	-.006	.003	1.187	1.184	-.028	-.025	1.269	1.220	-.071	-.074	1.381	1.349					
2.5	.025	.027	.878	.795	.009	.014	1.056	1.003	-.012	-.010	1.194	1.142	-.029	-.031	1.275	1.235	-.066	-.069	1.383	1.359					
3.0	.031	.013	.854	.808	.007	.004	1.049	1.013	-.008	-.015	1.182	1.150	-.018	-.022	1.266	1.241	-.052	-.063	1.377	1.363					
4.0	-.016	-.027	.834	.803	-.027	-.034	1.043	1.018	-.039	-.047	1.176	1.159	-.051	-.060	1.263	1.248	-.074	-.084	1.375	1.365					
5.0	-.030	-.036	.767	.760	-.039	-.044	1.017	1.012	-.048	-.064	1.161	1.159	-.058	-.064	1.250	1.248	-.076	-.079	1.367	1.365					
6.0	-.032	-.038	.623	.626	-.039	-.046	.995	.991	-.046	-.062	1.148	1.145	-.054	-.061	1.242	1.240	-.068	-.072	1.362	1.360					
7.0	-.002	-.030	.510	.506	-.029	-.038	1.002	1.003	-.035	-.044	1.151	1.151	-.042	-.050	1.245	1.245	-.064	-.068	1.363	1.363					
8.0	-.030	-.035	.659	.678	-.035	-.039	1.050	1.050	-.040	-.044	1.159	1.157	-.047	-.050	1.257	1.257	-.067	-.068	1.372	1.370					
9.0	-.027	-.030	.707	.716	-.029	-.035	1.021	1.028	-.035	-.040	1.157	1.171	-.041	-.045	1.254	1.259	-.049	-.061	1.368	1.373					
10.0	-.020	-.017		.520	-.024	-.021		1.028	-.030	-.025		1.171	-.034	-.031		1.259	-.041	-.037		1.372					
11.0	-.014	-.014		.442	-.019	-.019		1.045	-.028	-.025		1.184	-.026	-.027		1.269	-.035	-.032		1.378					
12.0	-.015	-.014		.278	-.016	-.019		1.082	-.020	-.022		1.209	-.023	-.025		1.287	-.031	-.021		1.388					
14.0	-.012	-.009		.474	-.014	-.013		1.159	-.017	-.017		1.262	-.021	-.020		1.328	-.026	-.022		1.411					
16.0	-.015	-.013		.778	-.017	-.017		1.221	-.080	-.021		1.306	-.022	-.022		1.360	-.026	-.025		1.438					
18.0	-.010	-.013		.917	-.012	-.016		1.270	-.014	-.018		1.342	-.016	-.022		1.388	-.021	-.024		1.448					
21.0	-.010	-.017		1.064	-.013	-.021		1.355	-.014	-.022		1.394	-.016	-.024		1.429	-.019	-.025		1.474					
24.0	-.007	-.014		1.170	-.009	-.016		1.388	-.011	-.016		1.435	-.013	-.020		1.463	-.015	-.022		1.497					
27.0	-.014	-.012		1.233	-.016	-.019		1.427	-.017	-.022		1.465	-.018	-.022		1.488	-.021	-.025		1.513					
31.0	-.017	-.023		1.275	-.019	-.025		1.453	-.020	-.025		1.483	-.022	-.027		1.502	-.023	-.027		1.523					
35.0	-.048	-.044			1.304	-.050	-.046		1.481	-.052	-.046			1.504	-.053	-.048			1.517	-.053	-.048		1.532		
37.0																									
40.0	-.028	-.029																							
45.0	-.021	-.025																							

Station	Outer shell, external				Outer shell, external				Outer shell, external				Outer shell, external				Outer shell, external				
	Circumferential distribution of C_p				Outer shell, external				Outer shell, external				Outer shell, external				Outer shell, external				
$\theta \rightarrow$	180°	216°	234°	252°	198°	216°	234°	252°	198°	216°	234°	252°	198°	216°	234°	252°	198°	216°	234°	252°	
0.5	0.177	0.176	0.172	0.161	0.100	0.097	0.092	0.086	0.014	0.013	0.006	-0.001	-0.063	-0.067	-0.075	-0.076	-0.187	-0.192	-0.195	-0.203	
14.0	-.015	-.080	-.017	-.017	-.019	-.024	-.023	-.014	-.022	-.027	-.024	-.017	-.026	-.031	-.026	-.021	-.051	-.034	-.033	-.024	
45.0	-.027	-.035	-.027	-.028	-.029	-.026	-.029	-.029	-.029	-.029	-.029	-.029	-.031	-.028	-.031	-.021	-.031	-.030	-.031	-.025	-.029

TABLE III - EXTERNAL AND INTERNAL PRESSURE COEFFICIENTS OF NACA 8-INCH RAM-JET CONFIGURATION
FOR FOUR ANGLES OF ATTACK - Continued
(a) Continued. - Free-stream Mach number of 1.69.



Station	$\alpha = 0^\circ; m_3/m_0 = 0.329$			$\alpha = 3^\circ; m_3/m_0 = 0.804$			$\alpha = 3^\circ; m_3/m_0 = 0.740$			$\alpha = 3^\circ; m_3/m_0 = 0.652$			$\alpha = 3^\circ; m_3/m_0 = 0.592$			
	Longitudinal distribution of C_p															
	Outer shell		Center body													
	External	Internal		External	Internal		External	Internal		External	Internal		External	Internal		
0	180°	270°	0°	180°	270°	0°	180°	270°	0°	180°	270°	0°	180°	270°	0°	
-1.5																
-1.0																
-0.5																
0																
.5	-0.331	-0.422	1.504	1.423	0.021	0.157	0.761	0.826	-0.020	0.103	0.921	0.928	-0.099	0.041	1.130	1.089
1.0	-0.214	-0.331	1.467	1.454	0.004	0.184	0.763	0.723	-0.028	0.090	0.960	0.891	-0.089	0.050	1.145	1.094
1.5	-0.166	-0.169	1.463	1.466	-0.012	0.063	0.796	0.732	-0.036	0.060	0.966	0.898	-0.082	0.021	1.156	1.106
2.0	-0.133	-0.139	1.482	1.469	-0.018	0.066	0.824	0.707	-0.038	0.041	0.967	0.892	-0.074	0.013	1.169	1.104
2.5	-0.122	-0.124	1.483	1.472	-0.028	0.066	0.824	0.769	-0.045	0.024	1.002	0.932	-0.071	0.005	1.179	1.150
3.0	-0.096	-0.103	1.480	1.474	-0.031	0.050	0.838	0.789	-0.047	0.018	1.091	0.948	-0.065	-0.002	1.171	1.141
4.0	-0.108	-0.115	1.480	1.475	-0.065	-0.024	0.826	0.793	-0.079	-0.051	1.089	0.961	-0.089	-0.044	1.178	1.154
5.0	-0.097	-0.105	1.477	1.475	-0.070	-0.040	0.768	0.755	-0.079	0.046	1.045	0.958	-0.091	-0.054	1.161	1.156
6.0	-0.085	-0.089	1.474	1.474	-0.064	-0.044	0.619	0.619	-0.071	-0.049	1.043	0.959	-0.079	-0.054	1.161	1.148
7.0	-0.066	-0.069	1.475	1.475	-0.049	-0.058	0.507	0.610	-0.063	-0.041	1.058	0.969	-0.061	-0.046	1.157	1.157
8.0	-0.066	-0.067	1.478	1.478	-0.049	-0.040	0.683	0.684	-0.063	-0.044	1.096	0.995	-0.058	-0.049	1.178	1.177
9.0	-0.067	-0.069	1.477	1.478	-0.041	-0.040	0.701	0.710	-0.045	-0.044	1.003	0.948	-0.048	-0.048	1.177	1.182
10.0	-0.047	-0.044	1.480	1.480	-0.054	-0.058	0.813	0.813	-0.058	-0.050	1.002	0.902	-0.040	-0.035	1.184	1.184
11.0	-0.039	-0.058	1.480	1.480	-0.066	-0.064	0.435	0.435	-0.050	-0.029	1.026	0.980	-0.030	-0.031	1.205	1.205
12.0	-0.034	-0.056	1.483	1.483	-0.082	-0.028	0.273	0.273	-0.024	-0.029	1.067	0.925	-0.025	-0.051	1.220	1.220
14.0	-0.029	-0.026	1.493	1.493	-0.018	-0.021	0.478	0.480	-0.026	-0.026	1.147	0.921	-0.026	-0.026	1.270	1.270
16.0	-0.028	-0.029	1.508	1.508	-0.018	-0.023	0.769	0.769	-0.020	-0.026	1.073	0.920	-0.028	-0.028	1.315	1.315
18.0	-0.028	-0.026	1.509	1.509	-0.013	-0.023	0.906	0.906	-0.014	-0.025	1.259	0.914	-0.026	-0.026	1.347	1.347
21.0	-0.031	-0.028	1.528	1.528	-0.013	-0.027	1.048	1.048	-0.016	-0.029	1.326	0.914	-0.029	-0.029	1.395	1.395
24.0	-0.016	-0.023	1.551	1.551	-0.018	-0.028	1.156	1.156	-0.017	-0.025	1.384	0.913	-0.025	-0.025	1.437	1.437
27.0	-0.020	-0.025	1.556	1.556	-0.016	-0.027	1.280	1.280	-0.020	-0.029	1.423	0.919	-0.029	-0.029	1.467	1.467
31.0	-0.022	-0.028	1.542	1.542	-0.022	-0.028	1.263	1.263	-0.025	-0.024	1.452	0.922	-0.033	-0.033	1.485	1.485
35.0	-0.053	-0.046			-0.051	-0.053			-0.054	-0.065		0.952	-0.053	-0.053	-0.053	-0.053
37.0	-0.031	-0.032	1.548	1.548	-0.039	-0.058		1.292	-0.030	-0.039	1.480	-0.029	-0.038	1.507	-0.029	-0.038
40.0	-0.031	-0.028			-0.021	-0.034			-0.029	-0.036		-0.021	-0.034	1.516	-0.021	-0.035
45.0	-0.031	-0.028														

Station	Circumferential distribution of C_p											
	Outer shell, external				Outer shell, external				Outer shell, external			
	Outer shell, external		Outer shell, external		Outer shell, external		Outer shell, external		Outer shell, external		Outer shell, external	
0	180°	216°	254°	282°	198°	216°	234°	252°	198°	216°	234°	252°
0.5	-0.383	-0.400	-0.408	-0.416	0.034	0.049	0.079	0.113	-0.028	-0.008	-0.025	-0.058
14.0	-0.034	-0.037	-0.037	-0.029	-0.023	-0.029	-0.023	-0.027	-0.028	-0.030	-0.027	-0.030
45.0	-0.031	-0.029	-0.030	-0.031	-0.039	-0.029	-0.058	-0.036	-0.029	-0.034	-0.036	-0.038

TABLE III - EXTERNAL AND INTERNAL PRESSURE COEFFICIENTS OF NACA 8-INCH RAM-JET CONFIGURATION
FOR FOUR ANGLES OF ATTACK - Continued
(a) Continued. - Free-stream Mach number of 1.69.



Station	$\alpha = 3^\circ; m_3/m_0 = 0.436$				$\alpha = 8^\circ; m_3/m_0 = 0.386$				$\alpha = 8^\circ; m_3/m_0 = 0.300$				$\alpha = 6^\circ; m_3/m_0 = 0.715$				$\alpha = 6^\circ; m_3/m_0 = 0.596$															
	Longitudinal distribution of C_p																Longitudinal distribution of C_p															
	Outer shell				Center body	Outer shell				Center body	Outer shell				Center body	Outer shell				Center body	Outer shell				Center body							
	External		Internal			External		Internal			External		Internal			External		Internal			External		Internal									
$\theta \rightarrow$	180°	270°	0°	0°	180°	270°	0°	0°	180°	270°	0°	0°	180°	270°	0°	180°	270°	0°	0°	180°	270°	0°	0°	180°	270°	0°	0°					
-1.5					1.117				1.201				1.687			0.680				0.987												
-1.0					1.170				1.252				.780			.982				1.104												
-0.5					1.210				1.300				.864			1.008				1.131												
0					1.251				1.351				.889			1.005				1.139												
0.5	-0.242	-0.198	1.350	1.287	-0.346	-0.375	1.473	1.401	-0.094	-0.174	0.492	.763	-0.145	0.075	0.919	.947	-0.251	-0.071	1.165	1.185												
1.0	-.806	-.106	1.354	1.317	-.309	-.315	1.463	1.431	-.083	-.169	.639	.494	-.140	.025	.981	.926	-.231	-.007	1.194	1.147												
1.5	-.171	-.077	1.354	1.331	-.251	-.159	1.463	1.445	-.096	-.118	.778	.700	-.130	.078	1.021	.950	-.203	.004	1.213	1.168												
2.0	-.146	-.064	1.359	1.335	-.211	-.129	1.465	1.480	-.096	-.071	.809	.795	-.122	.061	1.045	.980	-.180	.005	1.231	1.175												
2.5	-.183	-.058	1.387	1.344	-.183	-.106	1.467	1.455	-.099	-.060	.843	.762	-.120	.037	1.085	1.008	-.168	-.005	1.242	1.201												
3.0	-.120	-.058	1.387	1.351	-.165	-.095	1.466	1.458	-.098	-.030	.830	.785	-.112	.021	1.060	1.082	-.154	-.009	1.249	1.214												
4.0	-.123	-.072	1.363	1.357	-.150	-.190	1.467	1.462	-.116	-.050	.819	.786	-.126	-.038	1.063	1.040	-.157	-.055	1.246	1.229												
5.0	-.120	-.077	1.359	1.359	-.145	-.098	1.465	1.463	-.106	-.048	.782	.745	-.117	-.056	1.048	1.042	-.142	-.069	1.239	1.255												
6.0	-.103	-.074	1.363	1.357	-.120	-.086	1.463	1.462	-.082	-.057	.614	.618	-.095	-.061	1.036	1.051	-.116	-.073	1.225	1.228												
7.0	-.080	-.062	1.371	1.363	-.094	-.074	1.465	1.465	-.089	-.051	.505	.509	-.068	-.065	1.045	1.045	-.085	-.068	1.240	1.240												
8.0	-.071	-.061	1.372	1.371	-.079	-.066	1.467	1.467	-.068	-.061	.682	.695	-.060	-.064	1.075	1.073	-.071	-.080	1.257	1.257												
9.0	-.060	-.059	1.374	1.374	-.066	-.066	1.470	1.466	-.046	-.063	.688	.695	-.046	-.067	1.075	1.080	-.066	-.077	1.261	1.261												
10.0	-.060	-.046	1.376	1.376	-.066	-.063	1.471	1.471	-.038	-.064	.600	.600	-.040	-.068	1.061	1.047	-.068	-.068	1.263	1.263												
11.0	-.059	-.043	1.383	1.383	-.045	-.048	1.474	1.474	-.028	-.055	.423	.423	-.089	-.068	1.010	1.035	-.068	-.068	1.276	1.276												
12.0	-.054	-.041	1.393	1.386	-.047	1.478	1.478	-.021	-.057	.286	.286	-.023	-.059	1.083	1.080	-.069	-.069	1.292	1.292													
14.0	-.027	-.038	1.413	1.413	-.029	-.036	1.498	1.498	-.018	-.056	.597	.597	-.017	-.068	1.197	1.082	-.066	-.066	1.329	1.329												
16.0	-.026	-.035	1.433	1.433	-.025	-.038	1.496	1.496	-.015	-.053	.811	.811	-.016	-.055	1.261	1.260	-.063	-.063	1.361	1.361												
18.0	-.019	-.051	1.449	1.420	-.035	1.504	1.504	-.010	-.061	.928	.928	-.011	-.068	1.298	1.014	-.068	-.068	1.387	1.387													
21.0	-.019	-.035	1.472	1.472	-.030	-.036	1.515	1.511	-.011	-.064	1.061	1.011	-.064	1.353	1.014	-.068	1.425	1.425														
24.0	-.016	-.029	1.495	1.495	-.017	-.029	1.526	1.526	-.011	-.047	1.163	1.111	-.046	1.403	1.014	-.051	1.466	1.466														
27.0	-.021	-.031	1.510	1.510	-.022	-.032	1.533	1.533	-.018	-.061	1.236	1.217	-.051	1.439	1.021	-.054	1.488	1.488														
31.0	-.026	-.037	1.521	1.521	-.025	-.037	1.537	1.537	-.021	-.056	1.268	1.220	-.056	1.444	1.024	-.059	1.497	1.497														
35.0	-.054	-.056			-.064	-.066	1.542	1.542	-.025	-.068	1.297	1.297	-.049	-.074	1.491	1.491	-.053	-.078														
37.0	-.051	-.040	1.528	1.528	-.030	-.041			-.019	-.059	1.297	1.297	-.023	-.060	1.491	1.491	-.027	-.065														
40.0	-.023	-.037			-.022	-.037					-.017	-.059	1.297	1.297	-.023	-.060	1.491	1.491	-.020	-.062												

Station	Circumferential distribution of C_p							
	Outer shell, external				Outer shell, external			
$\theta \rightarrow$	198°	216°	234°	252°	198°	216°	234°	252°
0.5	-0.278	-0.268	-0.246	-0.226	-0.447	-0.447	-0.442	-0.408
14.0	-.232	-.058	-.059	-.035	-.035	-.040	-.042	-.031
43.0	-.050	-.080	-.056	-.058	-.029	-.029	-.034	-.037

TABLE III - EXTERNAL AND INTERNAL PRESSURE COEFFICIENTS OF NACA 8-INCH RAM-JET CONFIGURATION
FOR FOUR ANGLES OF ATTACK - Continued
(a) Concluded. - Free-stream Mach number of 1.59.



Station	$\alpha = 6^\circ; m_3/m_0 = 0.338$				$\alpha = 10^\circ; m_3/m_0 = 0.759$				$\alpha = 10^\circ; m_3/m_0 = 0.696$				$\alpha = 10^\circ; m_3/m_0 = 0.574$				$\alpha = 10^\circ; m_3/m_0 = 0.330$				
	Longitudinal distribution of C_p								Circumferential distribution of C_p												
	Outer shell		Center body	Outer shell		Center body	Outer shell		Center body	Outer shell		Center body	Outer shell		Center body	Outer shell		Center body	Outer shell		
	External	Internal		External	Internal		External	Internal		External	Internal		External	Internal		External	Internal		External	Internal	
$\theta \rightarrow$	180°	270°	0°	0°	180°	270°	0°	0°	0°	180°	270°	0°	0°	180°	270°	0°	0°	180°	270°	0°	0°
-1.5				1.899			0.767			0.806			1.016								1.251
-1.0				1.865			.875			.950			1.117								1.273
-0.5				1.806			.924			1.006			1.136								1.295
0				1.348			.908			.978			1.119								1.317
0.5	-0.586	-0.355	1.452	1.389	-0.170	0.261	0.288	.740	-0.243	0.106	0.743	.863	-0.295	-0.042	1.067	1.090	-0.347	-0.312	1.387	1.343	
1.0	-0.408	-0.204	1.451	1.420	-0.204	.186	.385	.421	-.259	.168	.911	.834	-.322	.029	1.145	1.096	-.475	-.184	1.400	1.369	
1.5	-0.354	-0.149	1.455	1.436	-0.200	.186	.356	.336	-.246	.101	.970	.892	-.293	.070	1.180	1.129	-.441	-.120	1.418	1.389	
2.0	-0.286	-0.118	1.459	1.443	-0.192	.079	.265	.188	-.238	.062	1.008	.918	-.267	.040	1.204	1.133	-.378	-.067	1.424	1.398	
2.5	-0.243	-.095	1.464	1.451	-0.186	.046	.762	.630	-.222	.031	1.037	.972	-.253	.012	1.222	1.178	-.351	-.064	1.451	1.412	
3.0	-0.234	-.083	1.464	1.455	-0.191	.026	.823	.764	-.201	.012	1.037	.998	-.234	-.006	1.222	1.197	-.324	-.070	1.435	1.420	
4.0	-0.211	-.098	1.457	1.468	-0.177	-.038	.810	.784	-.188	-.047	1.050	1.026	-.221	-.050	1.234	1.219	-.285	-.090	1.459	1.451	
5.0	-0.188	-.100	1.466	1.464	-0.185	-.064	.739	.733	-.154	-.070	1.039	1.032	-.184	-.081	1.231	1.227	-.244	-.105	1.459	1.438	
6.0	-0.163	-.095	1.455	1.464	-.094	-.079	.607	.608	-.104	-.065	1.029	1.022	-.126	-.094	1.229	1.226	-.179	-.116	1.459	1.458	
7.0	-0.113	-.083	1.469	1.467	-.071	-.081	.499	.504	-.075	-.085	1.040	1.040	-.095	-.094	1.237	1.237	-.112	-.114	1.442	1.442	
8.0	-0.090	-.085	1.472	1.472	-.061	-.098	.671	.677	-.064	-.092	1.070	1.068	-.066	-.101	1.265	1.262	-.079	-.114	1.446	1.444	
9.0	-0.070	-.088	1.478	1.474	-.045	-.098	.664	.674	-.051	-.107	1.070	1.075	-.062	-.114	1.254	1.257	-.058	-.127	1.444	1.444	
10.0	-0.054	-.082	1.475	1.475	-.037	-.105	.575	.604	-.110	-.110	1.078	1.078	-.040	-.115	1.261	1.261	-.042	-.132	1.444	1.444	
11.0	-0.039	-.080	1.478	1.478	-.028	-.112	.401	.401	-.088	-.115	1.068	1.068	-.089	-.122	1.278	1.278	-.029	-.157	1.449	1.449	
12.0	-0.031	-.083	1.482	1.482	-.018	-.180	.244	.244	-.021	-.184	1.189	1.189	-.022	-.189	1.288	1.288	-.023	-.146	1.456	1.456	
14.0	-0.023	-.076	1.492	1.492	-.011	-.189	.715	.715	-.014	-.133	1.194	1.194	-.015	-.139	1.326	1.326	-.016	-.154	1.467	1.467	
16.0	-0.021	-.072	1.500	1.500	-.011	-.186	.861	.861	-.018	-.141	1.245	1.245	-.012	-.146	1.356	1.356	-.013	-.163	1.479	1.479	
18.0	-0.016	-.065	1.507	1.507	-.008	-.156	.950	.950	-.007	-.141	1.286	1.286	-.007	-.149	1.383	1.383	-.008	-.169	1.490	1.490	
21.0	-0.016	-.053	1.519	1.519	-.008	-.128	1.060	1.060	-.007	-.126	1.345	1.345	-.007	-.129	1.422	1.422	-.008	-.145	1.506	1.506	
24.0	-0.016	-.055	1.539	1.539	-.004	-.108	1.153	1.153	-.008	-.110	1.397	1.397	-.006	-.111	1.456	1.456	-.008	-.114	1.518	1.518	
27.0	-0.023	-.056	1.536	1.536	-.013	-.113	1.214	1.214	-.014	-.115	1.433	1.433	-.014	-.114	1.480	1.480	-.016	-.117	1.535	1.535	
31.0	-0.026	-.045	1.541	1.541	-.014	-.110	1.255	1.255	-.014	-.112	1.459	1.459	-.014	-.111	1.498	1.498	-.018	-.114	1.532	1.532	
35.0	-0.054	-.076		1.545			-.054	-.129		1.484			-.055	-.128		1.512			-.056	-.130	
40.0	-0.028	-.063			-.080	-.112			-.020	-.112			-.020	-.114			-.023	-.114			
45.0	-0.021	-.060			-.080	-.110			-.030	-.110			-.030	-.109			-.023	-.110			



TABLE III - EXTERNAL AND INTERNAL PRESSURE COEFFICIENTS OF NACA 8-INCH RAM-JET CONFIGURATION
FOR FOUR ANGLES OF ATTACK - Continued
(b) Free-stream Mach number of 1.75.

Station	$\alpha = 0^\circ; m_3/m_0 = 0.915$			$\alpha = 0^\circ; m_3/m_0 = 0.903$			$\alpha = 0^\circ; m_3/m_0 = 0.842$			$\alpha = 0^\circ; m_3/m_0 = 0.796$			$\alpha = 0^\circ; m_3/m_0 = 0.667$						
	Longitudinal distribution of C_p .									Circumferential distribution of C_p .									
	Outer shell		Center body	Outer shell		Center body	Outer shell		Center body	Outer shell		Center body	Outer shell		Center body	Outer shell		Center body	
	External	Internal		External	Internal		External	Internal		External	Internal		External	Internal		External	Internal		
$\theta \rightarrow$	180°	270°	0°	0°	180°	270°	0°	0°	0°	180°	270°	0°	180°	270°	0°	180°	270°	0°	
-1.5				0.459			0.458			0.458			0.458					0.458	
-1.0				.505			.500			.501			.506					1.045	
-0.5				.503			.501			.584			1.034					1.252	
0				.555			.944			1.178			1.211					1.286	
0.5	0.269	1.036	1.069	0.238	0.812	1.107	1.087	0.176	0.151	1.211	1.153	0.097	0.075	1.289	1.207	-0.006	-0.036	1.410	
1.0	.171	0.167	1.017	.959	.188	1.153	1.083	1.028	.128	1.203	1.136	.088	.051	1.288	1.211	.034	.028	1.341	
1.5	.118	.116	1.006	.931	.109	.107	1.088	1.017	.092	.090	1.203	1.151	.055	.055	1.288	1.220	.028	.081	1.403
2.0	.083	.082	1.008	.892	.076	.076	1.098	.992	.064	.061	1.206	1.158	.044	.043	1.286	1.209	.020	.013	1.382
2.5	.059	.056	1.085	.919	.063	.063	1.105	1.033	.042	.059	1.214	1.156	.027	.024	1.299	1.258	.010	.008	1.409
3.0	.043	.040	1.008	.956	.058	.058	1.090	1.044	.028	.025	1.203	1.166	.017	.013	1.280	1.245	.007	-.003	1.403
4.0	-.006	-.010	.987	.955	-.011	-.013	1.078	1.049	-.017	-.019	1.197	1.174	-.025	-.029	1.277	1.253	-.032	-.041	1.388
5.0	-.025	-.023	.919	.915	-.026	-.026	1.040	1.028	-.034	-.031	1.188	1.170	-.059	-.058	1.267	1.255	-.045	-.047	1.393
6.0	-.024	-.026	.771	.771	-.028	-.028	1.004	.998	-.034	-.034	1.155	1.151	-.057	-.059	1.246	1.241	-.049	-.046	1.383
7.0	-.014	-.018	.654	.657	-.021	-.023	1.020	1.021	-.026	-.026	1.162	1.165	-.027	-.030	1.251	1.250	-.032	-.037	1.388
8.0	-.018	-.018	.741	.769	-.021	-.021	1.064	1.066	-.026	-.024	1.189	1.191	-.029	-.029	1.270	1.269	-.034	-.035	1.399
9.0	-.012	-.018	.853	.886	-.017	-.021	1.049	1.058	-.021	-.024	1.180	1.191	-.022	-.029	1.285	1.259	-.026	-.032	1.399
10.0	-.003		.774	-.007	-.007		1.058	-.010	-.012		1.192	-.018	-.018	-.015	1.267	-.017	-.019		1.403
11.0	.015	-.001	.587	.008	-.004		1.071	-.003	-.008		1.199	-.005	-.011		1.283	-.008	-.014		1.414
12.0	.012	.004	.422	.008	.008		1.135	.003	-.002		1.258	-.002	-.004		1.311	-.008	-.008		1.430
14.0	-.008	.002	.895	-.009	-.001		1.239	-.012	-.004		1.313	-.018	-.008		1.370	-.020	-.010		1.465
16.0	-.021	-.010	1.060	-.083	-.018		1.316	-.084	-.014		1.375	-.089	-.018		1.417	-.032	-.019		1.495
18.0	-.008	-.010	1.187	-.001	-.011		1.378	-.003	-.013		1.422	-.006	-.016		1.453	-.007	-.016		1.516
21.0	.001	-.003	1.292	-.001	-.006		1.459	-.003	-.008		1.487	-.005	-.010		1.508	-.007	-.011		1.561
24.0	.004	-.006	1.391	-.009	-.007		1.528	-.003	-.008		1.542	-.002	-.010		1.581	-.008	-.011		1.580
27.0	-.004	-.001	1.455	-.006	-.008		1.574	-.007	-.004		1.588	-.009	-.004		1.586	-.002	-.005		1.604
31.0	-.004	-.001	1.497	-.008	-.003		1.607	-.007	-.004		1.608	-.005	-.006		1.606	-.008	-.006		1.617
35.0	-.028	-.025		-.028	-.028		-.030	-.028			-.029	-.028			-.030	-.028			
37.0			1.530				1.644				1.644				1.640				1.639
40.0	-.016	-.016		-.018	-.004		-.018	-.018			-.018	-.018			-.019	-.019			
45.0	-.016	-.016		-.018	-.004		-.018	-.018			-.018	-.018			-.018	-.019			

TABLE III - EXTERNAL AND INTERNAL PRESSURE COEFFICIENTS OF NACA 8-INCH RAM-JET CONFIGURATION
FOR FOUR ANGLES OF ATTACK - Continued
(b) Continued. - Free-stream Mach number of 1.79.



Station	$\alpha = 0^\circ; m_3/m_0 = 0.644$				$\alpha = 3^\circ; m_3/m_0 = 0.914$				$\alpha = 3^\circ; m_3/m_0 = 0.854$				$\alpha = 3^\circ; m_3/m_0 = 0.783$				$\alpha = 3^\circ; m_3/m_0 = 0.661$				
	Longitudinal distribution of C_p																Outer shell				
	Outer shell		Center body	Outer shell		Center body	Outer shell		Center body	Outer shell		Center body	Outer shell		Center body	Outer shell		Center body	Outer shell		
	External	Internal		External	Internal		External	Internal		External	Internal		External	Internal		External	Internal		External	Internal	
$\theta \rightarrow$	180°	270°	0°	0°	180°	270°	0°	0°	180°	270°	0°	0°	180°	270°	0°	0°	180°	270°	0°	0°	0°
-1.5				0.722			0.554			0.540			0.534			0.536			0.536		
-1.0				1.254			.580			.610			.580			1.110			1.110		
-0.5				1.315			.591			.599			.769			1.252			1.252		
0				1.356			.541			1.015			1.185			1.274			1.274		
0.5	-0.120	-0.140	1.508	1.412	0.140	0.247	0.893	0.994	0.085	0.195	1.044	1.047	-0.007	0.096	1.210	1.164	-0.116	-0.026	1.361	1.298	
1.0	-.044	-.056	1.495	1.449	.081	.178	.920	.945	.055	.155	1.069	.998	.008	.103	1.227	1.162	-.066	-.023	1.367	1.312	
1.5	-.037	-.035	1.495	1.456	.042	.181	.941	.987	.024	.105	1.068	1.012	-.009	.074	1.240	1.180	-.056	-.023	1.376	1.338	
2.0	-.018	-.026	1.496	1.461	.015	.085	.970	.842	.003	.074	1.109	1.008	-.080	.061	1.255	1.176	-.054	-.013	1.385	1.332	
2.5	-.020	-.028	1.498	1.477	-.005	.067	1.000	.917	-.014	.048	1.126	1.065	-.030	.031	1.255	1.214	-.058	-.003	1.392	1.368	
3.0	-.017	-.027	1.495	1.481	-.016	.059	.992	.940	-.024	.031	1.119	1.073	-.034	.017	1.260	1.227	-.057	-.003	1.390	1.367	
4.0	-.047	-.055	1.495	1.488	-.065	-.009	.981	.948	-.061	-.016	1.121	1.092	-.065	-.026	1.255	1.245	-.081	-.040	1.394	1.388	
5.0	-.066	-.057	1.490	1.490	-.065	-.032	.913	.910	-.068	-.028	1.097	1.090	-.071	-.033	1.255	1.260	-.083	-.047	1.390	1.389	
6.0	-.061	-.054	1.486	1.487	-.068	-.087	.768	.767	-.063	-.033	1.076	1.069	-.065	-.028	1.248	1.243	-.075	-.048	1.387	1.385	
7.0	-.039	-.044	1.488	1.491	-.046	-.022	.653	.658	-.051	-.026	1.094	1.092	-.061	-.032	1.258	1.258	-.059	-.040	1.394	1.395	
8.0	-.039	-.040	1.496	1.496	-.059	-.084	.811	.845	-.044	-.028	1.134	1.134	-.046	-.035	1.282	1.284	-.054	-.040	1.411	1.411	
9.0	-.031	-.037	1.496	1.500	-.087	-.084	.840	.852	-.029	-.028	1.138	1.144	-.028	-.033	1.286	1.291	-.036	-.039	1.414	1.418	
10.0	-.020	-.023		1.501	-.017	-.011		.758	-.020	-.013		1.145	-.019	-.019		1.296	-.025	-.025		1.423	
11.0	-.004	-.018		1.506	-.018	-.005		.573	-.018	-.009		1.170	-.020	-.013		1.315	-.027	-.020		1.432	
12.0	-.009	-.011		1.618	-.015	-.007		.412	-.015	-.011		1.212	-.084	-.016		1.357	-.029	-.030		1.446	
14.0	-.063	-.013		1.537	-.022	-.018		.567	-.027	-.015		1.291	-.052	-.018		1.388	-.058	-.023		1.478	
15.0	-.034	-.022		1.556	-.084	-.019		.802	-.027	-.023		1.351	-.068	-.025		1.431	-.050	-.050		1.505	
18.0	-.008	-.018		1.571	-.001	-.019		.956	-.003	-.021		1.398	-.006	-.023		1.465	-.008	-.025		1.585	
21.0	-.007	-.013		1.593	-.008	-.015		1.128	-.003	-.015		1.468	-.006	-.018		1.506	-.008	-.021		1.654	
24.0	-.002	-.011		1.613	-.003	-.016		1.844	0	-.018		1.521	-.005	-.018		1.633	-.006	-.020		1.578	
27.0	-.009	-.005		1.629	-.007	-.009		1.325	-.009	-.015		1.567	-.009	-.011		1.618	-.012	-.013		1.599	
31.0	-.008	-.003		1.638	-.007	-.009		1.378	-.008	-.011		1.597	-.008	-.018		1.600	-.010	-.013		1.611	
35.0	-.026	-.026			-.080	-.034			-.030	-.034			-.030	-.035			-.033	-.036			
37.0				1.651				1.412				1.637				1.634				1.633	
40.0	-.018	-.019			-.017	-.026			-.019	-.026			-.018	-.026			-.020	-.027			
45.0	-.016	-.017			-.016	-.026			-.016	-.026			-.017	-.026			-.018	-.027			

Station	Circumferential distribution of C_p																
	Outer shell, external				Outer shell, external				Outer shell, external				Outer shell, external				
	Outer shell, external		Outer shell, external		Outer shell, external		Outer shell, external		Outer shell, external		Outer shell, external		Outer shell, external		Outer shell, external		
$\theta \rightarrow$	198°	216°	234°	252°	198°	216°	234°	252°	198°	216°	234°	252°	198°	216°	234°	252°	
0.5	-0.125	-0.127	-0.129	-0.135	0.144	0.168	0.185	0.215	0.068	0.105	0.139	0.158	-0.008	0.010	0.033	0.060	
14.0	-.024	-.024	-.020	-.015	-.024	-.027	-.019	-.018	-.028	-.030	-.018	-.022	-.033	-.018	-.024	-.025	-.028
45.0	-.018	-.016	-.016	-.018	-.019	-.016	-.028	-.024	-.020	-.020	-.020	-.020	-.024	-.021	-.021	-.023	-.026

TABLE III - EXTERNAL AND INTERNAL PRESSURE COEFFICIENTS OF NACA 8-INCH RAM-JET CONFIGURATION
FOR FOUR ANGLES OF ATTACK - Continued
(b) Continued. - Free-stream Mach number of 1.79.



Station	$\alpha = 3^\circ; m_3/m_0 = 0.446$				$\alpha = 6^\circ; m_3/m_0 = 0.911$				$\alpha = 6^\circ; m_3/m_0 = 0.869$				$\alpha = 6^\circ; m_3/m_0 = 0.784$				$\alpha = 6^\circ; m_3/m_0 = 0.669$					
	Longitudinal distribution of C_p								Circumferential distribution of C_p								Circumferential distribution of C_p					
	Outer shell		Center body	Outer shell		Center body	Outer shell		Center body	Outer shell		Center body	Outer shell		Center body	Outer shell		Center body	Outer shell			
	External	Internal		External	Internal		External	Internal		External	Internal		External	Internal		External	Internal		External	Internal		
$\theta \rightarrow$	180°	270°	0°	0°	180°	270°	0°	0°	180°	270°	0°	0°	180°	270°	0°	0°	180°	270°	0°	180°	270°	0°
-1.5	-0.509	-0.307	1.584	1.445	0.015	0.261	0.658	.921	-0.058	0.800	0.926	0.983	-0.115	0.102	1.135	1.125	-0.195	-0.008	1.308	1.268	1.614	
-1.0	-1.06	-1.107	1.617	1.483	-.008	.187	.713	.633	-.034	.163	1.014	.926	-.086	.109	1.185	1.122	-.144	.038	1.329	1.278	1.133	
-.5	-1.145	-.072	1.580	1.600	-.080	.129	.918	.697	-.050	.118	1.061	.973	-.085	.084	1.818	1.158	-.128	.056	1.350	1.308	1.245	
0	-1.181	-.067	1.584	1.508	-.047	.090	.961	.948	-.060	.061	1.092	.987	-.085	.085	1.840	1.180	-.119	.028	1.366	1.311	1.269	
1.0	-1.113	-.050	1.587	1.589	-.057	.061	.991	.913	-.070	.068	1.118	1.049	-.090	.036	1.858	1.205	-.118	.015	1.377	1.345	1.278	
1.5	-1.08	-.045	1.527	1.580	-.068	.042	.981	.935	-.072	.035	1.116	1.072	-.088	.081	1.288	1.828	-.111	.004	1.379	1.357	1.278	
2.0	-1.113	-.050	1.587	1.589	-.057	.061	.991	.913	-.070	.068	1.118	1.049	-.090	.036	1.858	1.205	-.118	.015	1.377	1.345	1.278	
2.5	-1.06	-.067	1.530	1.587	-.068	-.011	.967	.958	-.098	-.016	1.181	1.004	-.108	.085	1.266	1.248	-.124	-.037	1.386	1.377	1.308	
3.0	-1.09	-.065	1.530	1.531	-.090	-.088	.908	.898	-.097	-.038	1.101	1.095	-.106	-.040	1.269	1.257	-.118	-.048	1.386	1.396	1.308	
3.5	-1.092	-.065	1.530	1.531	-.079	-.055	.762	.761	-.084	-.059	1.085	1.077	-.091	-.045	1.254	1.251	-.101	-.055	1.386	1.386	1.308	
4.0	-1.074	-.065	1.534	1.537	-.068	-.053	.648	.656	-.061	-.057	1.108	1.101	-.065	-.048	1.266	1.287	-.074	-.048	1.393	1.396	1.308	
4.5	-1.065	-.051	1.548	1.548	-.040	-.058	.817	.850	-.045	-.042	1.148	1.142	-.049	-.046	1.890	1.290	-.053	-.052	1.410	1.411	1.411	
5.0	-1.045	-.048	1.546	1.451	-.038	-.041	.826	.838	-.039	-.044	1.150	1.154	-.044	-.048	1.294	1.299	-.048	-.054	1.413	1.418	1.418	
5.5	-1.034	-.035	1.540	1.540	-.034	-.031	.744	.744	-.037	-.053	1.169	1.169	-.048	-.037	1.305	1.305	-.046	-.042	1.422	1.422	1.422	
6.0	-1.034	-.027	1.584	1.584	-.031	-.031	.681	.681	-.034	-.035	1.185	1.185	-.039	-.037	1.319	1.319	-.041	-.043	1.432	1.432	1.432	
6.5	-1.035	-.029	1.559	1.559	-.033	-.038	.402	.402	-.034	-.041	.822	.822	-.039	-.045	1.341	1.341	-.041	-.049	1.444	1.444	1.444	
7.0	-1.040	-.029	1.571	1.571	-.034	-.045	.863	.863	-.036	-.046	1.294	1.294	-.059	-.061	1.390	1.390	-.040	-.054	1.475	1.475	1.475	
7.5	-1.033	-.035	1.581	1.581	-.008	-.058	.700	.700	-.010	-.04	.850	.813	-.087	1.429	1.429	-.140	-.061	1.500	1.500	1.500		
8.0	-1.011	-.031	1.590	1.590	-.003	-.053	.865	.865	-.004	-.054	1.593	1.593	-.005	-.066	1.480	1.480	-.008	-.058	1.581	1.581	1.581	
8.5	-1.011	-.024	1.503	1.503	-.008	-.041	1.037	1.037	-.004	-.044	1.458	1.458	-.005	-.045	1.501	1.501	-.007	-.048	1.548	1.548	1.548	
9.0	-1.008	-.024	1.515	1.515	-.001	-.043	1.155	1.155	-.003	-.046	1.508	1.508	-.004	-.047	1.556	1.556	-.004	-.048	1.574	1.574	1.574	
9.5	-1.013	-.017	1.525	1.525	-.006	-.036	1.856	1.856	-.009	-.038	1.647	1.647	-.010	-.038	1.584	1.584	-.011	-.039	1.603	1.603	1.603	
10.0	-1.018	-.016	1.550	1.550	-.007	-.038	1.312	1.312	-.008	-.033	1.578	1.578	-.008	-.034	1.584	1.584	-.008	-.034	1.603	1.603	1.603	
10.5	-1.004	-.037	1.637	1.637	-.031	-.061	1.353	1.353	-.032	-.058	1.622	1.622	-.018	-.061	1.620	1.620	-.018	-.063	1.625	1.625	1.625	
11.0	-1.019	-.028			-.014	-.061			-.015	-.062			-.015	-.061			-.015	-.053				

TABLE III - EXTERNAL AND INTERNAL PRESSURE COEFFICIENTS OF NACA 8-INCH RAM-JET CONFIGURATION
FOR FOUR ANGLES OF ATTACK - Continued
(b) Concluded. - Free-stream Mach number of 1.79.



Station	$\alpha = 6^\circ; m_3/m_0 = 0.410$				$\alpha = 10^\circ; m_3/m_0 = 0.867$				$\alpha = 10^\circ; m_3/m_0 = 0.793$				$\alpha = 10^\circ; m_3/m_0 = 0.631$				$\alpha = 10^\circ; m_3/m_0 = 0.583$				
	Longitudinal distribution of C_p								Circumferential distribution of C_p								Outer shell, external				
	Outer shell		Center body	Outer shell		Center body	Outer shell		Center body	Outer shell		Center body	Outer shell		Center body	Outer shell		Center body	Outer shell		
	External	Internal		External	Internal		External	Internal		External	Internal		External	Internal		External	Internal		External	Internal	
$\theta \rightarrow$	180°	270°	0°	0°	180°	270°	0°	0°	0°	180°	270°	0°	0°	0°	0°	180°	270°	0°	180°	270°	0°
-1.5				1.275			0.723			0.723			0.774			0.774			1.257		
-1.0				1.332			.817			.815			1.017			1.017			1.302		
-0.5				1.375			.801			.800			1.144			1.144			1.356		
0				1.420			.798			1.004			1.155			1.155			1.366		
0.5	-0.351	-0.231	1.530	1.466	-0.140	0.296	0.446	.847	-0.180	0.178	0.805	.923	-0.246	0.029	1.091	1.116	-0.249	-0.183	1.437	1.398	
1.0	-0.288	-0.125	1.599	1.502	-0.120	.194	.523	.557	-0.154	.180	.986	.994	-0.236	.067	1.164	1.181	-0.320	-0.087	1.458	1.429	
1.5	-0.237	-0.066	1.555	1.520	-0.126	.142	.476	.257	-0.155	.125	1.087	.978	-0.229	.070	1.212	1.161	-0.298	-0.048	1.473	1.453	
2.0	-0.204	-0.064	1.541	1.525	-0.132	.098	.904	.603	-0.149	.080	1.106	1.012	-0.219	.068	1.246	1.181	-0.270	-0.032	1.487	1.465	
2.5	-0.189	-0.064	1.548	1.535	-0.137	.065	.991	.908	-0.148	.051	1.142	1.080	-0.214	.055	1.272	1.229	-0.287	-0.028	1.497	1.488	
3.0	-0.172	-0.048	1.548	1.541	-0.157	.043	1.007	.976	-0.142	.032	1.151	1.112	-0.208	.017	1.274	1.252	-0.240	-0.022	1.499	1.498	
4.0	-0.167	-0.070	1.563	1.550	-0.147	.015	1.018	.988	-0.161	.083	1.171	1.149	-0.199	.004	1.291	1.279	-0.224	-0.058	1.509	1.507	
5.0	-0.161	-0.073	1.566	1.555	-0.123	.037	.988	.985	-0.132	.043	1.170	1.166	-0.174	-.051	1.287	1.281	-0.194	-0.059	1.509	1.515	
6.0	-0.127	-0.073	1.555	1.555	-0.078	.061	.984	.989	-0.095	.066	1.170	1.164	-0.128	-.065	1.292	1.286	-0.151	-0.078	1.511	1.514	
7.0	-0.045	-0.065	1.560	1.560	-0.084	.062	.986	.996	-0.073	.068	1.194	1.192	-0.093	-.065	1.295	1.295	-0.112	-0.077	1.519	1.521	
8.0	-0.070	-0.067	1.565	1.565	-0.063	.061	1.060	1.061	-0.069	.065	1.227	1.233	-0.078	-.068	1.303	1.305	-0.090	-0.080	1.523	1.527	
9.0	-0.060	-0.067	1.569	1.571	-0.066	.068	1.093	1.099	-0.060	.070	1.252	1.257	-0.067	-.078	1.294	1.301	-0.073	-0.091	1.524	1.528	
10.0	-0.053	-0.065	1.574	1.574	-0.048	.068	1.122	1.122	-0.063	.073	1.270	1.270	-0.058	-.080	1.294	1.294	-0.063	-0.099	1.530	1.530	
11.0	-0.048	-0.057	1.577	1.577	-0.041	.079	1.151	1.151	-0.047	.082	1.291	1.291	-0.050	-.088	1.309	1.309	-0.053	-0.099	1.533	1.540	
12.0	-0.047	-0.062	1.581	1.581	-0.058	.090	1.187	1.187	-0.042	.093	1.317	1.317	-0.045	-.099	1.330	1.330	-0.047	-0.110	1.540	1.540	
14.0	-0.044	-0.065	1.589	1.589	-0.011	.102	1.252	1.252	-0.018	.106	1.366	1.366	-0.018	-.111	1.380	1.380	-0.020	-0.191	1.553	1.553	
16.0	-0.018	-0.070	1.597	1.597	-0.004	.118	1.305	1.305	-0.007	.120	1.406	1.406	-0.009	-.126	1.420	1.420	-0.013	-0.155	1.564	1.574	
18.0	-0.012	-0.067	1.604	1.604	-0.001	.150	1.344	1.344	-0.002	.152	1.435	1.435	-0.005	-.138	1.450	1.450	-0.007	-0.145	1.574	1.589	
21.0	-0.010	-0.055	1.613	1.613	-0.001	.128	1.397	1.397	-0.002	.125	1.474	1.474	-0.004	-.156	1.494	1.494	-0.007	-0.143	1.603	1.614	
24.0	-0.009	-0.063	1.621	1.621	-0.005	.113	1.447	1.447	-0.003	.115	1.506	1.506	-0.001	-.183	1.532	1.532	-0.003	-0.128	1.620	1.620	
27.0	-0.015	-0.043	1.629	1.629	0	.107	1.486	1.486	-0.002	.108	1.533	1.533	-0.007	-.113	1.559	1.559	-0.008	-0.113	1.624	1.624	
31.0	-0.012	-0.038	1.633	1.633	.002	.094	1.519	1.519	-0.002	.086	1.555	1.555	-0.003	-.088	1.578	1.578	-0.007	-0.087	1.620	1.620	
35.0	-0.035	-0.062			-0.060	.108			-0.032	.108			-0.034	-.111			-0.036	-.091			1.625
37.0			1.638	1.638	-0.010	.103			-0.012	.103			-0.014	-.106			-0.015	-.104			
40.0	-0.019	-0.054			-0.014	.101			-0.015	.101			-0.017	-.103			-0.024	-.108			
45.0	-0.018	-0.064																			



TABLE III - EXTERNAL AND INTERNAL PRESSURE COEFFICIENTS OF NACA 8-INCH RAM-JET CONFIGURATION
FOR FOUR ANGLES OF ATTACK - Continued
(e) Free-stream Mach number of 1.79 with model rotated 180°.

Station	$\alpha = 0^\circ; m_3/m_0 = 0.915$			$\alpha = 0^\circ; m_3/m_0 = 0.870$			$\alpha = 0^\circ; m_3/m_0 = 0.800$			$\alpha = 0^\circ; m_3/m_0 = 0.651$			$\alpha = 0^\circ; m_3/m_0 = 0.401$							
	Longitudinal distribution of C_p .																			
	Outer shell		Center body	Outer shell		Center body	Outer shell		Center body	Outer shell		Center body	Outer shell		Center body					
	External	Internal		External	Internal		External	Internal		External	Internal		External	Internal						
$\theta \rightarrow$	0°	90°	180°	180°	0°	90°	180°	180°	0°	90°	180°	0°	90°	180°	180°					
-1.0																				
-1.5																				
-1.0																				
-0.5																				
0																				
0.5																				
1.0																				
1.5																				
2.0																				
2.5																				
3.0																				
4.0																				
5.0																				
6.0																				
7.0																				
8.0																				
9.0																				
10.0																				
11.0																				
12.0																				
13.0																				
14.0																				
15.0																				
16.0																				
17.0																				
18.0																				
19.0																				
20.0																				
21.0																				
22.0																				
23.0																				
24.0																				
25.0																				
26.0																				
27.0																				
28.0																				
29.0																				
30.0																				
31.0																				
32.0																				
33.0																				
34.0																				
35.0																				
36.0																				
37.0																				
38.0																				
39.0																				
40.0																				
41.0																				
42.0																				
43.0																				
	Circumferential distribution of C_p .																			
Station	Outer shell, external				Outer shell, external				Outer shell, external				Outer shell, external							
	180°	360°	540°	720°	180°	360°	540°	720°	180°	360°	540°	720°	180°	360°	540°	720°				
0	0.275	0.283	0.286	0.278	0.218	0.224	0.226	0.221	0.127	0.129	0.129	0.122	-0.026	-0.025	-0.021	-0.024	-0.049	-0.243	-0.240	-0.241
0.5	-0.003	-0.005	-0.006	-0.005	-0.006	-0.006	-0.009	-0.008	-0.008	-0.010	-0.010	-0.010	-0.014	-0.015	-0.018	-0.006	-0.028	-0.022	-0.024	-0.023
1.0	-0.011	-0.009	-0.012	-0.012	-0.010	-0.012	-0.013	-0.010	-0.010	-0.011	-0.011	-0.010	-0.010	-0.010	-0.012	-0.013	-0.013	-0.013	-0.013	-0.015

TABLE III - EXTERNAL AND INTERNAL PRESSURE COEFFICIENTS OF MACA 8-INCH RAM-JET CONFIGURATION
FOR FOUR ANGLES OF ATTACK - Continued

(c) Continued. - Free-stream Mach number of 1.79 with model rotated 180°.



Station	$\alpha = 3^\circ; m_3/m_0 = 0.914$				$\alpha = 3^\circ; m_3/m_0 = 0.869$				$\alpha = 3^\circ; m_3/m_0 = 0.793$				$\alpha = 3^\circ; m_3/m_0 = 0.527$				$\alpha = 3^\circ; m_3/m_0 = 0.384$						
	Longitudinal distribution of C_p								Circumferential distribution of C_p								Outer shell, external						
	Outer shell		Center body	Outer shell		Center body	Outer shell		Center body	Outer shell		Center body	Outer shell		Center body	Outer shell		Center body	Outer shell		Center body		
	External	Internal		External	Internal		External	Internal		External	Internal		External	Internal		External	Internal		External	Internal			
0 →	0°	90°	180°	0°	90°	180°	0°	90°	180°	0°	90°	180°	0°	90°	180°	0°	90°	180°	0°	90°	180°		
-1.5				0.421			0.422			0.417			0.392			0.382			1.262			1.283	
-1.0				.466			.467			.464			1.024			1.024			1.526			1.516	
-0.5				.455			.456			1.242			1.593			1.593			1.593			1.469	
0				.849			1.091																
0.5	0.405			1.163	1.108	0.360	1.279	1.193	0.275	1.369	1.266	0.006	1.556	1.450	-0.121	1.625			1.521			1.521	
1.0	.276	0.196		1.116	1.068	0.266	1.241	1.175	.232	1.344	1.275	.073	-0.010	1.536	1.487	-0.118	-0.114	1.608			1.570		
1.5	.202	.141		1.086	1.022	.189	.125	1.225	1.158	.170	.097	1.332	1.275	.072	-0.011	1.531	1.500	.010	-0.071	1.505		1.585	
2.0	.185	.104		1.073	.977	.154	.092	1.216	1.134	.135	.072	1.327	1.262	.068	-0.006	1.526	1.497	.028	-0.064	1.600		1.582	
2.5	.107	.076		1.080	1.002	.098	.065	1.217	1.153	.064	.050	1.325	1.278	.056	-0.010	1.528	1.506	.003	-0.045	1.600		1.587	
3.0	.117	.060		1.051	1.004	.108	.052	1.198	1.155	.065	.058	1.312	1.281	.051	-0.010	1.523	1.509	.024	-0.059	1.597		1.590	
4.0	.064	.007		1.024	.979	.048	-.002	1.179	1.145	.057	-.011	1.300	1.275	.007	-0.041	1.506	1.508	.010	-0.059	1.594		1.588	
5.0	.039	-.010		.947	.942	.086	-.016	1.141	1.156	.016	-.023	1.276	1.274	-.007	-0.047	1.511	1.511	-.021	-0.069	1.590		1.588	
6.0	.022	-.015		.789	.797	.019	-.080	1.106	1.102	.011	-.036	1.254	1.254	-.009	-0.045	1.504	1.508	-.019	-0.066	1.588		1.585	
7.0		-.010		.683	.676			1.104	1.105			1.251	1.253			1.501	1.505			1.583		1.583	
8.0	.018	-.015		.881	.885	.015	-.020	1.126	1.126	.009	-.024	1.256	1.259	-.006	-0.039	1.508	1.504	-.014	-0.046	1.583		1.588	
9.0	.038	-.010		.872	.881	.059	-.015	1.093	1.108	.034	-.019	1.256	1.245	.056	-0.032	1.494	1.500	.081	-0.059	1.580		1.580	
10.0		-.010			.790			.014		.075		.016		1.231		.028		1.496		.035		1.576	
11.0	.082	-.010			.608	.019	.015		1.100	.014	-.018	1.244		.002	-.029	1.499		-.003	-.034		1.574		
12.0	.020	-.008			.441	.018	.011		1.157	.012	-.015	1.276		.025		1.509		-.003	-.029		1.579		
14.0	.017	-.005			.754	.014	-.007		1.881	.008	-.011	1.346		.001	-.019	1.534		-.003	-.028		1.583		
16.0	.012	-.005			1.006	.010	-.008		1.352	.006	-.011	1.403		-.008	-.019	1.556		-.006	-.022		1.606		
18.0	.016	-.003			1.129	.014	-.007		1.397	.011	-.009	1.447		.004	-.016	1.578		.001	-.019		1.615		
21.0	.016	-.005			1.264	.015	-.008		1.476	.012	-.009	1.611		.006	-.015	1.602		-.003	-.017		1.630		
24.0	.060	-.005			1.366	.019	-.004		1.541	.016	-.006	1.550		.011	-.010	1.685		-.003	-.018		1.643		
27.0	.013	-.001			1.429	.015	-.003		1.584	.009	-.004	1.596		.006	-.009	1.645		-.004	-.010		1.688		
31.0	.014	-.008			1.476	.012	-.009		1.615	.010	-.003	1.617		.008	-.004	1.649		-.005	-.003		1.655		
35.0	-.010	-.002				-.014	-.007		1.650	-.014	-.009		1.648		-.015	-.010		1.662		-.016	-.011		1.682
37.0					1.510																		
40.0	-.003	-.011				-.004	-.017			-.004	-.019			-.007	-.019			-.009	-.020				
45.0	-.006	-.006				-.009	-.015			-.009	-.016			-.011	-.016			-.012	-.017				

TABLE III - EXTERNAL AND INTERNAL PRESSURE COEFFICIENTS OF NACA 8-INCH RAM-JET CONFIGURATION
FOR FOUR ANGLES OF ATTACK - Continued

(c) Continued. - Free-stream Mach number of 1.79 with model rotated 180°.



Station	$\alpha = 6^\circ; m_3/m_0 = 0.911$			$\alpha = 6^\circ; m_3/m_0 = 0.869$			$\alpha = 6^\circ; m_3/m_0 = 0.785$			$\alpha = 6^\circ; m_3/m_0 = 0.554$			$\alpha = 6^\circ; m_3/m_0 = 0.386$		
	Longitudinal distribution of C_p														
	Outer shell		Center body												
	External	Internal		External	Internal		External	Internal		External	Internal		External	Internal	
0 →	0°	90°	180°	180°	0°	90°	180°	180°	0°	90°	180°	180°	0°	90°	180°
-1.5			0.351			0.351			0.352			0.353			0.353
-1.0			.394			.393			.712			.904			1.211
-0.5			.388			.850			1.143			1.142			1.521
0			.870			.934			1.400			1.400			1.483
0.5	0.526	0.801	1.237	1.074	0.502	1.363	1.802	0.427	1.449	1.351	0.158	1.484	-0.007	1.648	1.551
1.0	.569	0.801	1.178	1.158	.542	1.307	1.280	.521	1.410	1.350	.199	-0.027	1.555	1.503	1.589
1.5	.581	.139	1.143	1.066	.282	.126	1.287	.247	.061	1.390	.176	-.003	1.645	1.515	1.596
2.0	.239	.108	1.119	1.037	.100	.092	1.268	.202	.213	1.377	.157	.001	1.559	1.509	1.597
2.5	.172	.072	1.114	1.040	.170	.063	1.260	.202	.158	1.369	.112	-.002	1.555	.080	1.616
3.0	.180	.069	1.074	1.033	.175	.060	1.250	.196	.163	1.352	.124	-.003	1.558	.097	1.610
4.0	.108	.001	1.037	.968	.101	-.004	1.204	.170	.064	1.332	.100	-.011	1.520	.049	1.598
5.0	.075	-.015	.954	.949	.071	-.021	1.187	.182	.065	1.302	.129	-.049	1.500	.030	1.597
6.0	.065	-.024	.791	.808	.062	-.028	1.110	.110	.067	1.272	.127	-.053	1.495	.027	1.592
7.0	-.028	.682	.674	.626	-.026	.098	1.103	.038	.125	1.258	.129	-.047	1.486	-.056	1.587
8.0	.058	-.031	.861	.885	.051	-.053	1.108	.046	.058	1.253	.031	-.063	1.481	.021	1.583
9.0	.068	-.032	.877	.865	.071	-.053	1.042	.064	.070	1.206	.013	-.061	1.463	.063	1.573
10.0	-.032		.794	.794	-.053		.980		.058	1.177		-.061	1.458	-.056	1.563
11.0	.053	-.036	.610	.610	-.051	-.038	1.009	.048	.041	1.180	.036	-.061	1.457	-.068	1.583
12.0	.048	-.036	.442	.446	-.046	-.056	1.088	.044	.041	1.230	.051	-.061	1.471	.038	1.568
14.0	.043	-.034	.684	.686	-.059	-.056	1.216	.036	.041	1.315	.088	-.049	1.503	.023	1.588
16.0	.035	-.037	.991	.955	-.055	-.059	1.305	.051	.048	1.382	.026	-.061	1.553	.091	1.599
18.0	.036	-.037	1.121	.985	-.059	-.059	1.372	.052	.041	1.434	.024	-.047	1.556	.081	1.612
21.0	.038	-.037	1.259	.931	-.058	-.058	1.460	.050	.041	1.506	.023	-.045	1.592	.019	1.631
24.0	.034	-.032	1.358	.932	-.053	-.053	1.539	.052	.034	1.582	.026	-.037	1.621	.023	1.645
27.0	.027	-.031	1.422	.925	-.051	-.051	1.570	.056	.038	1.594	.021	-.054	1.558	.018	1.656
31.0	.026	-.016	1.468	.926	-.017	-.017	1.500	.083	-.017	1.613	.080	-.080	1.644	.018	1.656
35.0	-.003	-.029			-.003	-.032		-.005	-.032		-.005	-.031		-.007	-.031
37.0							1.637			1.642			1.658		
40.0	.006	-.042			.006	-.042		.006	-.044		.006	-.045		.003	-.042
45.0	0	-.040			.001	-.039		0	-.038		-.002	-.040		-.003	-.038

Station	Circumferential distribution of C_p											
	Outer shell, external			Outer shell, external			Outer shell, external			Outer shell, external		
0 →	180°	360°	540°	720°	180°	360°	540°	720°	180°	360°	540°	720°
0.5	0.516	0.497	0.448	0.373	0.485	0.466	0.420	0.319	0.416	0.378	0.306	0.210
14.0	.036	.021	-.018	-.014	.034	.019	-.008	-.015	.032	.016	-.009	-.017
43.0	0	-.014	-.028	-.048	.001	-.013	-.028	-.043	0	-.014	-.029	-.044

TABLE III - EXTERNAL AND INTERNAL PRESSURE COEFFICIENTS OF NACA 8-INCH RAM-JET CONFIGURATION
FOR FOUR ANGLES OF ATTACK - Continued

(c) Concluded. - Free-stream Mach number of 1.79 with model rotated 180°.



CONFIDENTIAL

NACA RM E50J26

Station	$\alpha = 10^\circ; m_2/m_0 = 0.867$			$\alpha = 10^\circ; m_2/m_0 = 0.782$			$\alpha = 10^\circ; m_2/m_0 = 0.644$			$\alpha = 10^\circ; m_2/m_0 = 0.510$			$\alpha = 10^\circ; m_2/m_0 = 0.371$							
	Longitudinal distribution of C_p									Circumferential distribution of C_p										
	Outer shell		Center body	Outer shell		Center body	Outer shell		Center body	Outer shell		Center body	Outer shell		Center body	Outer shell		Center body		
	External	Internal		External	Internal		External	Internal		External	Internal		External	Internal		External	Internal			
0+	0°	90°	180°	180°	0°	90°	180°	180°	0°	90°	180°	180°	0°	90°	180°	180°	0°	90°	180°	
-1.6				0.266			0.450			0.843			0.915						1.069	
-1.0				.314			.787			.910			1.042						1.285	
-0.5				.616			.916			.980			1.193						1.588	
0				.747			.928			1.067			1.315						1.481	
0.5	0.670	0.215	1.226	.865	0.645	1.877	1.059	0.677	1.424	1.169	0.442	1.488	1.409	0.203	1.662	1.557				
1.0	0.484	0.215	1.156	1.128	0.476	0.184	1.265	1.104	.444	1.456	1.286	.359	-0.009	1.490	1.474	.264	-0.101	1.654	1.569	
1.5	0.383	0.151	1.121	1.157	.379	.156	1.364	1.310	.368	.090	1.371	1.368	.380	.022	1.504	1.507	.260	-.055	1.632	1.612
2.0	0.333	0.112	1.091	1.058	.331	.096	1.551	1.542	.307	.075	1.396	1.404	.276	.039	1.614	1.516	.235	-.039	1.634	1.610
2.5	0.286	0.082	1.081	1.018	.254	.044	1.559	1.548	.237	.049	1.409	1.414	.216	.080	1.520	1.516	.184	-.021	1.619	1.606
3.0	0.263	0.060	1.037	.998	.264	.045	1.555	1.544	.246	.051	1.408	1.416	.223	.012	1.519	1.517	.195	-.020	1.611	1.606
4.0	0.178	-.003	1.007	.952	.182	-.018	1.510	1.297	.170	-.023	1.409	1.407	.185	-.036	1.517	1.514	.134	-.064	1.502	1.506
5.0	.142	-.006	.928	.928	.144	-.034	1.264	1.266	.133	-.048	1.396	1.400	.120	-.065	1.509	1.511	.105	-.067	1.590	1.590
6.0	.128	-.009	.772	.783	.128	-.046	1.221	1.226	.120	-.052	1.384	1.389	.109	-.063	1.499	1.504	.096	-.074	1.578	1.578
7.0	-.064	-.004	.658	.658	.061	-.061	1.197	1.202	.056	-.056	1.396	1.389	.084	-.054	1.500	1.503	.074	-.074	1.568	1.568
8.0	.108	-.066	.829	.840	.108	-.061	1.181	1.179	.108	-.067	1.393	1.395	.092	-.075	1.503	1.504	.082	-.085	1.569	1.566
9.0	.116	-.063	.865	.975	.128	-.069	1.096	1.107	.180	-.073	1.389	1.397	.114	-.061	1.499	1.504	.107	-.089	1.539	1.540
10.0	-.069	-.077	.599	.784	-.074	1.084	1.079	1.089	-.079	1.400	1.400	.085	1.506	1.506	-.093	1.529	1.527			
11.0	.104	-.077	.599	.103	-.061	1.089	1.089	-.099	-.086	1.410	1.410	.092	-.092	1.509	1.509	.085	-.096	1.537	1.537	
12.0	.099	-.083	.432	.100	-.068	1.110	1.110	-.094	-.091	1.426	1.426	.068	-.097	1.519	1.519	.080	-.103	1.537	1.537	
14.0	.091	-.093	.476	.090	-.066	1.288	1.288	-.096	1.021	1.458	1.458	.080	-.106	1.538	1.538	.074	-.110	1.559	1.559	
15.0	.055	-.105	.954	.951	-.105	1.315	1.315	-.079	1.111	1.455	1.455	.074	-.115	1.544	1.544	.097	-.120	1.578	1.578	
18.0	.076	-.112	1.091	.076	-.115	1.388	1.388	-.073	1.119	1.510	1.510	.088	-.184	1.571	1.571	.085	-.127	1.594	1.594	
21.0	.073	-.120	1.286	.072	-.124	1.470	1.470	-.069	1.129	1.544	1.544	.065	-.135	1.563	1.563	.062	-.137	1.618	1.618	
24.0	.073	-.110	1.384	.072	-.113	1.555	1.555	-.069	1.120	1.576	1.576	.066	-.124	1.615	1.615	.063	-.127	1.626	1.626	
27.0	.063	-.098	1.385	.065	-.100	1.573	1.573	-.060	1.103	1.598	1.598	.067	-.105	1.629	1.629	.066	-.105	1.648	1.648	
31.0	.057	-.070	1.496	.055	-.070	1.593	1.593	-.054	-.072	1.615	1.615	.063	-.075	1.639	1.639	.060	-.072	1.649	1.649	
35.0	.024	-.082		.023	-.088			.023	-.091			.080	-.094					.030	-.083	
37.0			1.467				1.626			1.630			1.648						1.655	
40.0	.098	-.099		.086	-.098			.025	-.099			.025	-.101			.083	-.100			
45.0	.023	-.095		.081	-.094			.020	-.094			.080	-.094			.030	-.093			



TABLE III - EXTERNAL AND INTERNAL PRESSURE COEFFICIENTS OF NACA 8-INCH RAM-JET CONFIGURATION
FOR FOUR ANGLES OF ATTACK - Continued
(d) Free-stream Mach number of 1.99.

Station	$\alpha = 0^\circ; m_3/m_0 = 1.00$				$\alpha = 0^\circ; m_3/m_0 = 0.965$				$\alpha = 0^\circ; m_3/m_0 = 0.885$				$\alpha = 0^\circ; m_3/m_0 = 0.773$				$\alpha = 0^\circ; m_3/m_0 = 0.559$							
	Longitudinal distribution of C_p .																							
	Outer shell		Center body	Outer shell		Center body	Outer shell		Center body	Outer shell		Center body	Outer shell		Center body	Outer shell		Center body	Outer shell		Center body			
	External	Internal		External	Internal		External	Internal		External	Internal		External	Internal		External	Internal		External	Internal				
0 →	180°	270°	0°	0°	180°	270°	0°	0°	180°	270°	0°	0°	180°	180°	0°	0°	180°	180°	0°	0°	0°	0°		
-1.5				0.448			0.444			0.444			0.444			0.444								
-1.0				.486			.480			.482			.492			.492								
-.5				.485			.480			.511			.498			.498								
0				.461			.533			1.175			1.175			1.175								
.5	0.293	0.281	0.577	.553	0.269	0.255	1.146	1.206	0.206	0.190	1.327	1.296	0.107	0.068	1.445	1.345	0.020	-0.006	1.591	1.499				
1.0	.186	.189	.508	.599	.178	.173	1.156	1.146	.148	.145	1.385	1.287	.102	.048	1.441	1.376	0.007	.012	1.591	1.555				
1.5	.153	.152	.553	.457	.181	.119	1.156	1.124	.104	.103	1.327	1.264	.078	.078	1.443	1.394	.006	.003	1.591	1.554				
2.0	.069	.078	.551	.550	.094	.088	1.163	1.099	.079	.074	1.350	1.247	.061	.057	1.445	1.383	.003	.006	1.593	1.558				
2.5	.073	.073	.668	.488	.068	.068	1.180	1.144	.056	.051	1.337	1.288	.045	.038	1.450	1.411	.006	.001	1.593	1.568				
3.0	.065	.064	.589	.458	.063	.044	1.175	1.159	.043	.035	1.330	1.293	.035	.020	1.446	1.420	.006	-.009	1.586	1.575				
4.0	.014	.011	.500	.511	.009	.003	1.170	1.173	0	-.003	1.387	1.306	-.006	-.011	1.445	1.433	-.004	-.031	1.587	1.583				
5.0	-.002	-.006	.543	.615	-.006	-.009	1.154	1.168	-.013	-.014	1.312	1.310	-.018	-.081	1.438	1.438	-.034	-.036	1.587	1.588				
6.0	0	-.008	.620	.538	-.010	-.004	1.134	1.141	-.016	-.013	1.298	1.294	-.019	-.020	1.451	1.450	-.038	-.033	1.587	1.587				
7.0	0	-.001	.633	.575	-.006	-.007	1.150	1.159	-.010	-.013	1.308	1.306	-.014	-.018	1.436	1.438	-.026	-.030	1.592	1.593				
8.0	-.004	-.005	.606	.489	-.010	-.009	1.186	1.201	-.015	-.014	1.397	1.350	-.019	-.080	1.460	1.458	-.039	-.050	1.600	1.600				
9.0	-.003	-.008	.633	.478	-.008	-.012	1.198	1.199	-.013	-.017	1.325	1.332	-.017	-.081	1.458	1.457	-.086	-.030	1.608	1.604				
10.0	0	-.008	.633	.764	-.005	-.004	1.185	1.185	-.010	-.006	1.350	1.350	-.015	-.013	1.460	1.460	-.028	-.021	1.607	1.612				
11.0	.005	-.001	.670	.670	-.001	-.004	1.218	1.218	-.008	-.008	1.348	1.348	-.010	-.013	1.470	1.470	-.019	-.081	1.612	1.612				
12.0	.003	0	.901	0	-.004		1.269	1.269	-.003	-.006	1.378	1.378	-.009	-.011	1.490	1.490	-.017	-.019	1.622	1.622				
13.0	.005	-.001	1.163	.003	0		1.361	1.361	0	-.004	1.444	1.444	-.005	-.006	1.530	1.530	-.018	-.013	1.630	1.630				
14.0	.005	.001	1.283	.003	-.008		1.431	1.431	0	-.004	1.494	1.494	-.004	-.006	1.564	1.564	-.011	-.013	1.657	1.657				
15.0	.008	.008	1.374	.007	.001		1.487	.008	-.002	1.537	1.537	0.001	-.006	1.593	1.593	-.004	-.011	1.672	1.672					
16.0	.013	.005	1.493	.011	.003		1.586	.006	-.003	1.598	1.598	0.006	-.001	1.636	1.636	0.001	-.006	1.696	1.696					
17.0	.019	.016	1.595	.016	.013		1.630	.013	.011	1.652	1.652	.011	-.009	1.676	1.676	-.006	-.003	1.716	1.716					
18.0	-.009	.003	1.651	-.010	.001		1.678	-.011	0	1.692	1.692	.014	-.008	1.708	1.708	-.018	-.006	1.730	1.730					
19.0	-.005	-.006	1.696	-.001	-.008		1.707	.001	-.008	1.714	1.714	-.001	-.008	1.773	1.773	-.004	-.008	1.738	1.738					
20.0	-.030	-.016	1.751	-.031	-.020		1.748	-.023	-.020	1.748	1.748	-.023	-.023	1.744	1.744	-.024	-.035	1.748	1.748					
21.0	-.013	-.013	1.751	-.014	-.013		1.748	-.014	-.015	1.748	1.748	-.011	-.013	1.744	1.744	-.017	-.015	1.748	1.748					
22.0	-.008	-.011	1.751	-.009	-.012		1.748	-.009	-.013	1.748	1.748	-.011	-.013	1.744	1.744	-.018	-.014	1.748	1.748					

Station	Outer shell, external																				
	198°	216°	234°	252°	198°	216°	234°	252°	198°	216°	234°	252°	198°	216°	234°	252°	198°	216°	234°	252°	
0 →	0.269	0.273	0.271	0.262	0.206	0.206	0.204	0.198	0.103	0.100	0.099	0.093	0.020	0.019	0.017	0.016	0.014	0.013	0.012	0.011	
14.0	0.003	0.001	0	0.005	-.003	-.001	-.002	-.003	-.011	-.005	-.008	-.009	-.006	-.007	-.004	-.014	-.017	-.007	-.013	-.013	-.013
43.0	-.011	-.009	-.011	-.013	-.012	-.011	-.012	-.013	-.013	-.011	-.013	-.014	-.013	-.013	-.013	-.016	-.016	-.013	-.016	-.016	-.016



TABLE III - EXTERNAL AND INTERNAL PRESSURE COEFFICIENTS OF NACA 6-INCH RAM-JET CONFIGURATION
FOR FOUR ANGLES OF ATTACK - Continued
(d) Continued. - Free-stream Mach number of 1.09.

Station	$\alpha = 0^\circ; m_3/m_0 = 0.576$			$\alpha = 0^\circ; m_3/m_0 = 0.992$			$\alpha = 3^\circ; m_3/m_0 = 0.999$			$\alpha = 3^\circ; m_3/m_0 = 0.954$			$\alpha = 3^\circ; m_3/m_0 = 0.861$			
	Longitudinal distribution of C_p						Circumferential distribution of C_p									
	Outer shell		Center body	Outer shell		Center body	Outer shell		Center body	Outer shell		Center body	Outer shell		Center body	
	External	Internal		External	Internal		External	Internal		External	Internal		External	Internal		
$\theta \rightarrow$	180°	270°	0°	0°	180°	270°	0°	0°	0°	180°	270°	0°	0°	180°	270°	0°
-1.5			1.208				0.440			0.521			0.520			0.521
-1.0			1.421				.479			.561			.561			.563
-0.5			1.467				.478			.559			.559			.561
0			1.530				.631			.548			.561			1.230
.5	-0.238	-0.233	1.660	1.590	0.251	0.236	1.234	1.269	0.208	0.282	0.637	0.400	0.158	0.263	1.094	1.214
1.0	-.108	-.113	1.550	1.684	.164	.165	1.238	1.195	.142	.157	.565	.286	.094	.178	1.137	1.097
1.5	-.060	-.065	1.648	1.638	.117	.113	1.240	1.188	.071	.151	.487	.411	.058	.118	1.161	1.108
2.0	-.036	-.044	1.651	1.636	.100	.083	1.244	1.165	.046	.098	.575	.254	.032	.088	1.175	1.001
2.5	-.032	-.038	1.652	1.647	.063	.059	1.254	1.204	.025	.070	.441	.364	.012	.062	1.195	1.148
3.0	-.084	-.059	1.653	1.646	.048	.045	1.246	1.215	.013	.061	.300	.444	.001	.046	1.800	1.173
4.0	-.040	-.048	1.655	1.653	-.001	.008	1.244	1.232	-.035	.009	.487	.277	-.034	.007	1.214	1.197
5.0	-.047	-.049	1.656	1.657	-.011	-.011	1.289	1.232	-.036	-.008	.355	.493	-.045	-.006	1.202	1.201
6.0	-.042	-.042	1.657	1.657	-.015	-.010	1.211	1.210	-.037	-.018	.568	.507	-.045	-.010	1.190	1.185
7.0	-.033	-.037	1.658	1.680	-.008	-.008	1.281	1.235	-.030	-.010	.693	.780	-.037	-.011	1.207	1.205
8.0	-.037	-.037	1.662	1.662	-.012	-.011	1.261	1.267	-.028	-.014	.704	.704	-.035	-.013	1.245	1.247
9.0	-.038	-.036	1.664	1.685	-.011	-.013	1.244	1.256	-.026	-.016	.863	.864	-.032	-.017	1.252	1.257
10.0	-.028	-.027		1.666	-.006	-.005		1.249	-.021	-.010		.882	-.026	-.010	1.261	-.027
11.0	-.024	-.025		1.668	-.001	-.006		1.271	-.018	-.010		.979	-.018	-.011	1.286	-.020
12.0	-.022	-.023		1.672	-.001	-.003		1.313	-.007	-.011		1.079	-.010	-.012	1.324	-.017
14.0	-.017	-.018		1.681	.002	-.001		1.389	-.003	-.012		1.223	-.006	-.011	1.392	-.011
16.0	-.014	-.016		1.687	-.008	-.005		1.452	-.001	-.003		1.385	-.008	-.008	1.446	-.008
18.0	-.008	-.014		1.695	-.006	0		1.505	-.008	-.003		1.405	-.004	-.006	1.471	0
21.0	-.001	-.008		1.704	.010	.003		1.573	.081	-.003		1.507	.019	-.005	1.556	.018
24.0	-.002	-.002		1.713	.015	.013		1.653	.008	.008		1.594	.004	.007	1.613	.003
27.0	-.080	-.008		1.720	-.011	0		1.576	-.013	-.006		1.655	-.015	-.006	1.681	-.017
31.0	-.005	-.018		1.723	-.008			1.706	.002	-.016		1.700	0	-.015	1.692	-.001
35.0	-.027	-.027			-.022	-.020		1.743	-.022	-.026		1.738	-.012	-.027		-.024
37.0				1.726											1.755	
40.0	-.018	-.015			-.015	-.015			-.012	-.023		-.012	-.023		-.014	-.023
45.0	+.013	-.015			-.008	-.013			-.008	-.020		-.008	-.020		-.008	-.021

TABLE III - EXTERNAL AND INTERNAL PRESSURE COEFFICIENTS OF NACA 8-INCH RAM-JET CONFIGURATION
FOR FOUR ANGLES OF ATTACK - Continued
(d) Continued. - Free-stream Mach number of 1.99.



Station	$\alpha = 3^\circ; m_3/m_0 = 0.740$				$\alpha = 3^\circ; m_3/m_0 = 0.511$				$\alpha = 3^\circ; m_3/m_0 = 0.445$				$\alpha = 6^\circ; m_3/m_0 = 0.995$				$\alpha = 6^\circ; m_3/m_0 = 0.944$						
	Longitudinal distribution of C_p								Circumferential distribution of C_p								Outer shell						
	Outer shell		Center body	Outer shell		Center body	Outer shell		Center body	Outer shell		Center body	Outer shell		Center body	Outer shell		Center body	Outer shell				
	External	Internal		External	Internal		External	Internal		External	Internal		External	Internal		External	Internal		External	Internal			
$\theta \rightarrow$	180°	270°	0°	0°	180°	270°	0°	0°	180°	270°	0°	0°	180°	270°	0°	0°	180°	270°	0°	0°	180°	270°	0°
-1.5				0.581			0.581			1.031			0.601								0.601		
-1.0				0.564			1.374			1.410			0.645								0.645		
-.5				1.245			1.416			1.458			0.645								0.645		
0				1.364			1.444			1.238			0.638								0.638		
0.5	-0.019	0.075	1.407	1.540	-0.168	-0.084	1.562	1.479	-0.247	-0.180	1.510	1.555	0.182	0.282	0.441	.494	0.074	0.270	0.798	.657			
1.0	.008	.095	1.417	1.555	-.098	-.013	1.559	1.516	-.140	-.069	1.604	1.572	.051	.189	.507	.768	.068	.182	1.001	.928			
1.5	0.008	.075	1.489	1.581	-.065	.006	1.565	1.541	-.108	-.038	1.608	1.594	.014	.184	.474	.552	-.005	.135	1.028	1.030			
2.0	-.005	-.056	1.458	1.577	-.061	.008	1.570	1.541	-.079	-.084	1.612	1.594	-.005	.097	.535	-.006	-.020	.098	1.135	1.046			
2.5	-.017	.038	1.448	1.410	-.052	.005	1.577	1.560	-.075	-.081	1.617	1.608	-.082	.069	.386	.501	-.036	.071	1.155	1.118			
3.0	-.060	.018	1.446	1.482	-.049	-.009	1.577	1.567	-.068	-.026	1.618	1.614	-.051	.050	.239	.386	-.046	.058	1.160	1.143			
4.0	-.049	-.012	1.465	1.441	-.067	-.038	1.584	1.579	-.061	-.041	1.524	1.524	-.062	.005	.413	.235	-.075	.007	1.171	1.169			
5.0	-.066	-.028	1.451	1.451	-.070	-.036	1.588	1.589	-.079	-.045	1.628	1.623	-.068	-.014	.798	.683	-.078	-.018	1.175	1.176			
6.0	-.064	-.022	1.451	1.450	-.065	-.035	1.584	1.591	-.075	-.041	1.631	1.632	-.062	-.021	.845	.846	-.078	-.019	1.168	1.161			
7.0	-.046	-.022	1.460	1.465	-.065	-.032	1.597	1.599	-.060	-.039	1.636	1.637	-.052	-.022	.830	.831	-.059	-.020	1.179	1.165			
8.0	-.046	-.024	1.479	1.481	-.068	-.033	1.608	1.608	-.058	-.039	1.643	1.643	-.044	-.026	.950	.950	-.053	-.022	1.214	1.201			
9.0	-.039	-.027	1.488	1.491	-.046	-.035	1.613	1.616	-.050	-.041	1.647	1.650	-.038	-.031	.999	1.006	-.048	-.031	1.216	1.228			
10.0	-.032	-.019	1.498	1.498	-.038	-.038	1.621	1.621	-.043	-.051	1.655	1.655	-.029	-.029	1.031	1.032	-.027	-.027	1.228	1.228			
11.0	-.025	-.019	1.510	1.510	-.051	-.027	1.627	1.627	-.058	-.051	1.657	1.657	-.022	-.035	1.065	1.065	-.028	-.031	1.256	1.256			
12.0	-.022	-.020	1.525	1.525	-.027	-.037	1.633	1.633	-.031	-.031	1.663	1.663	-.017	-.031	1.168	1.168	-.017	-.038	1.297	1.297			
14.0	-.015	-.017	1.556	1.556	-.019	-.023	1.647	1.647	-.024	-.027	1.671	1.671	-.004	-.035	1.264	1.264	-.006	-.035	1.374	1.374			
16.0	-.010	-.017	1.585	1.585	-.014	-.022	1.661	1.661	-.017	-.026	1.690	1.690	-.005	-.036	1.348	1.348	-.001	-.038	1.438	1.438			
18.0	-.003	-.012	1.604	1.604	-.007	-.016	1.671	1.671	-.010	-.022	1.688	1.688	-.010	-.037	1.412	1.412	-.005	-.038	1.486	1.486			
21.0	-.015	-.010	1.639	1.639	-.011	-.014	1.690	1.690	-.007	-.017	1.696	1.696	-.020	-.034	1.498	1.498	-.016	-.036	1.555	1.555			
24.0	0	.008	1.671	1.671	-.004	-.003	1.707	1.707	-.007	-.006	1.708	1.708	-.008	-.023	1.576	1.576	-.005	-.024	1.615	1.615			
27.0	-.019	-.009	1.698	1.698	-.022	-.013	1.719	1.719	-.025	-.017	1.715	1.715	-.015	-.029	1.652	1.652	-.016	-.030	1.681	1.681			
31.0	-.003	-.017	1.714	1.714	-.004	-.018	1.728	1.728	-.007	-.028	1.720	1.720	-.003	-.041	1.671	1.671	0	-.041	1.695	1.695			
35.0	-.025	-.030			-.027	-.031			-.029	-.034			-.024	-.061			-.024	-.058			1.736		
37.0																	1.707						
40.0	-.014	-.023			-.014	-.035			-.017	-.036			-.010	-.048			-.011	-.049					
45.0	-.009	-.020			-.011	-.031			-.012	-.034			-.007	-.046			-.007	-.048					

TABLE III - EXTERNAL AND INTERNAL PRESSURE COEFFICIENTS OF NACA 8-INCH RAM-JET CONFIGURATION
FOR FOUR ANGLES OF ATTACK - Concluded

(d) Concluded. - Free-stream Mach number of 1.99.



Station	$\alpha = 6^\circ; m_3/m_0 = 0.733$				$\alpha = 6^\circ; m_3/m_0 = 0.374$				$\alpha = 10^\circ; m_3/m_0 = 0.956$				$\alpha = 10^\circ; m_3/m_0 = 0.902$				$\alpha = 10^\circ; m_3/m_0 = 0.710$							
	Longitudinal distribution of C_p												Circumferential distribution of C_p											
	Outer shell		Center body	Outer shell		Center body	Outer shell		Center body	Outer shell		Center body	Outer shell		Center body	Outer shell		Center body	Outer shell		Center body			
	External	Internal		External	Internal		External	Internal		External	Internal		External	Internal		External	Internal		External	Internal				
0 →	180°	270°	0°	0°	180°	270°	0°	0°	180°	270°	0°	0°	180°	270°	0°	0°	180°	270°	0°	0°	180°	270°	0°	
-1.5	-0.064	0.100	1.295	1.264	-0.251	-0.126	1.531	1.470	-0.001	0.291	0.586	0.594	-0.053	0.298	0.414	0.771	-0.142	0.185	0.946	1.055	0.781			
-1.0	-0.058	.106	1.333	1.272	-.212	-.050	1.532	1.494	-.044	.201	.436	.713	-.062	.213	.692	.647	-.154	.130	1.046	.981	.875			
-0.5	-0.070	.083	1.361	1.307	-.187	-.026	1.541	1.520	-.072	.142	.533	.264	-.080	.156	.893	.580	-.158	.110	1.128	1.055	.937			
0	-0.062	.084	1.378	1.312	-.157	-.014	1.550	1.522	-.082	.104	.768	.578	-.098	.116	1.008	.865	-.157	.098	1.175	1.061	1.053			
0.5	-0.075	.045	1.395	1.308	-.180	-.012	1.566	1.542	-.098	.072	.754	.568	-.098	.082	1.084	1.060	-.158	.085	1.210	1.161				
1.0	-0.076	.034	1.398	1.375	-.137	-.019	1.564	1.551	-.099	.051	.757	.524	-.100	.068	1.133	1.116	-.158	.041	1.224	1.197				
1.5	-0.095	.009	1.413	1.402	-.136	-.036	1.564	1.563	-.110	.003	.918	.856	-.116	.007	1.172	1.184	-.162	-.002	1.250	1.238				
2.0	-0.095	.023	1.415	1.417	-.123	-.046	1.569	1.566	-.104	.018	1.008	1.007	-.110	.016	1.175	1.173	-.151	-.080	1.247	1.234				
2.5	-0.084	.026	1.416	1.417	-.108	-.045	1.554	1.565	-.090	.026	1.024	1.024	-.098	.026	1.181	1.175	-.137	-.050	1.237	1.245				
3.0	-0.069	.029	1.422	1.433	-.088	-.045	1.560	1.564	-.076	.026	1.050	1.063	-.068	.035	1.208	1.207	-.094	-.059	1.249	1.251				
3.5	-0.061	.034	1.452	1.456	-.075	-.050	1.554	1.560	-.065	.048	1.100	1.100	-.065	.047	1.253	1.285	-.072	-.062	1.254	1.266				
4.0	-0.051	.039	1.461	1.469	-.061	-.055	1.546	1.532	-.054	.058	1.182	1.189	-.041	.057	1.288	1.288	-.065	-.061	1.224	1.245				
4.5	-0.041	.034		1.478	-.061	-.060		1.546	-.065	.058	1.182	1.189	-.030	.068	1.312	-.041	-.061		1.204					
5.0	-0.032	.032		1.493	-.040	-.058		1.550	-.015	.063	1.177	1.171	-.021	.055	1.359	-.038	-.059		1.183					
5.5	-0.026	.040		1.505	-.034	-.058		1.557	-.010	.071	1.812	1.015	-.071	1.367	-.021	-.076		1.210						
6.0	-0.017	.044		1.536	-.028	-.056		1.576	-.008	.080	1.282	-.003	-.080	1.484	-.010	-.085		1.295						
6.5	-0.010	.044		1.562	-.015	-.053		1.592	-.007	.090	1.359	-.009	-.090	1.471	-.008	-.095		1.359						
7.0	-0.003	.043		1.583	-.007	-.050		1.604	-.014	.097	1.385	-.016	-.099	1.508	-.007	-.102		1.406						
7.5	-0.007	.039		1.614	-.001	-.046		1.625	-.004	.108	1.449	-.002	-.106	1.561	-.006	-.112		1.464						
8.0	-0.007	.036		1.644	-.018	-.017		1.647	-.006	.111	1.514	-.006	-.111	1.611	-.011	-.116		1.515						
8.5	-0.020	.034		1.669	-.018	-.026		1.658	-.001	.104	1.589	-.004	-.104	1.647	0	-.118		1.545						
9.0	-0.003	.044		1.686	-.005	-.046		1.662	-.007	.107	1.583	-.008	-.107	1.669	-.003	-.118		1.580						
9.5	-0.028	.064		1.710	-.008	-.056		1.867	-.020	.123	1.605	-.020	-.123	1.692	-.024	-.129		1.691						
10.0	-.010	-.049			-.012	-.050			-.008	-.108			-.002	-.097		-.006	-.101							
10.5	-.008	-.045			-.012	-.046			-.008	-.108			-.006	-.093		-.010	-.096							

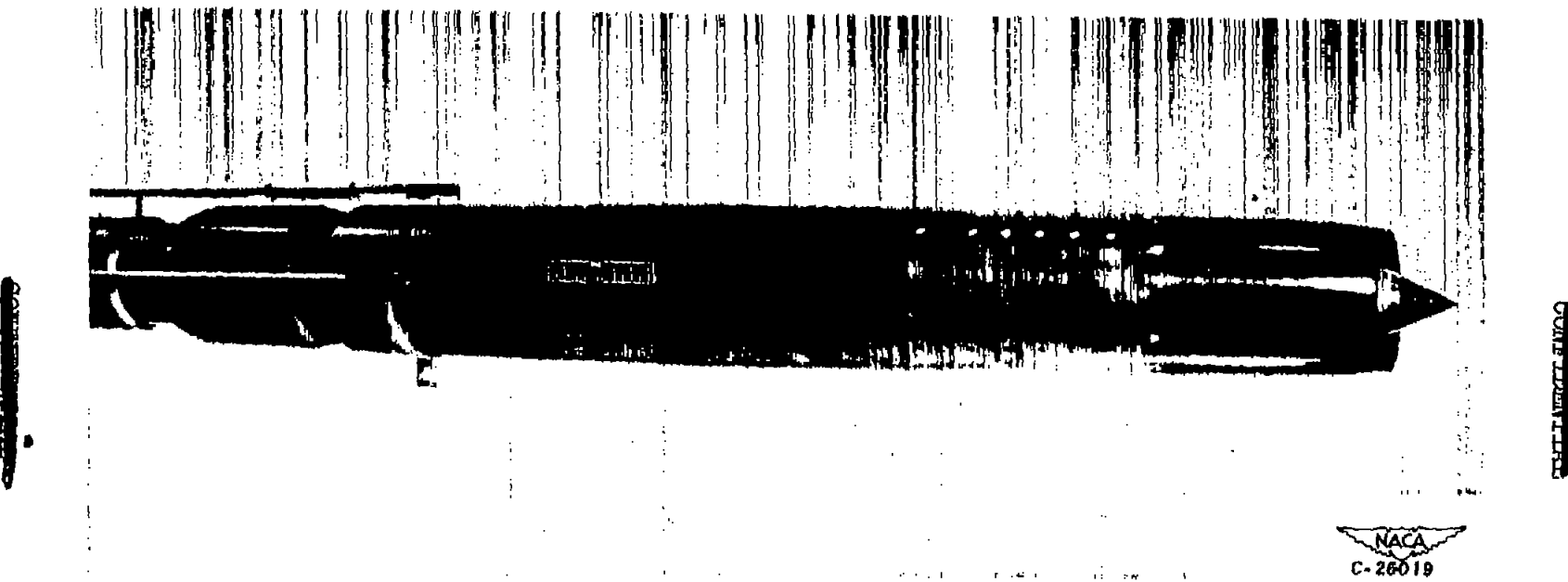


Figure 1. - Pressure model of NACA 6-inch ram-jet configuration.

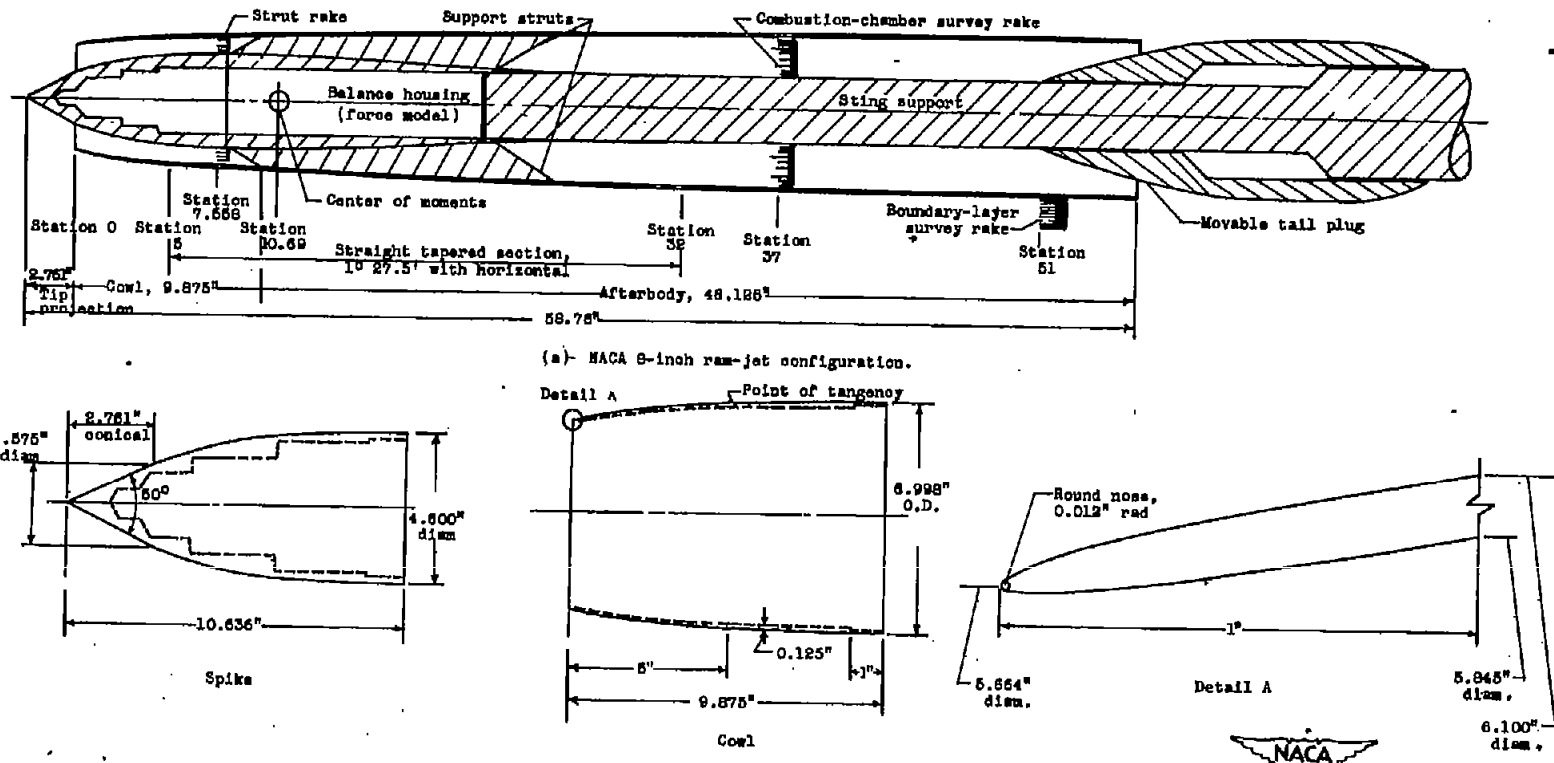


Figure 2. - Schematic diagram of NACA 8-inch ram-jet configuration showing principal dimensions of model and details of all-external compression inlet.

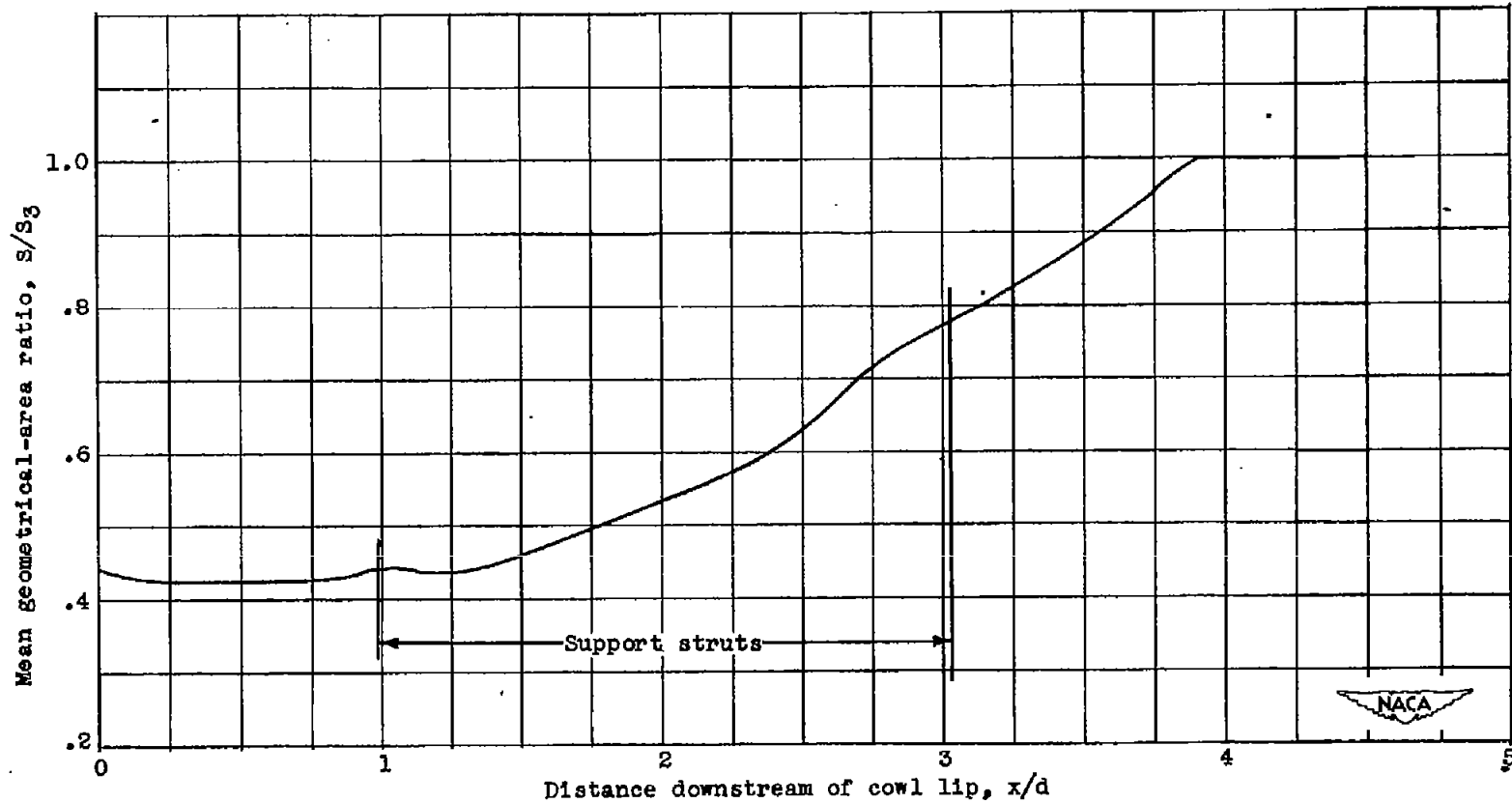
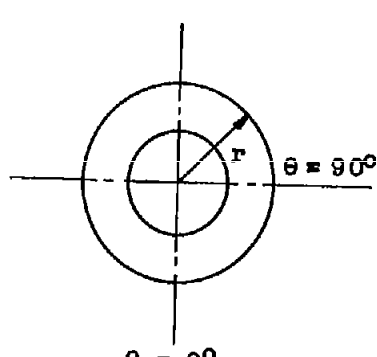
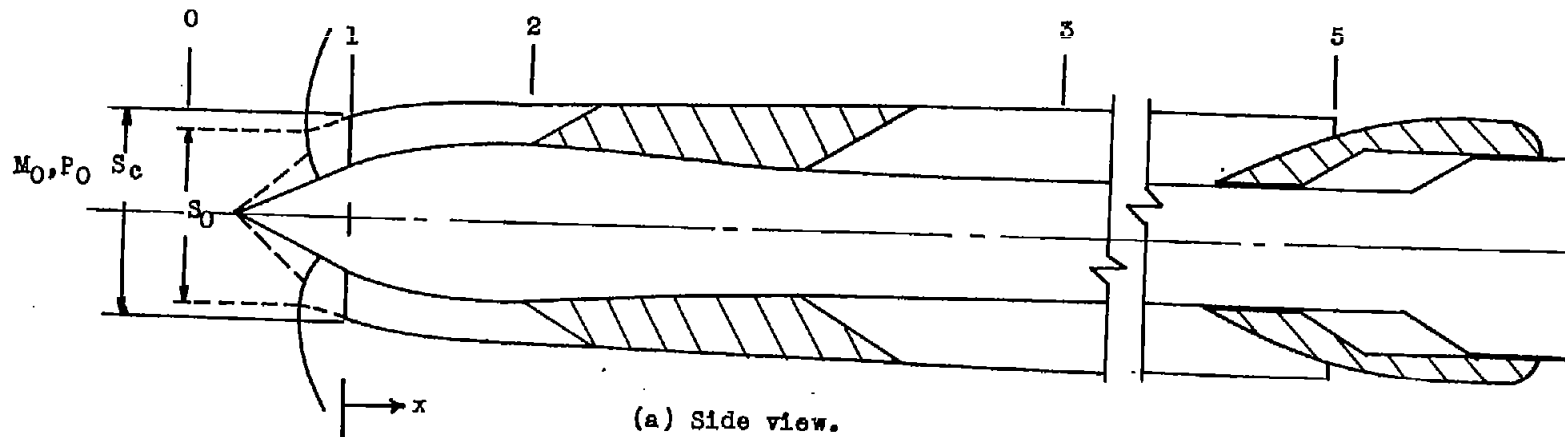


Figure 3. - Longitudinal variation of mean geometrical-area ratio.



(b) Front view.



Figure 4. - Notation for 8-inch ram-jet configuration.

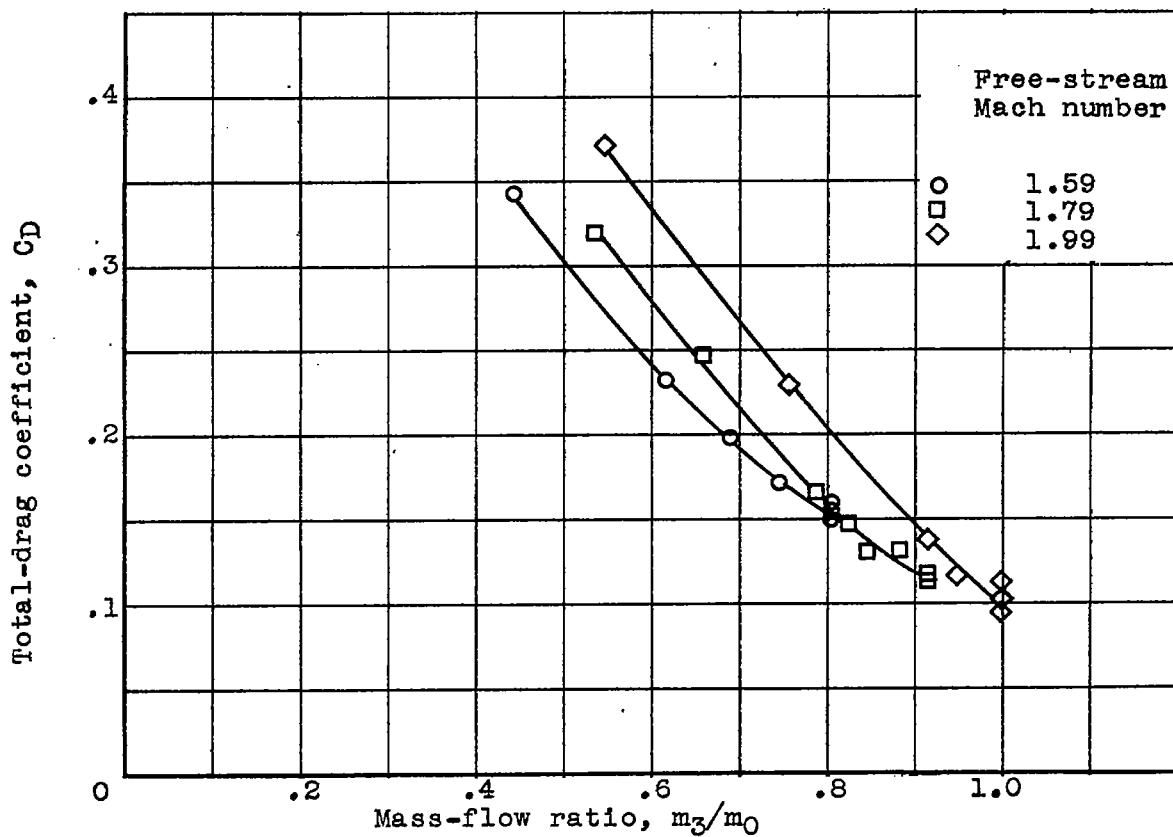


Figure 5. - Variation of total-drag coefficient with mass flow at zero angle of attack for three Mach numbers.

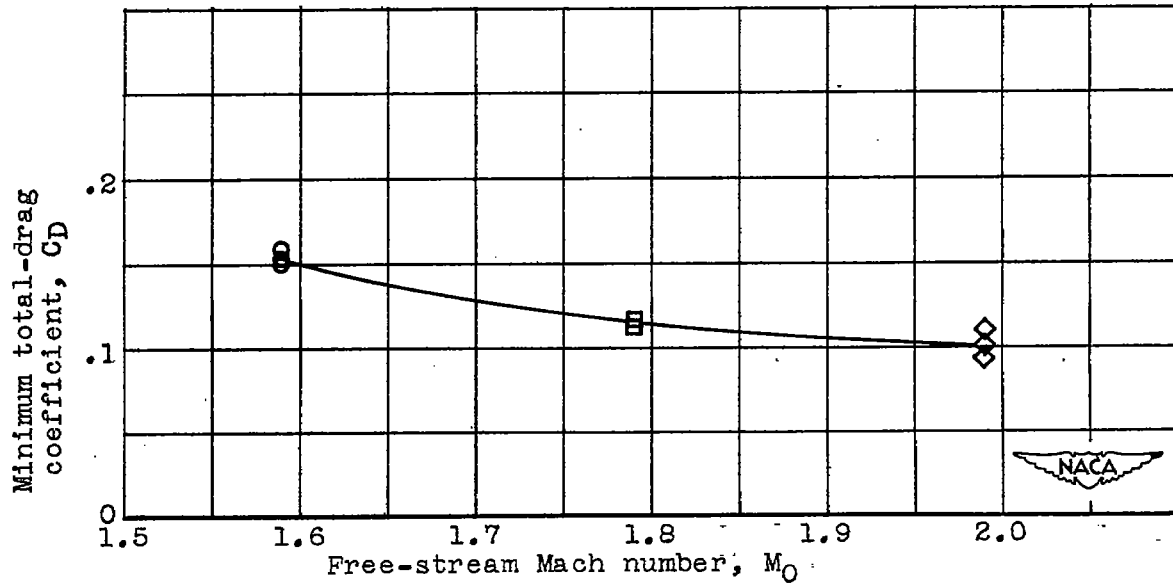
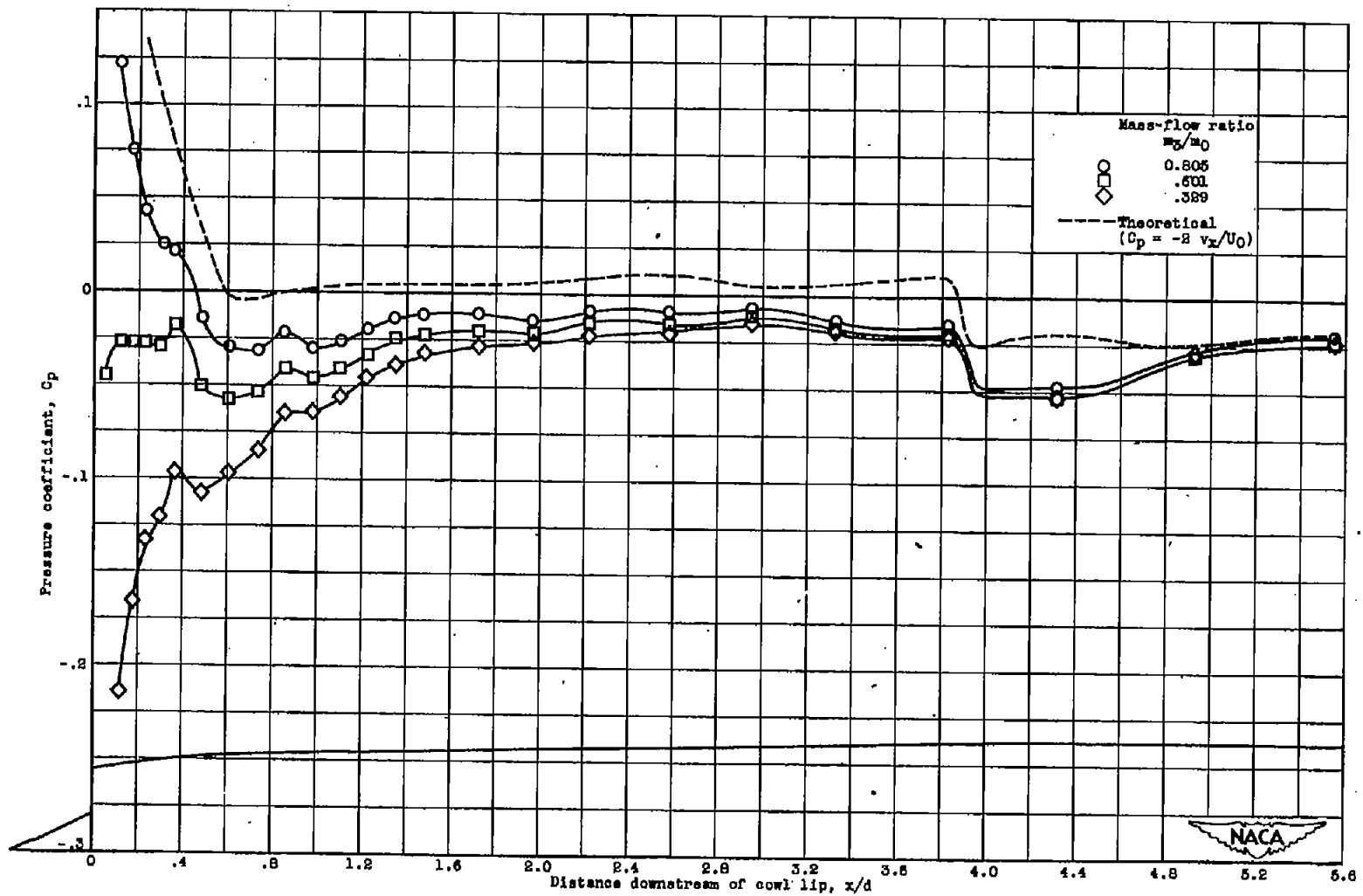


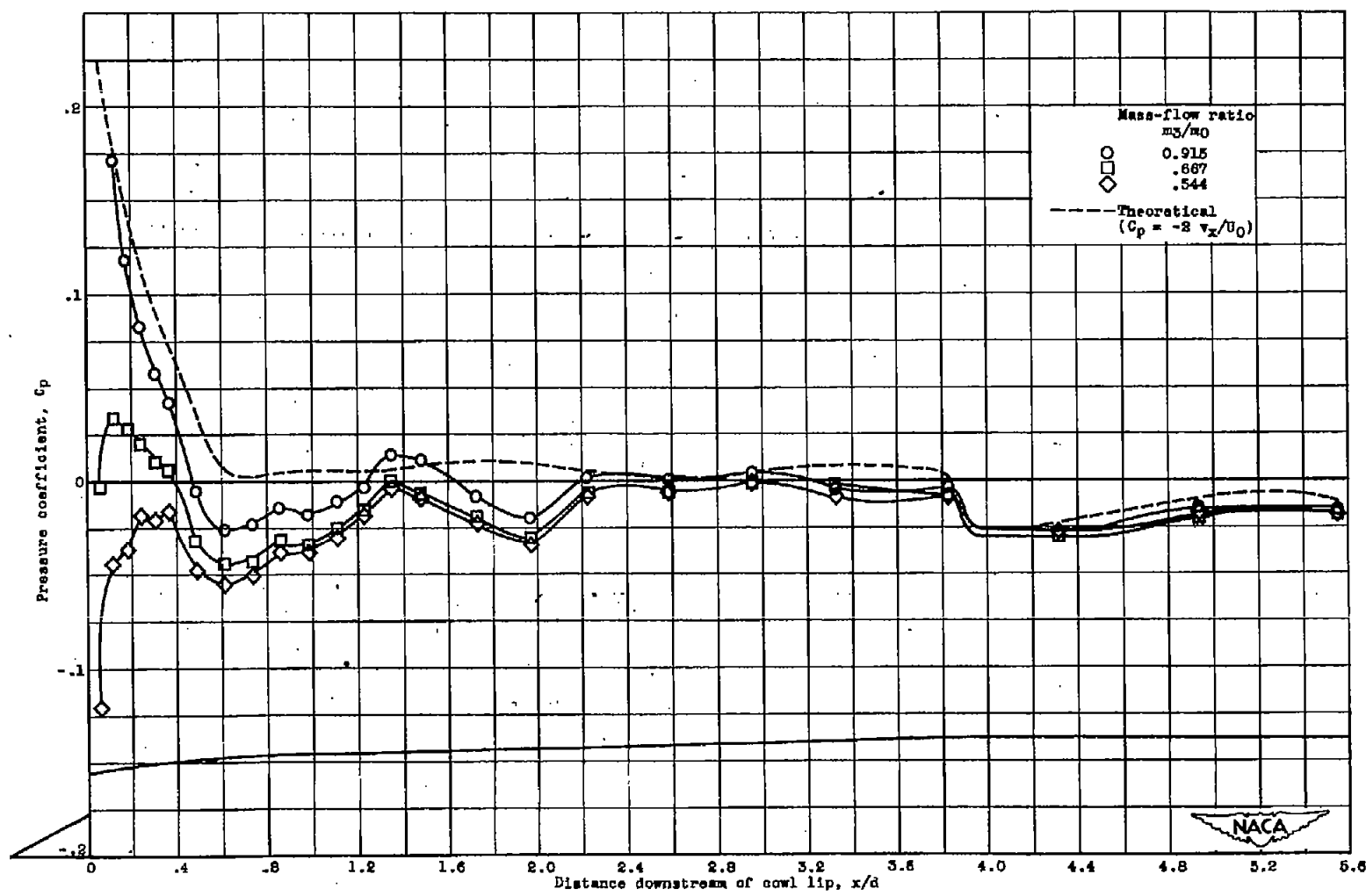
Figure 6. - Variation of minimum total-drag coefficient with free-stream Mach number at zero angle of attack.

CONFIDENTIAL



(a) Free-stream Mach number, 1.59.

Figure 7. - Longitudinal variation of external pressure coefficient at zero angle of attack for range of mass flows at three Mach numbers. Cylindrical coordinate θ , 180° .



(b) Free-stream Mach number, 1.79.

Figure 7. - Continued. Longitudinal variation of external pressure coefficient at zero angle of attack for range of mass flows at three Mach numbers.
 Cylindrical coordinate $\theta, 180^\circ$.

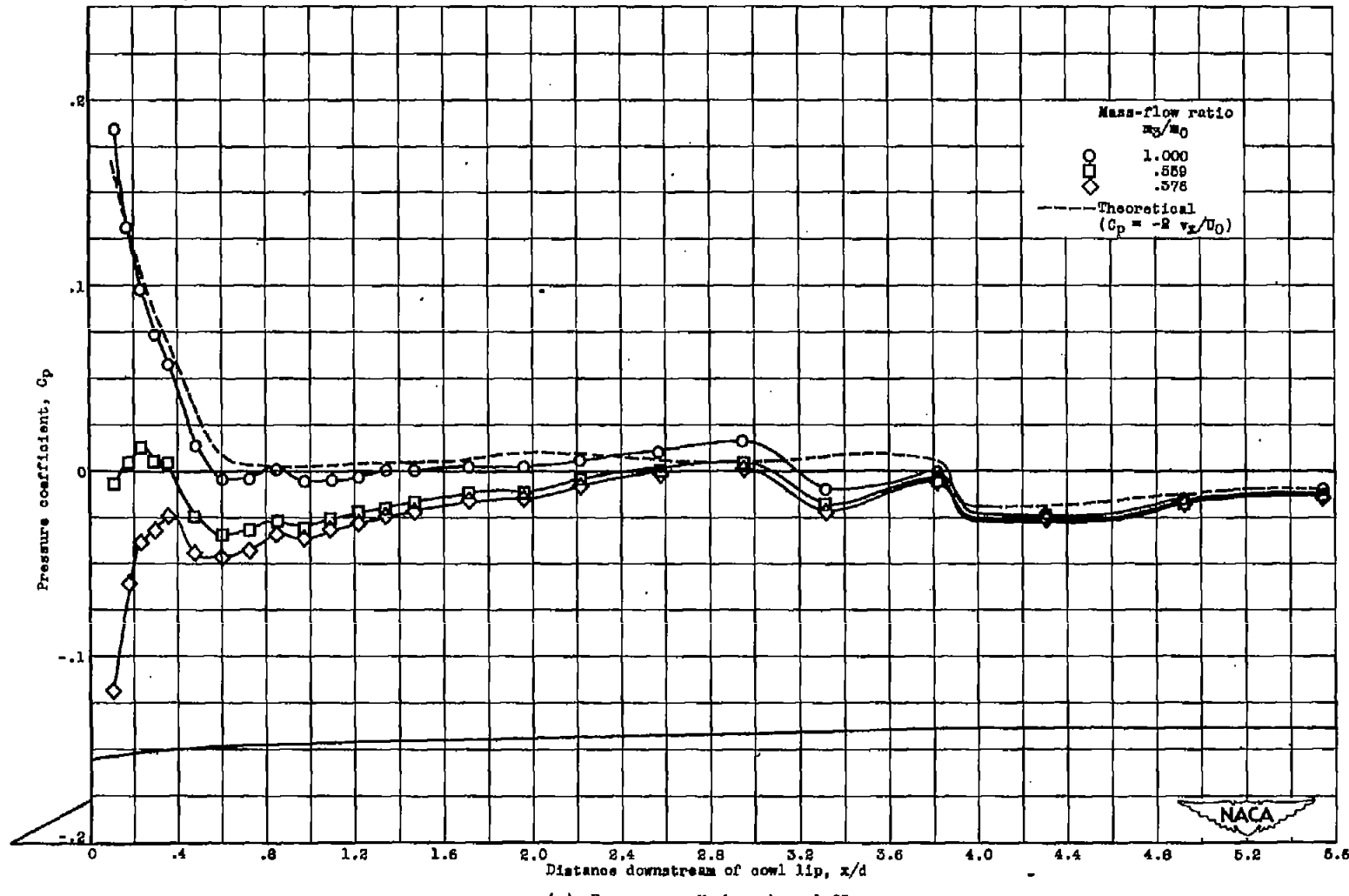
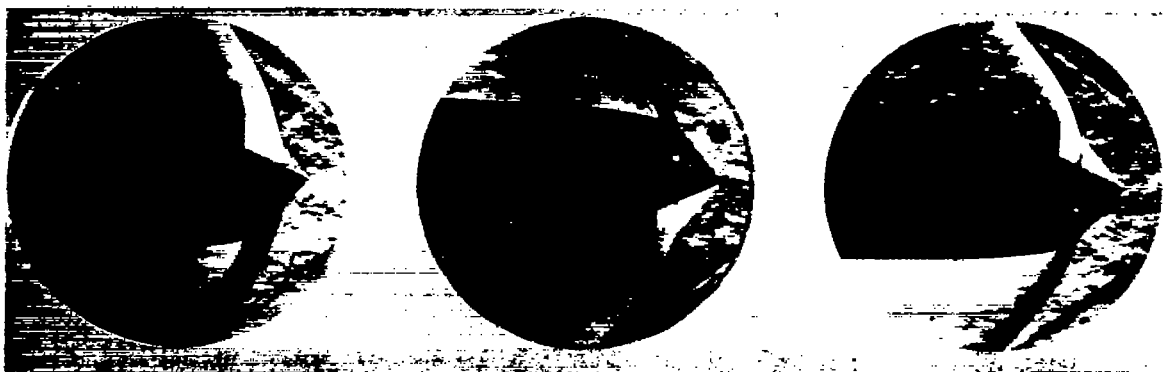


Figure 7. - Concluded. Longitudinal variation of external pressure coefficient at zero angle of attack for range of mass flows at three Mach numbers. Cylindrical coordinate θ , 180°.

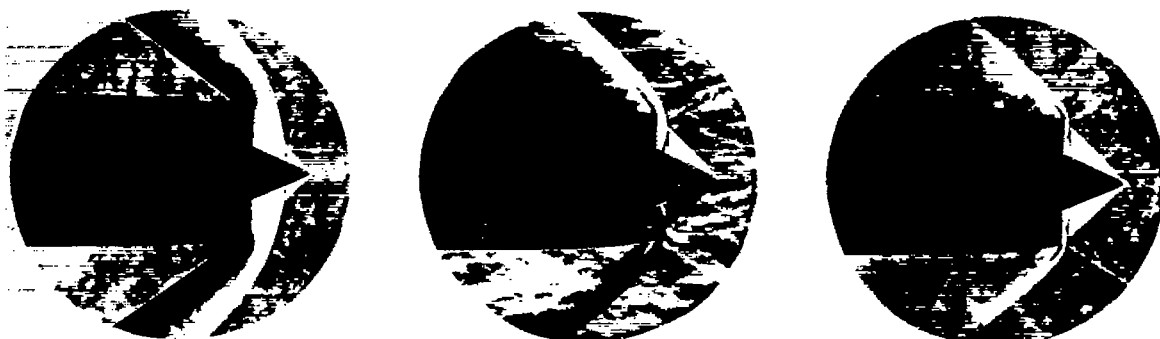


Mass-flow ratio 0.617

0.732

0.805

(a) Free-stream Mach number, 1.59.



Mass-flow ratio 0.544

0.870

0.915

(b) Free-stream Mach number, 1.79.



Mass-flow ratio 0.559

0.996

1.00


C-26039

(c) Free-stream Mach number, 1.99.

Figure 8. - Typical schlieren photographs at zero angle of attack for three Mach numbers.

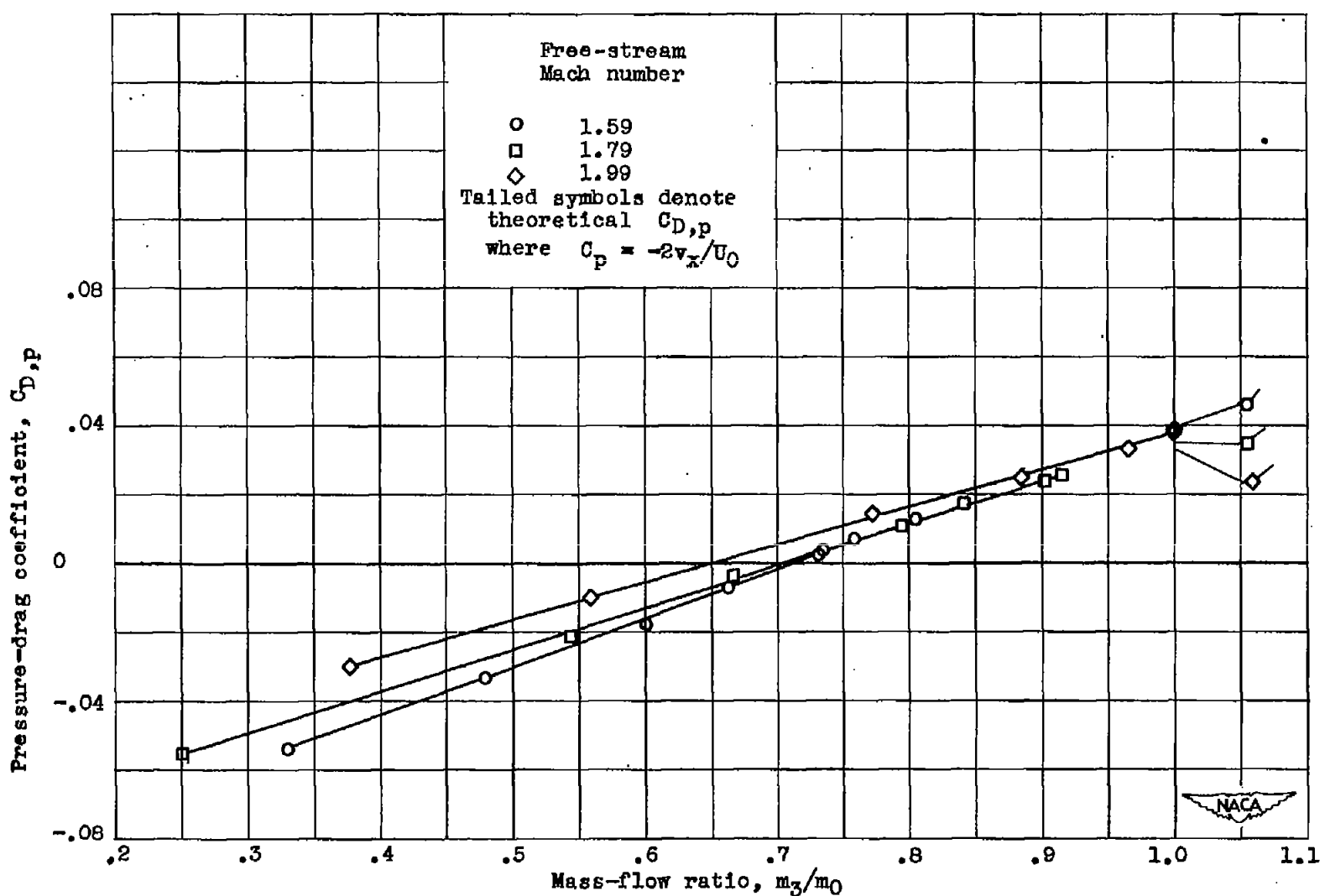


Figure 9. - Variation of pressure-drag coefficient with mass flow at zero angle of attack for three Mach numbers.

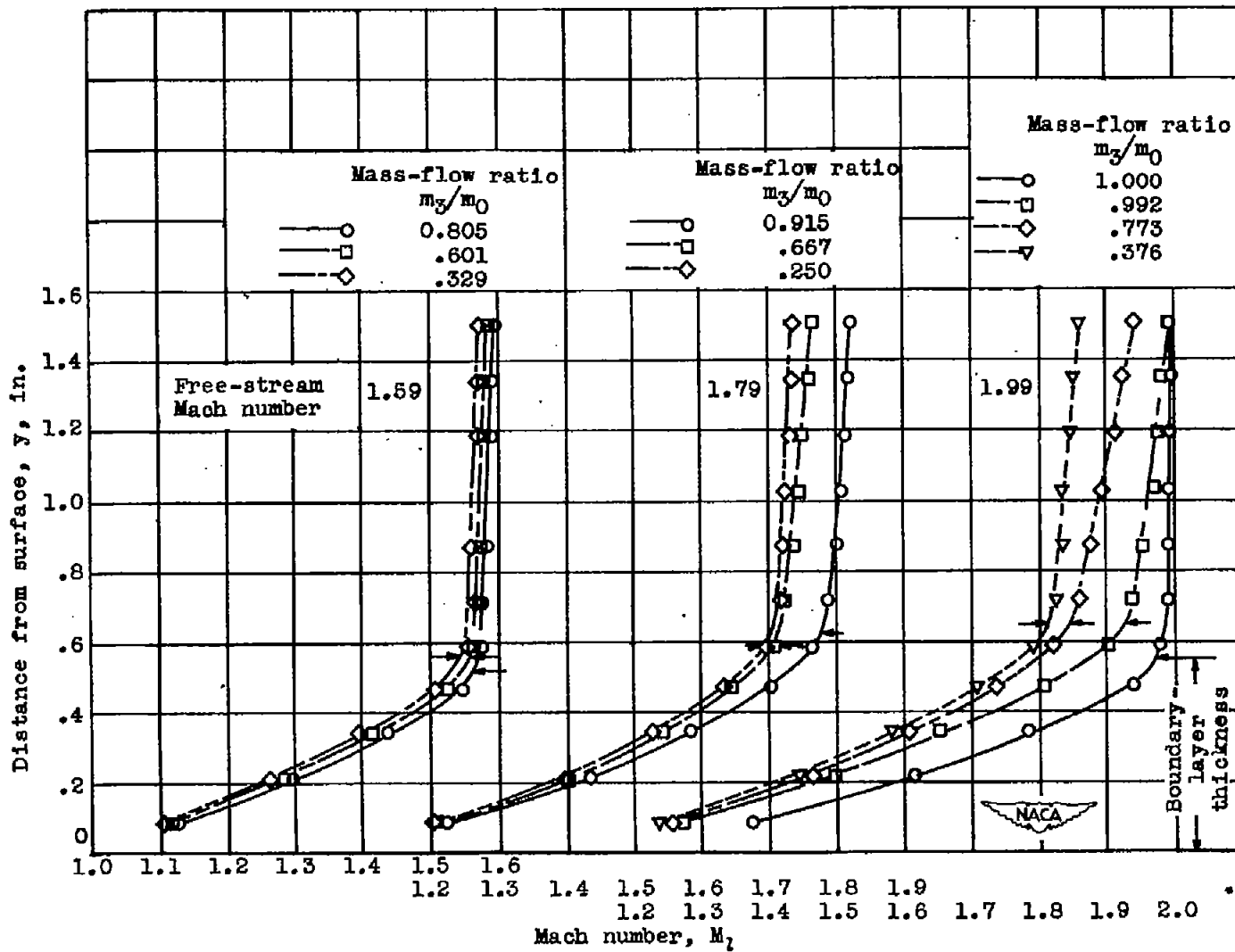


Figure 10. - Variation of Mach number distribution in boundary layer at zero angle of attack for range of mass flows at three Mach numbers. (Station 51.)

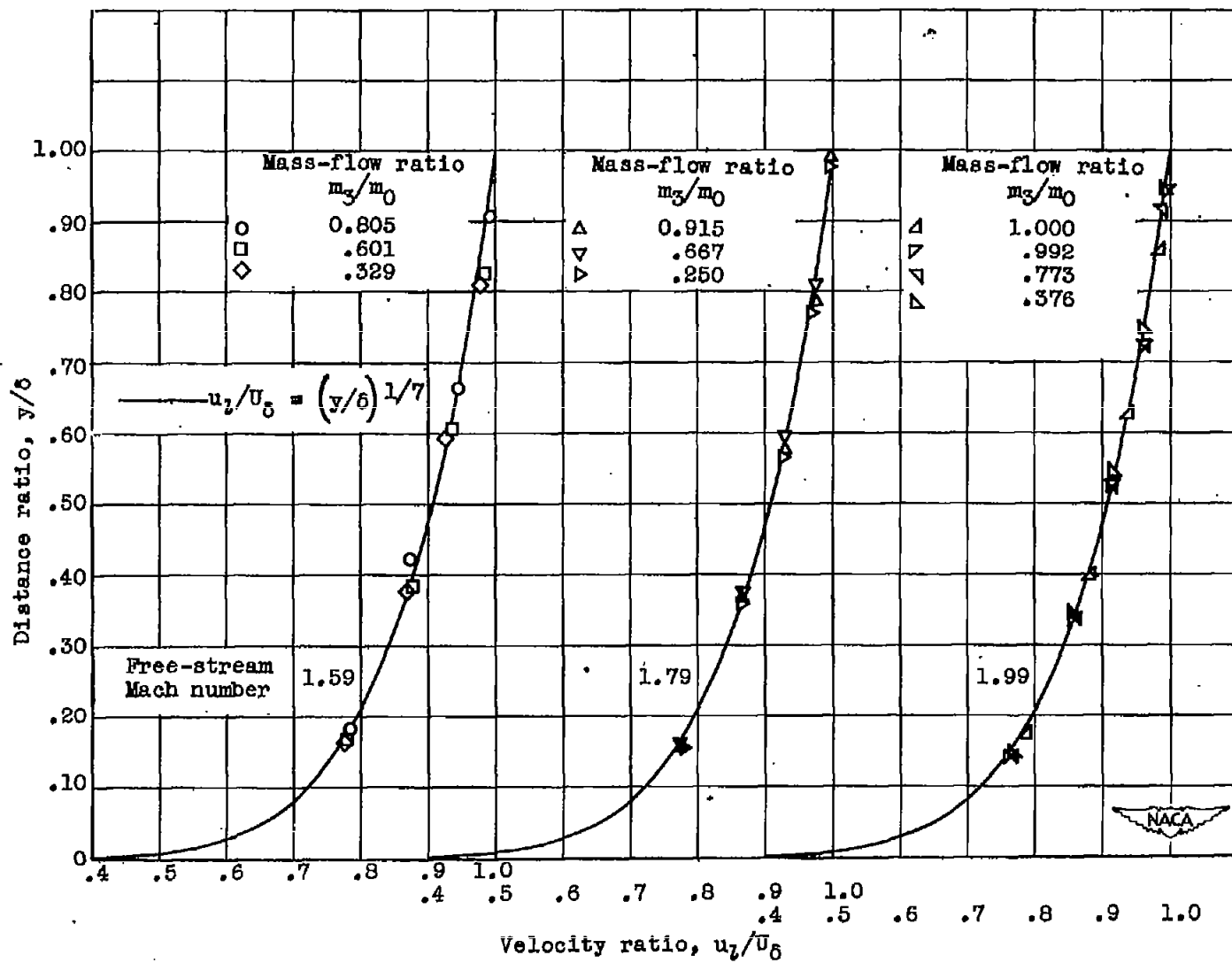


Figure 11. - Comparison of experimental and theoretical boundary-layer profiles at zero angle of attack for range of mass flows and three free-stream Mach numbers.

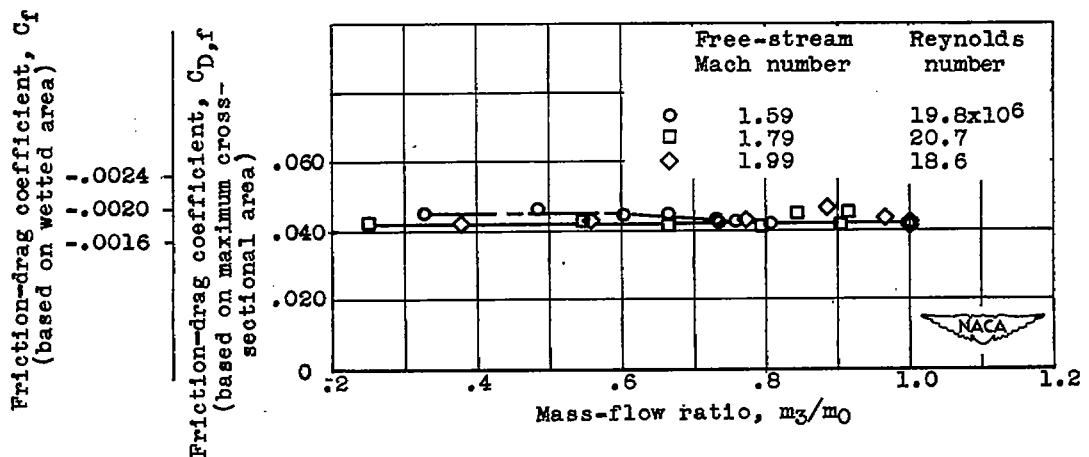


Figure 12. - Variation of friction-drag coefficient with mass flow at zero angle of attack for three Mach numbers.

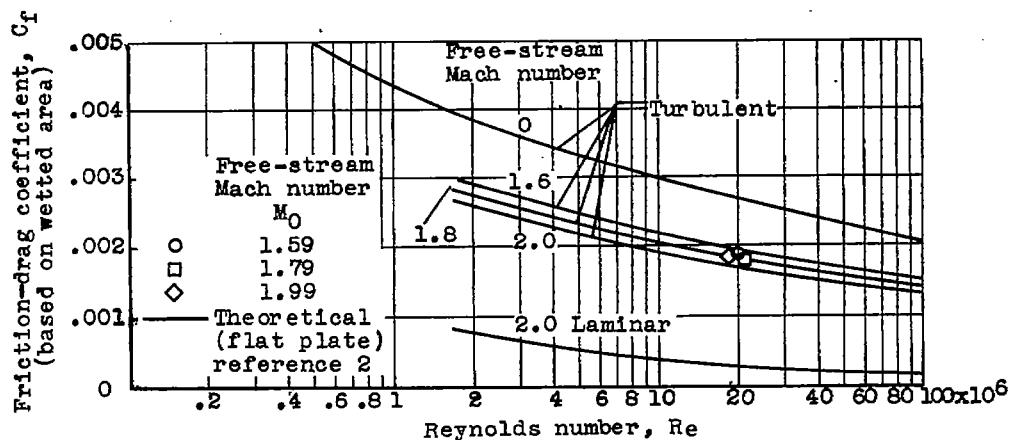


Figure 13. - Comparison of experimental friction-drag coefficient with two-dimensional compressible-flow theory at three Mach numbers.

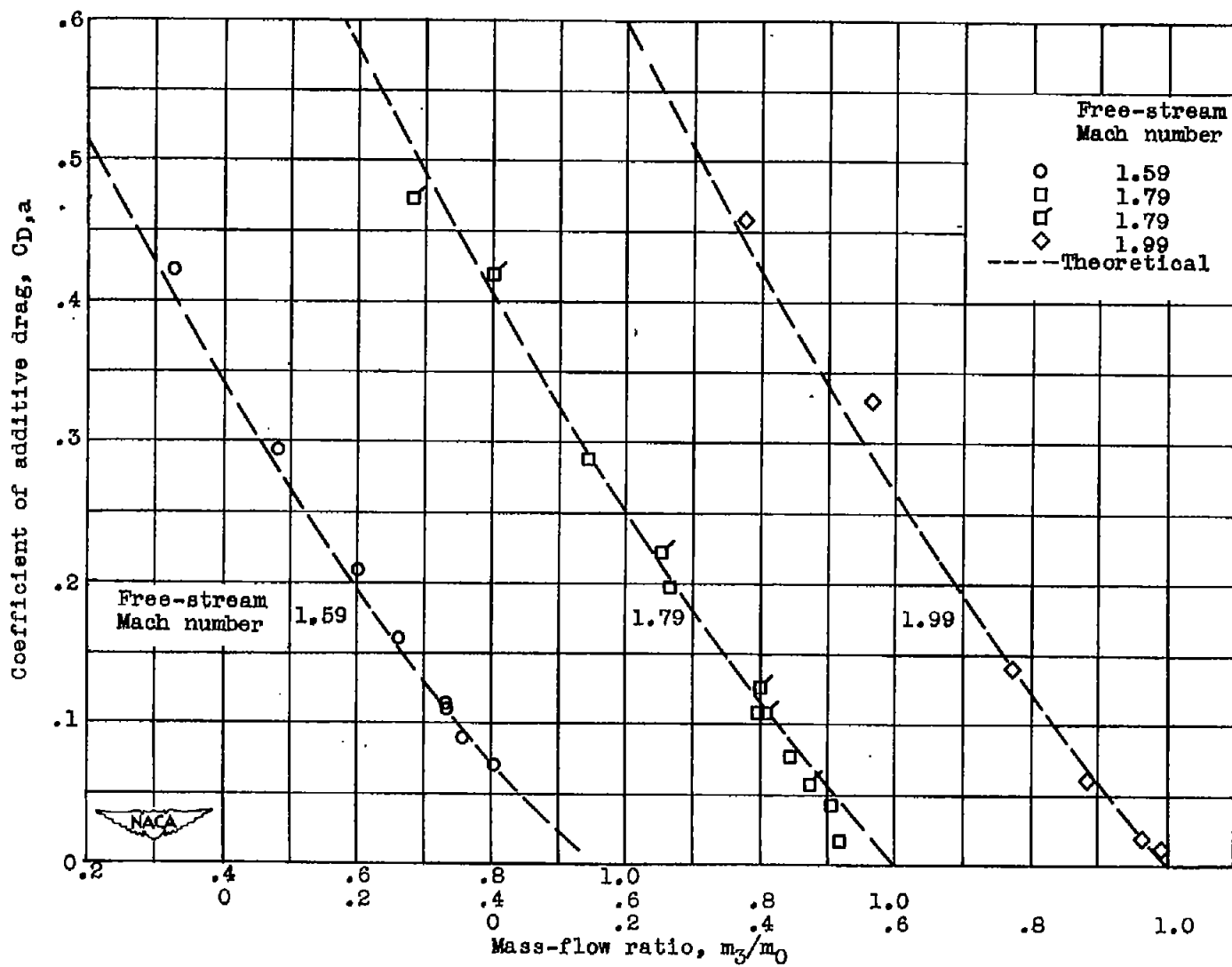
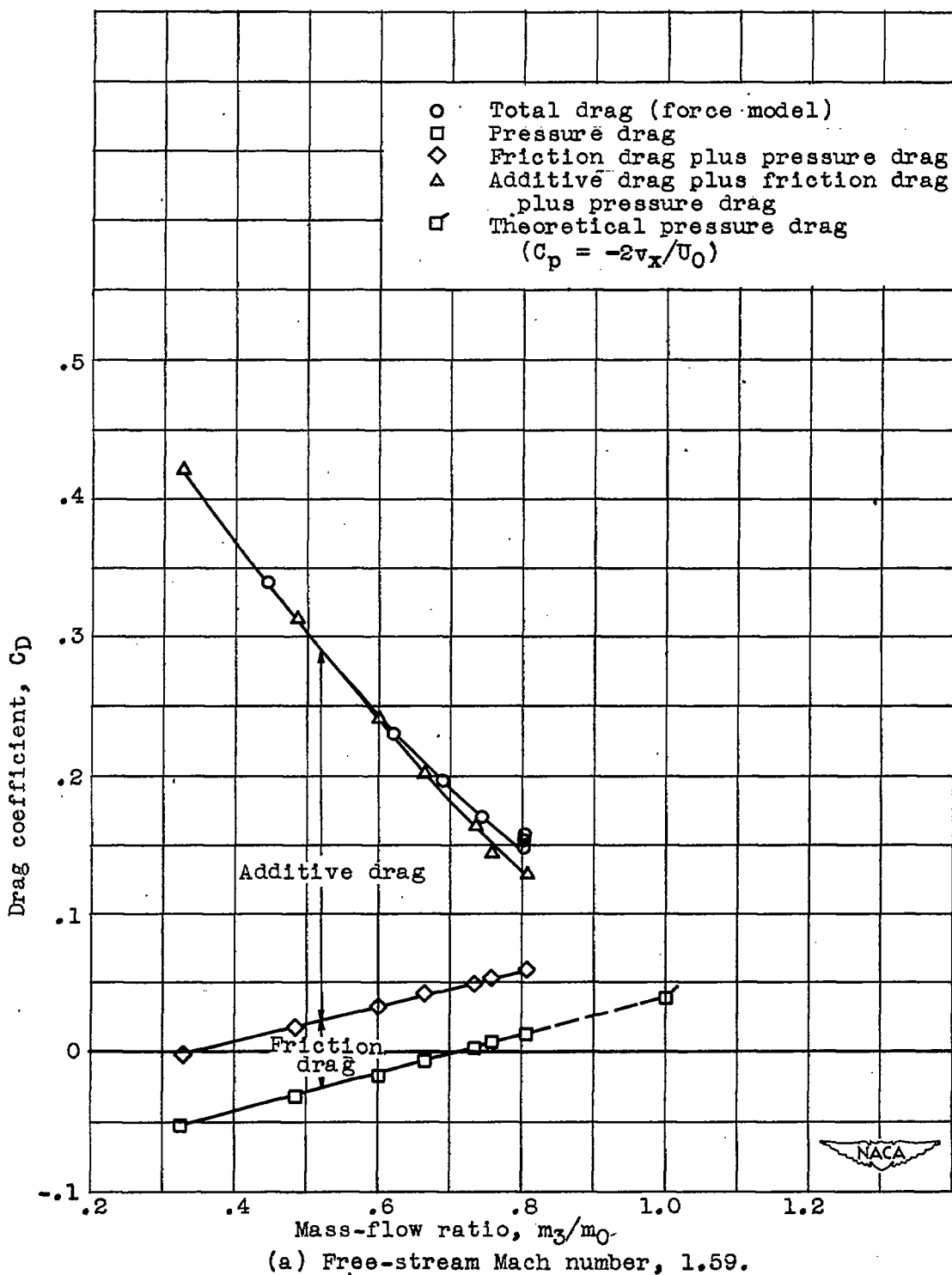
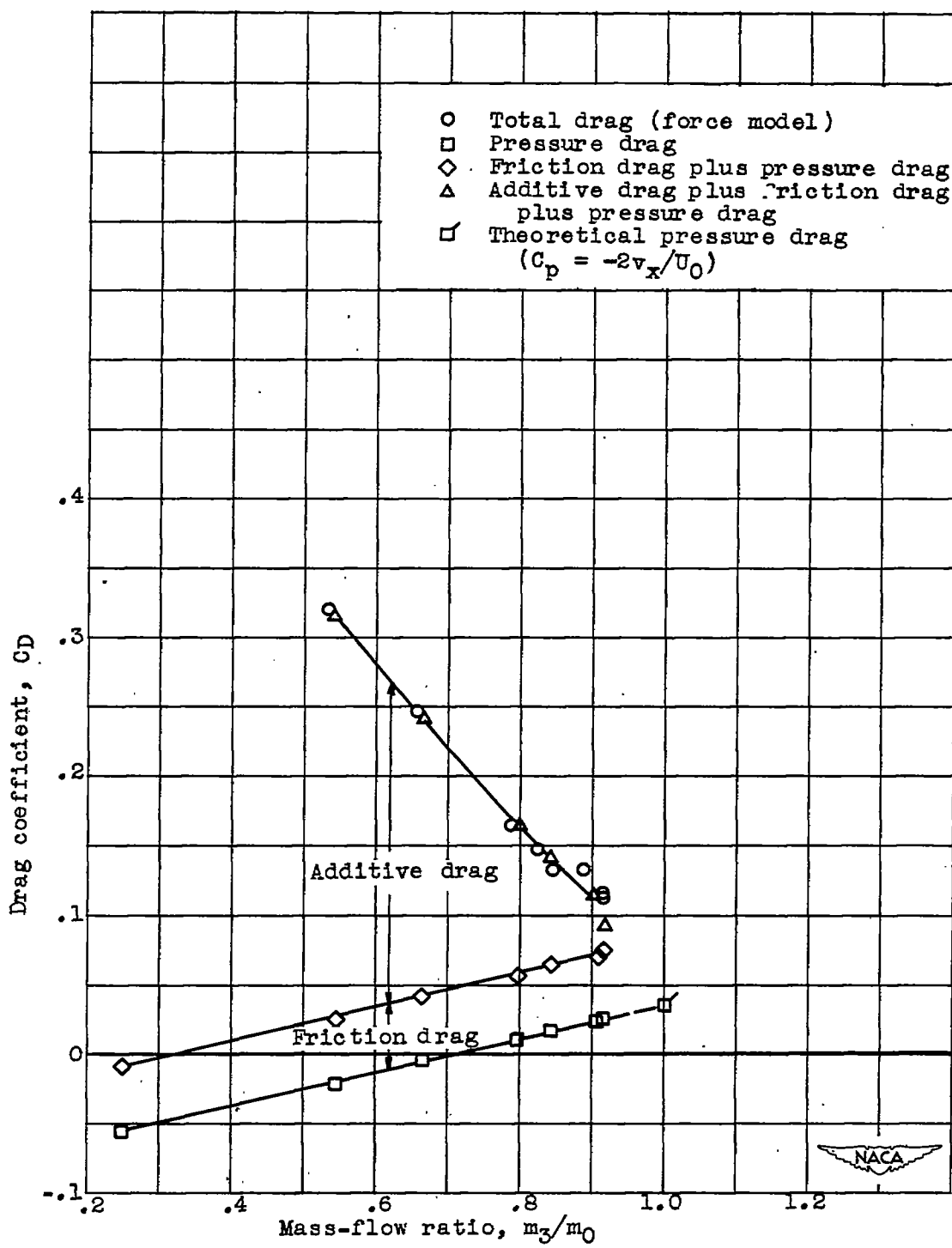


Figure 14. -- Comparison of experimental additive-drag coefficient with one-dimensional theory for range of mass flows at three Mach numbers.



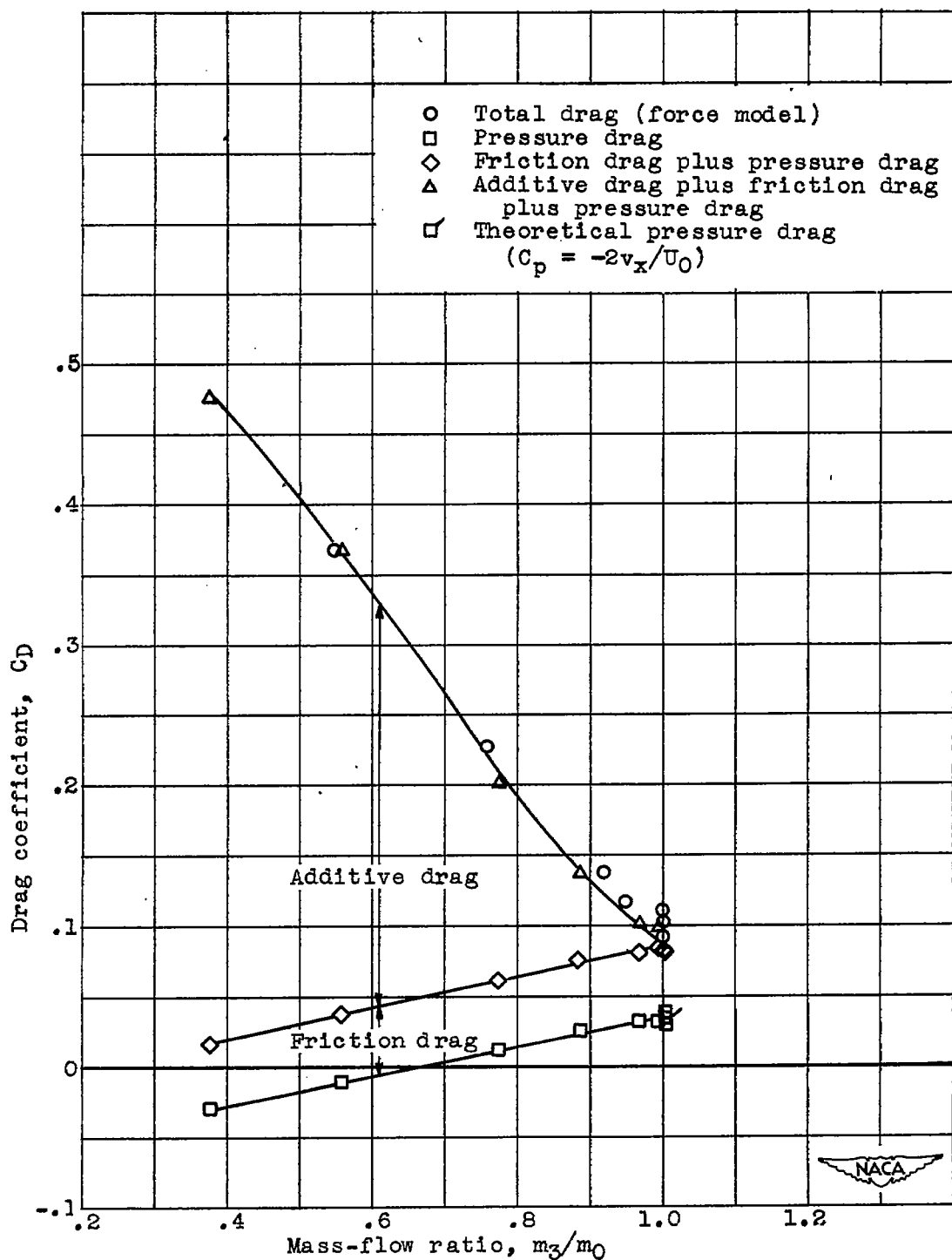
(a) Free-stream Mach number, 1.59.

Figure 15. - Variation of components of total-drag coefficient with mass flow at zero angle of attack for three Mach numbers.



(b) Free-stream Mach number, 1.79.

Figure 15. - Continued. Variation of components of total-drag coefficient with mass flow at zero angle of attack for three Mach numbers.



(c) Free-stream Mach number, 1.99.

Figure 15. -- Concluded. Variation of components of total-drag coefficient with mass flow at zero angle of attack for three Mach numbers.

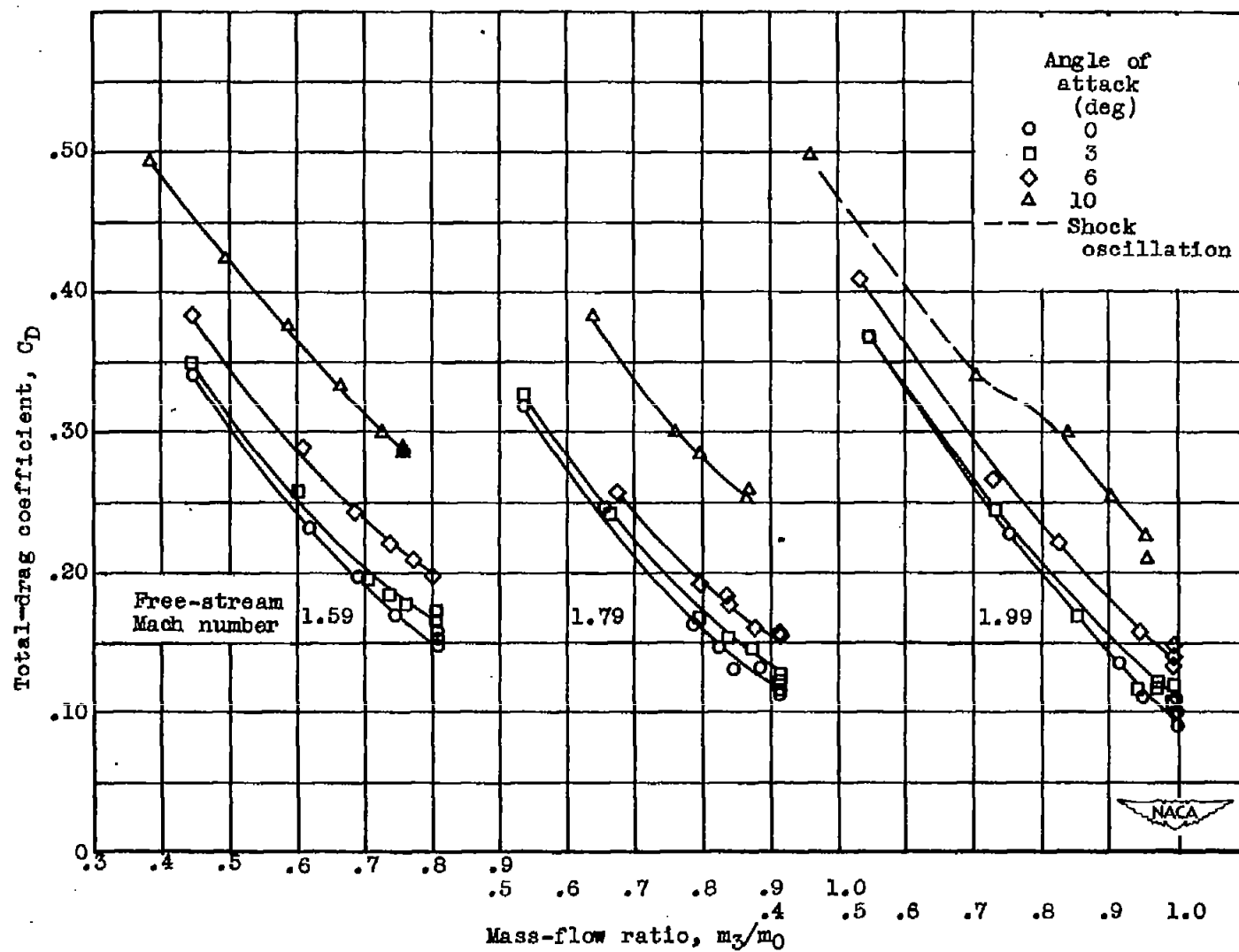


Figure 16. - Variation of total-drag coefficient with mass flow at four angles of attack for three Mach numbers.

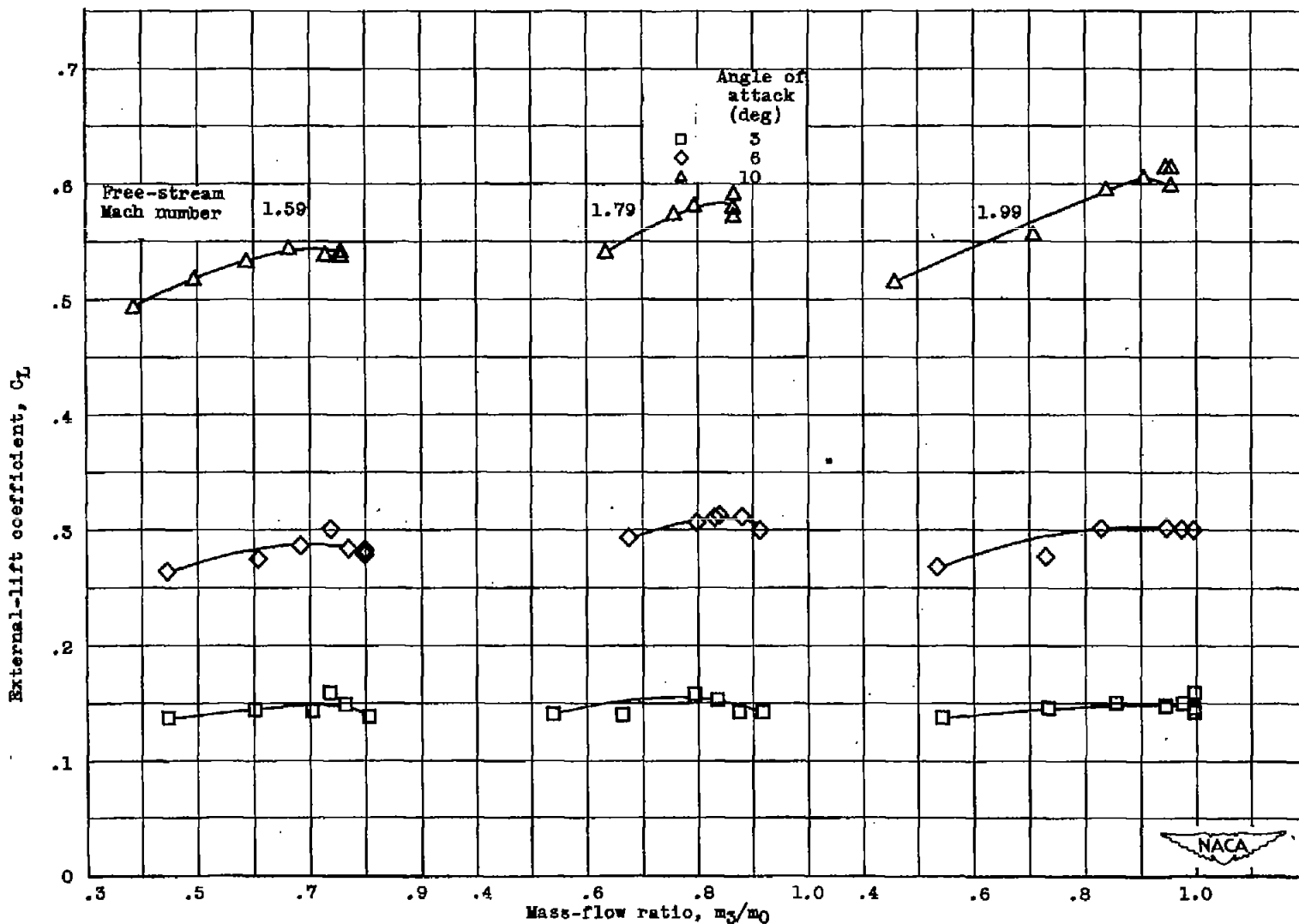


Figure 17. - Variation of external-lift coefficient with mass flow at three angles of attack for three Mach numbers.

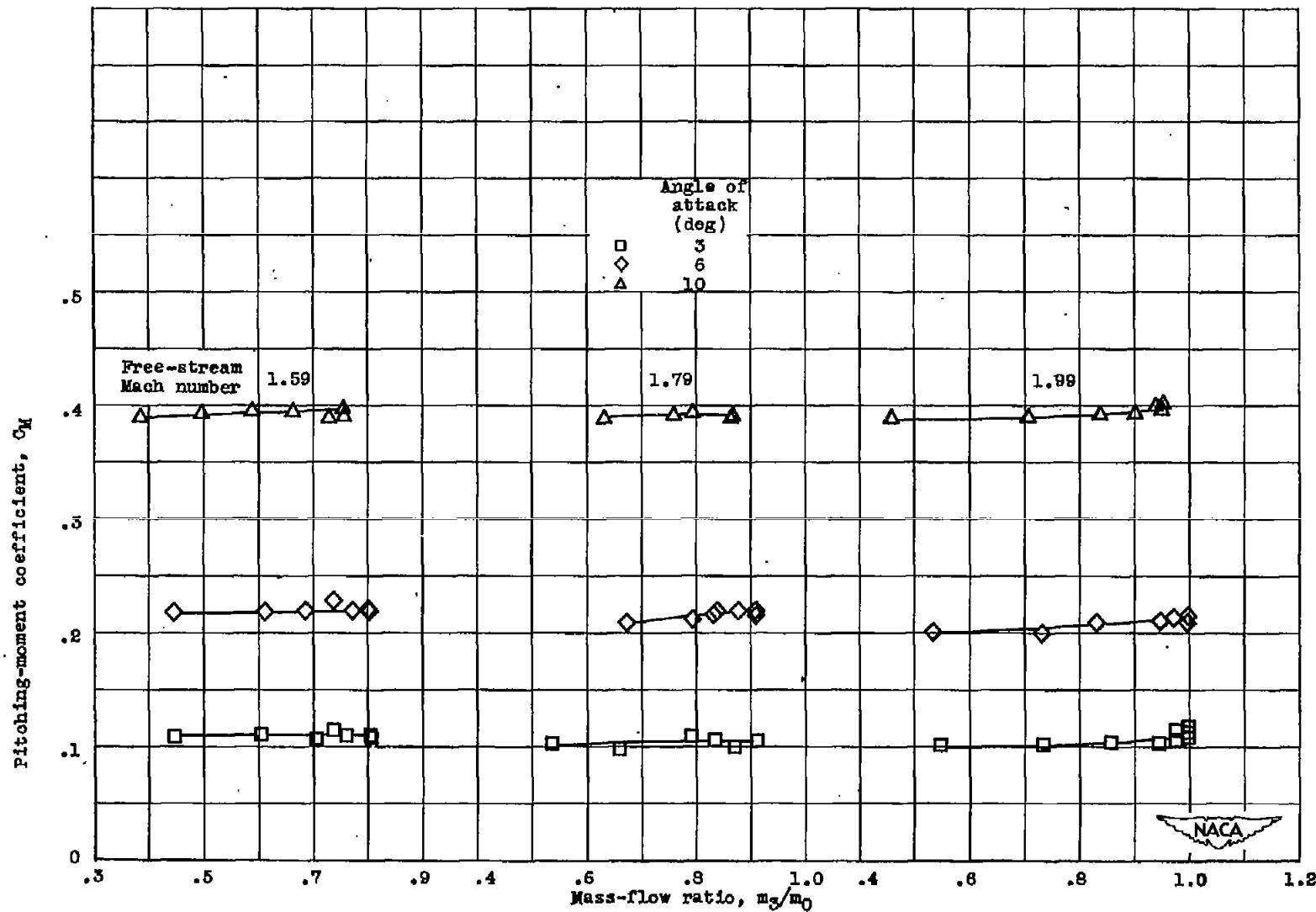


Figure 18. - Variation of external pitching-moment coefficient about base of model with mass flow at three angles of attack for three Mach numbers.

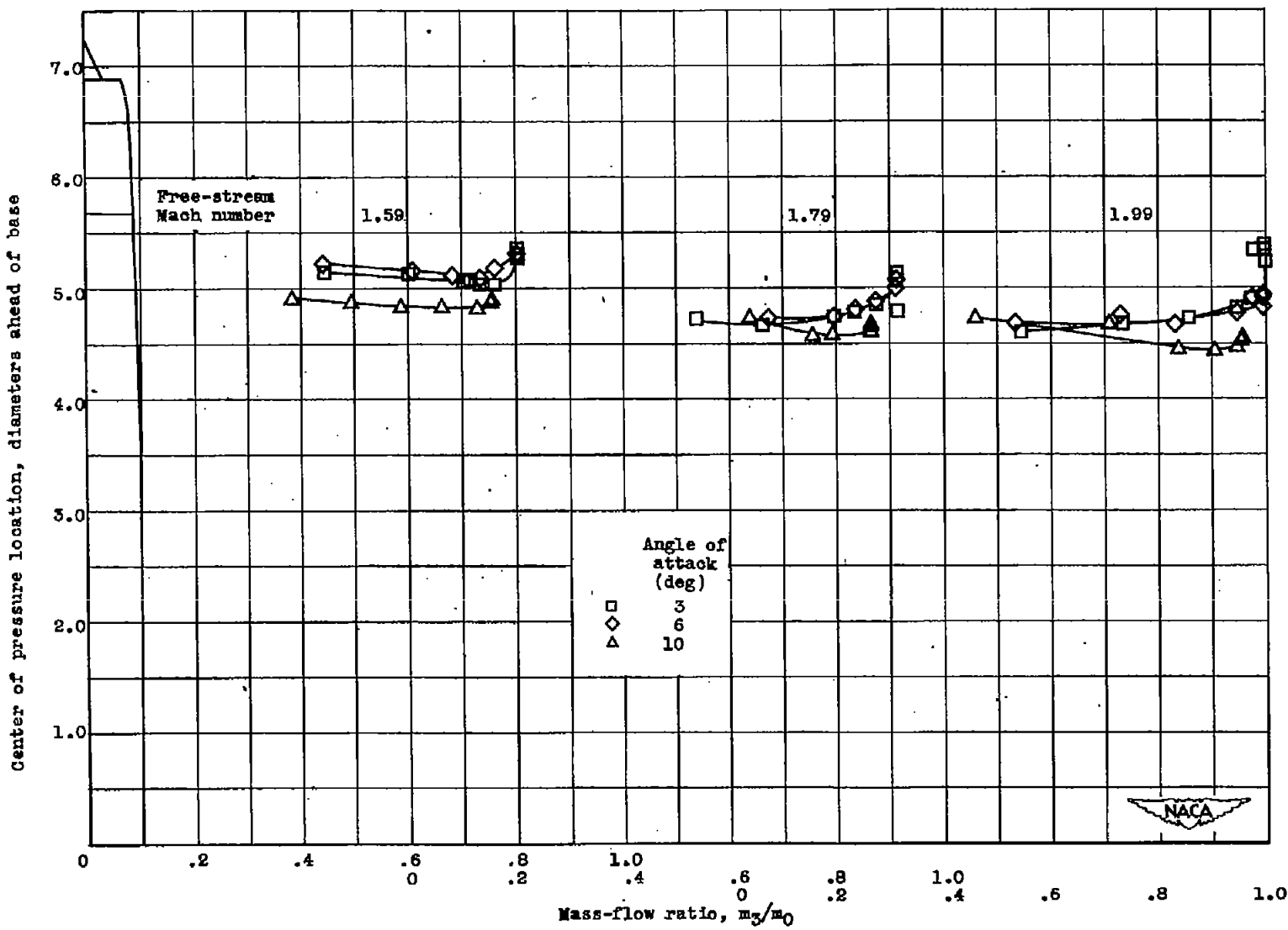


Figure 19. - Variation of center of pressure location with mass flow at three angles of attack for three Mach numbers.

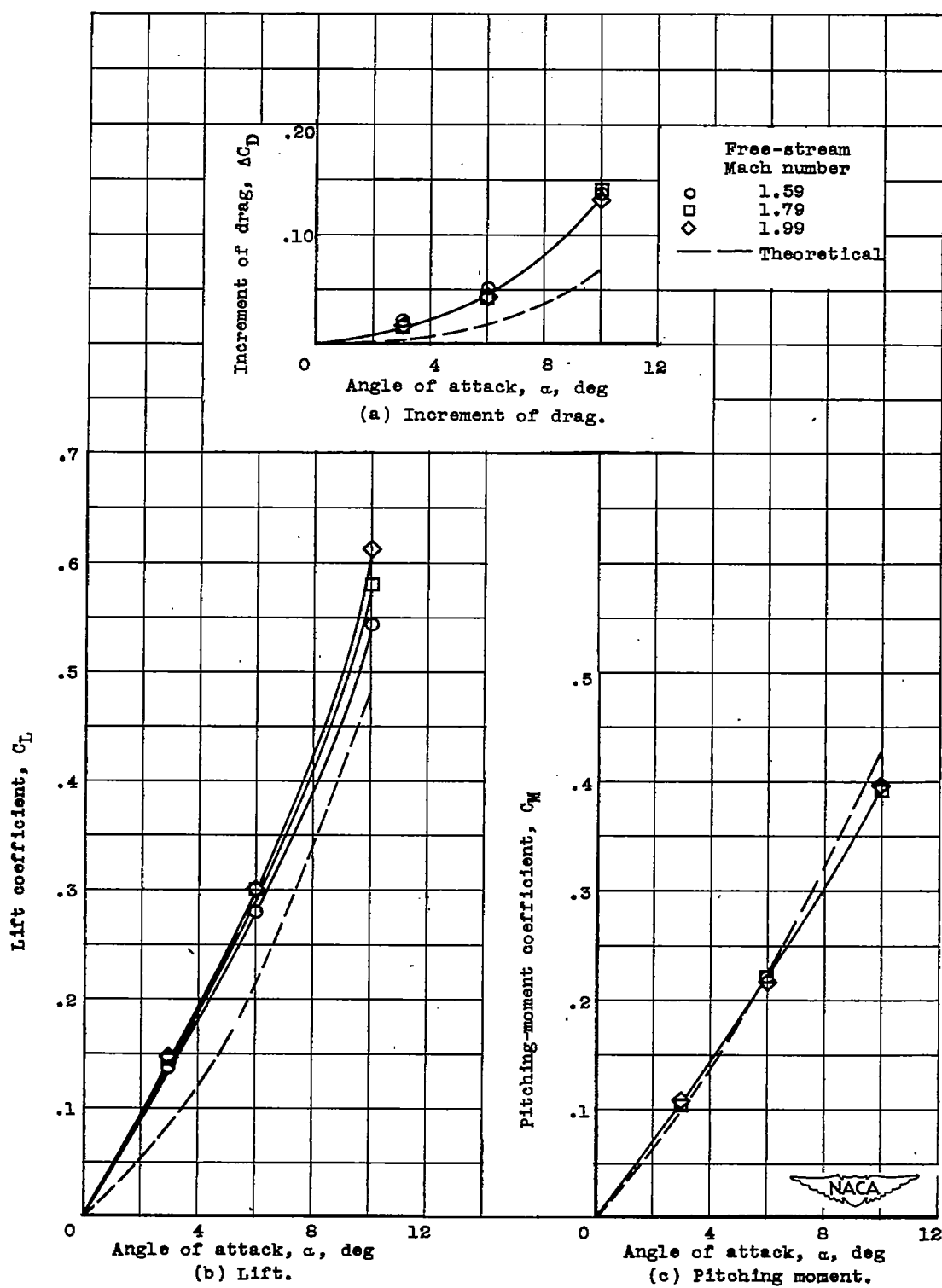


Figure 20. - Variation of external drag increment, lift and pitching-moment coefficients with angle of attack at critical mass flow for three Mach numbers.

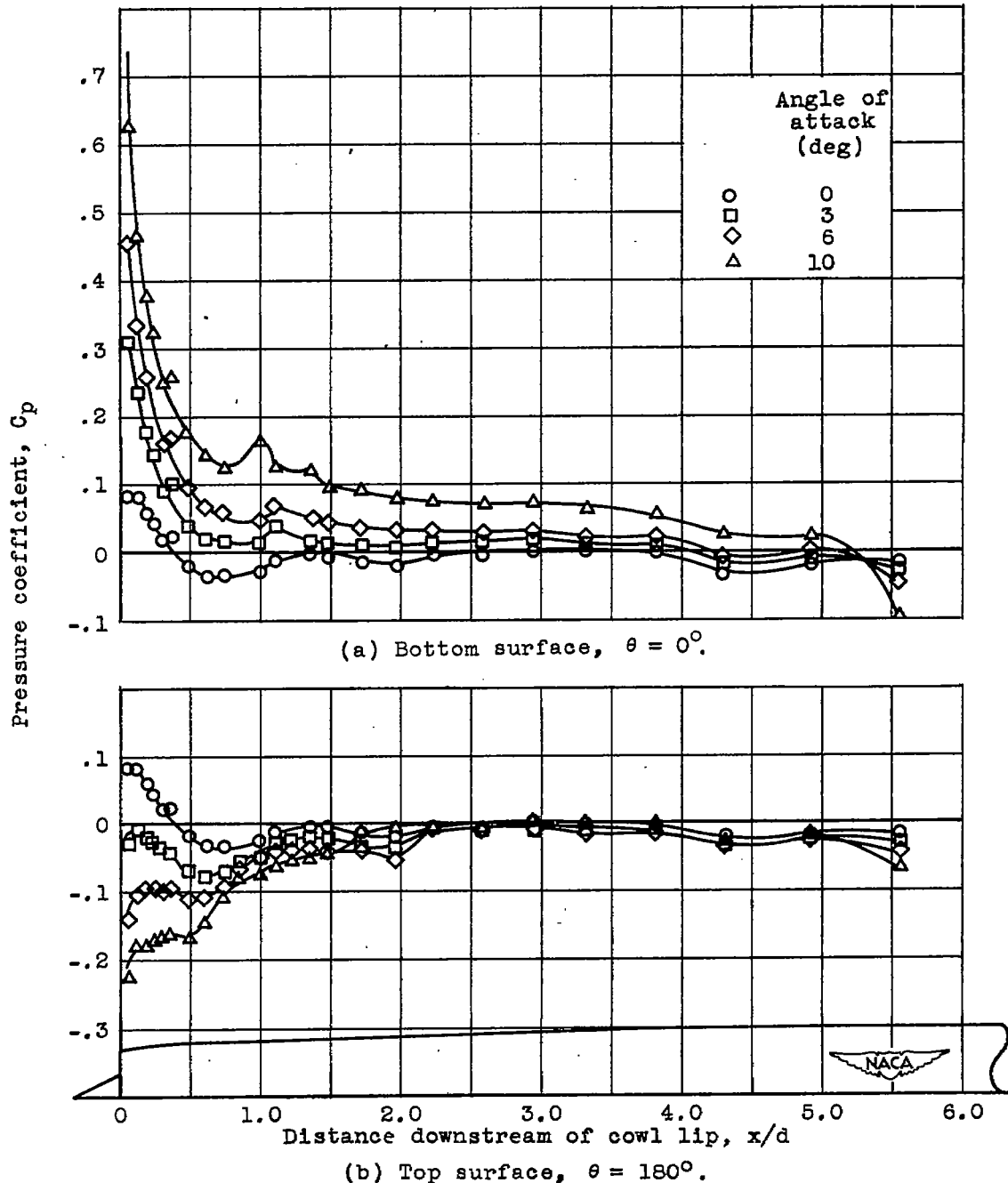


Figure 21. - Longitudinal variation of external-pressure coefficients for four angles of attack. Mass-flow ratio, 0.750; Mach number, 1.79.

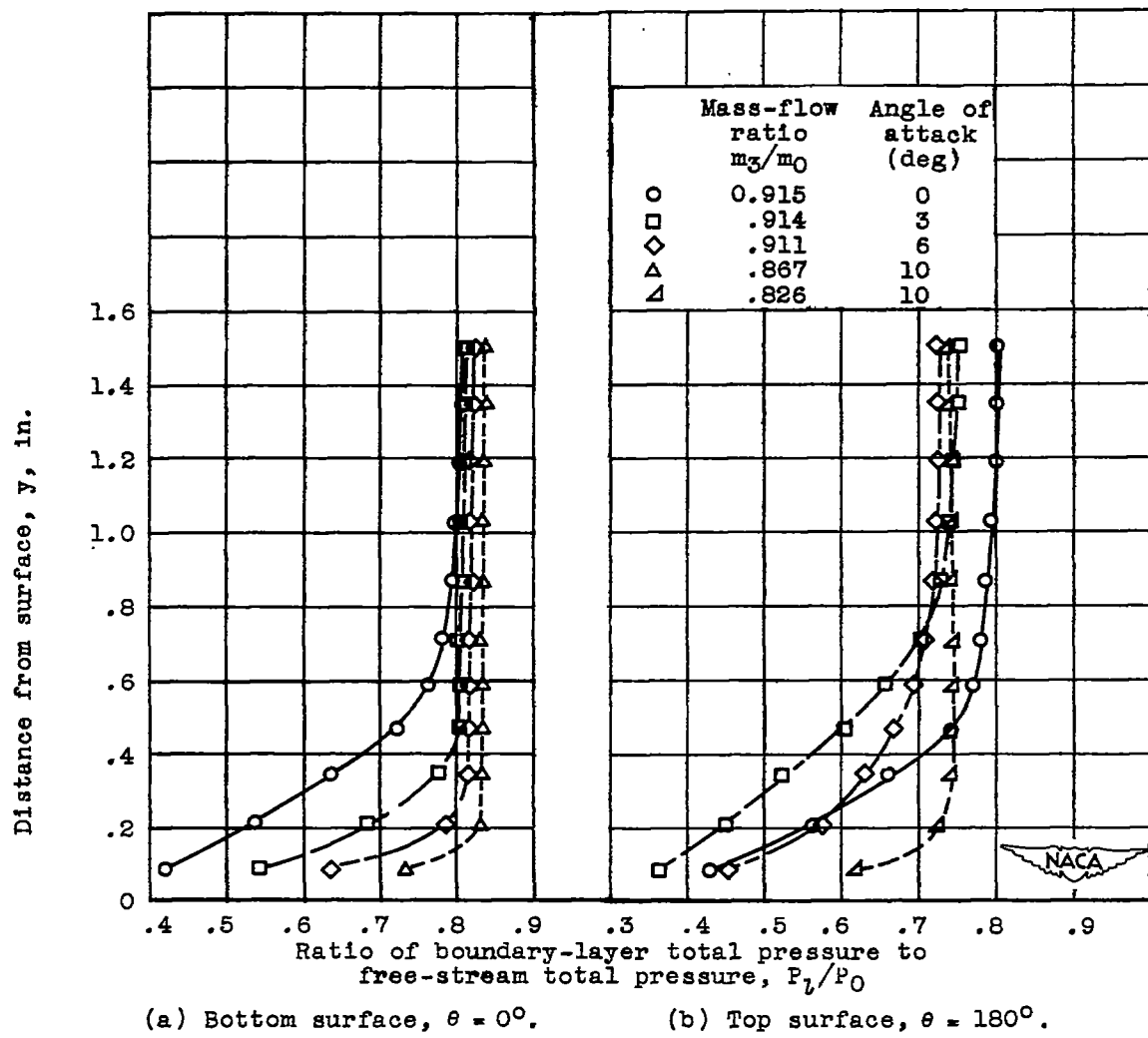


Figure 22. - Variation of total pressure in boundary layer over upper and lower surfaces of model at station 51 for four angles of attack. Mach number, 1.79.

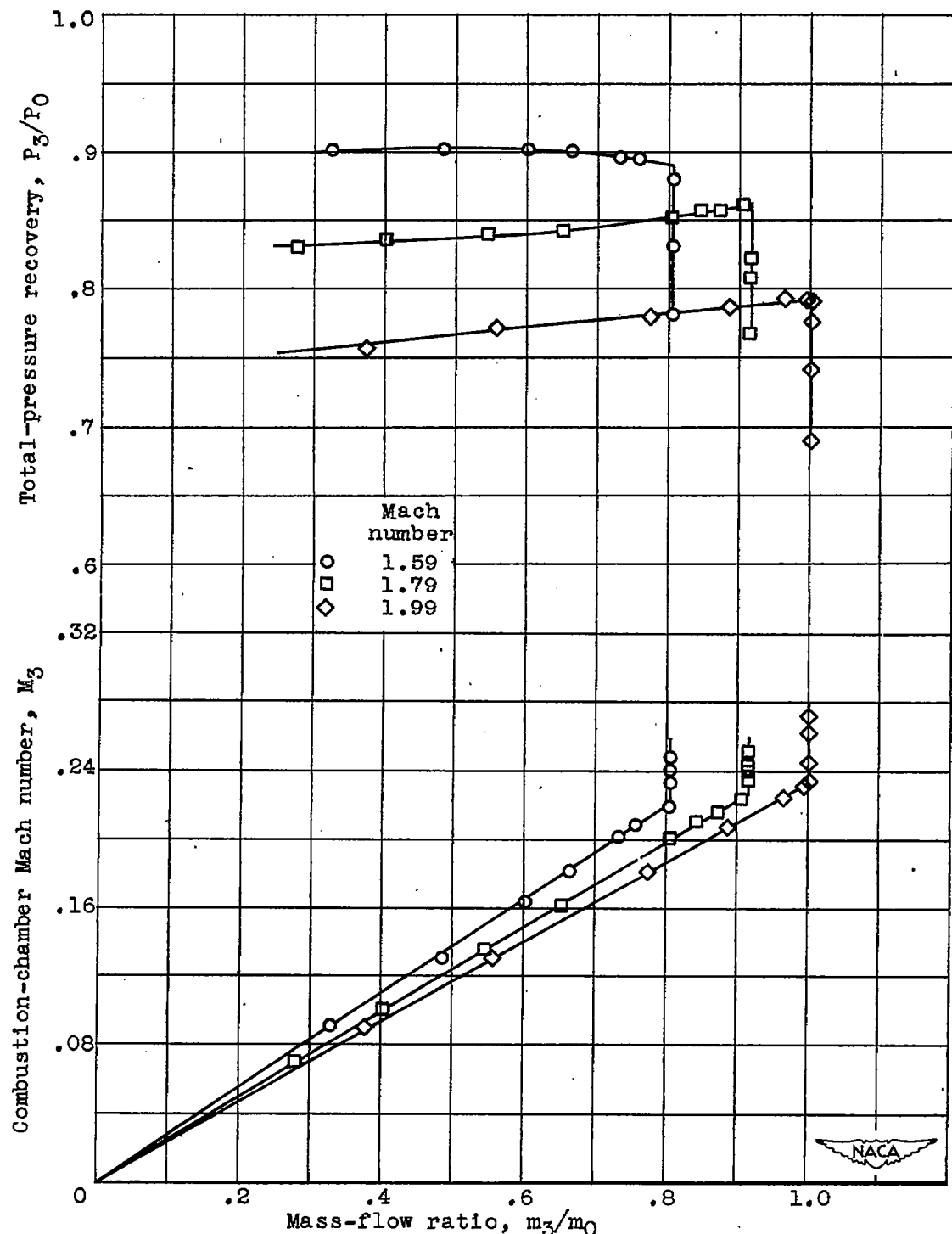


Figure 23. - Variation of total-pressure recovery and combustion-chamber Mach number with mass flow at zero angle of attack for three Mach numbers.

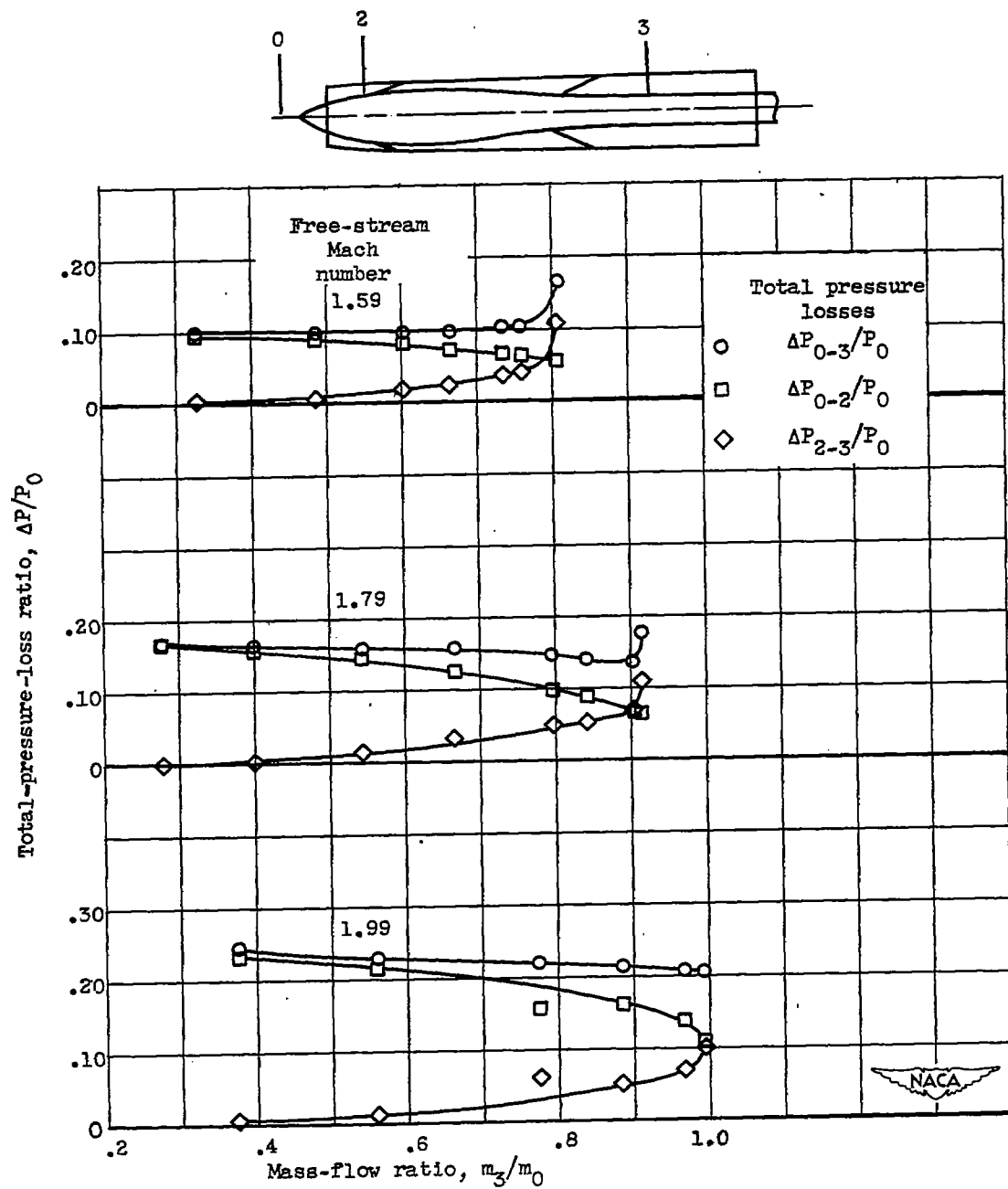
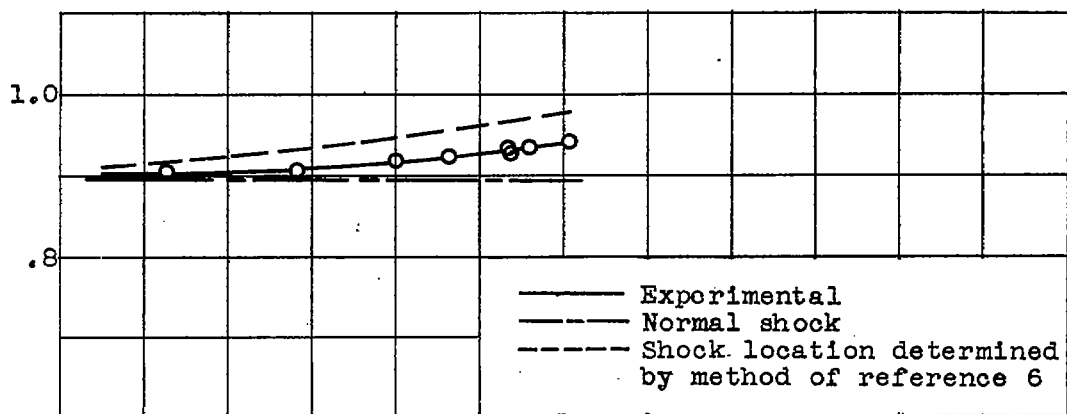
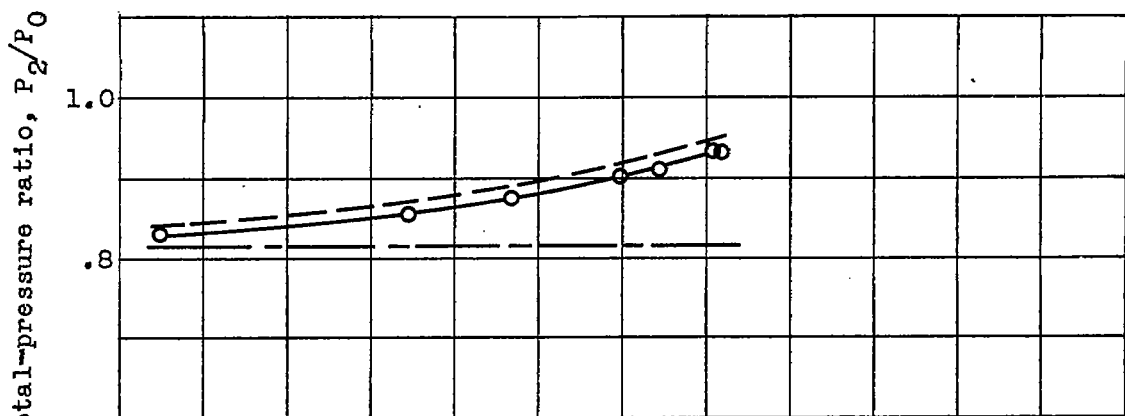


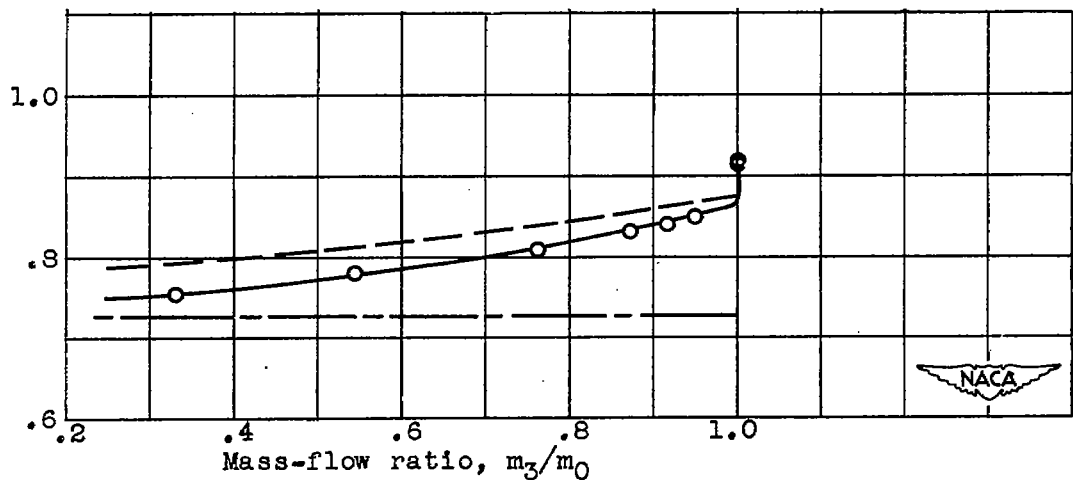
Figure 24. - Components of total-pressure loss at zero angle of attack for range of mass flows at three Mach numbers.



(a) Free-stream Mach number, 1.59.



(b) Free-stream Mach number, 1.79.



(c) Free-stream Mach number, 1.99.

Figure 25. - Comparison of experimental inlet losses with theory at zero angle of attack for range of mass flows at three Mach numbers.

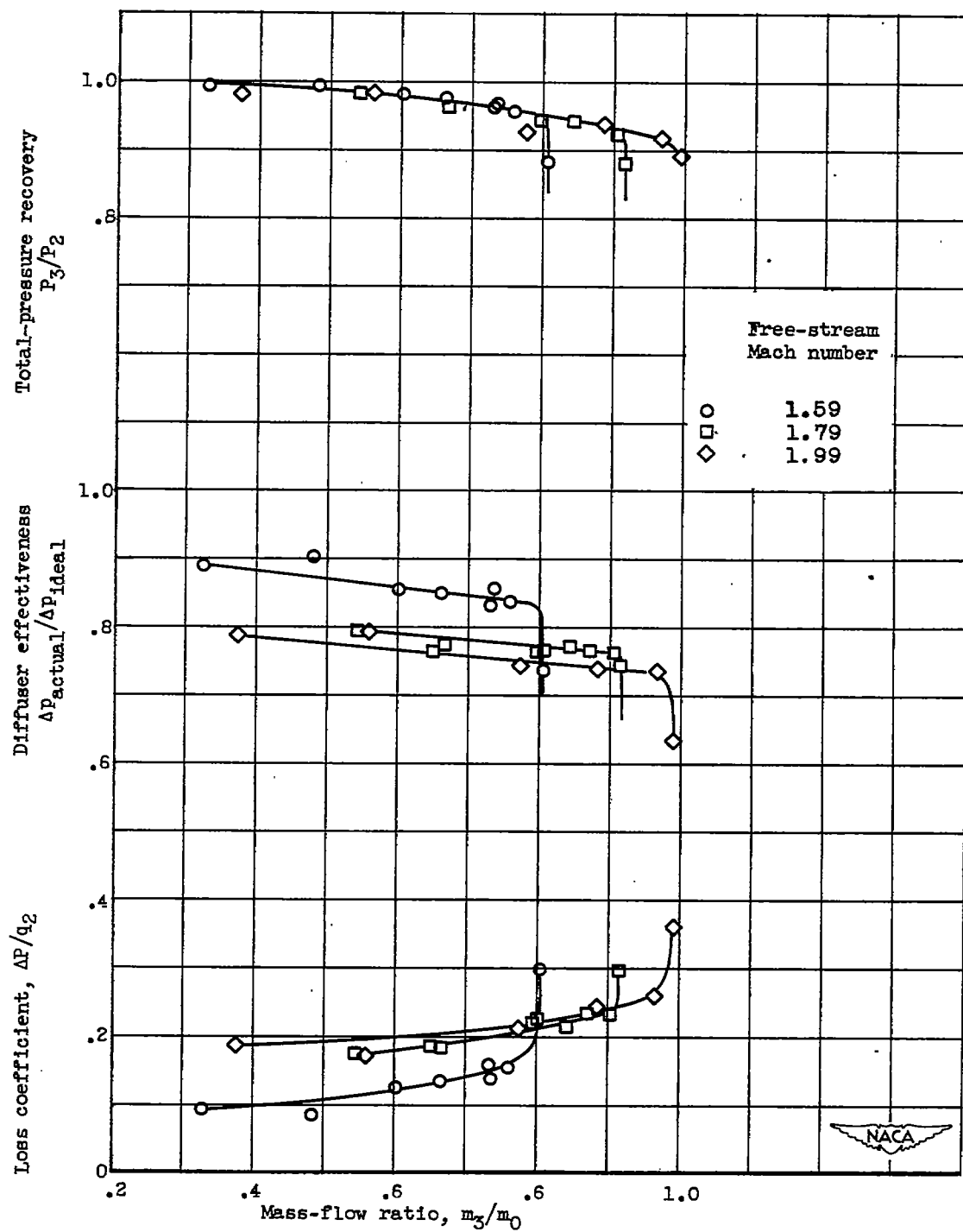


Figure 26. - Subsonic diffuser characteristics at zero angle of attack for range of mass flows at three Mach numbers.

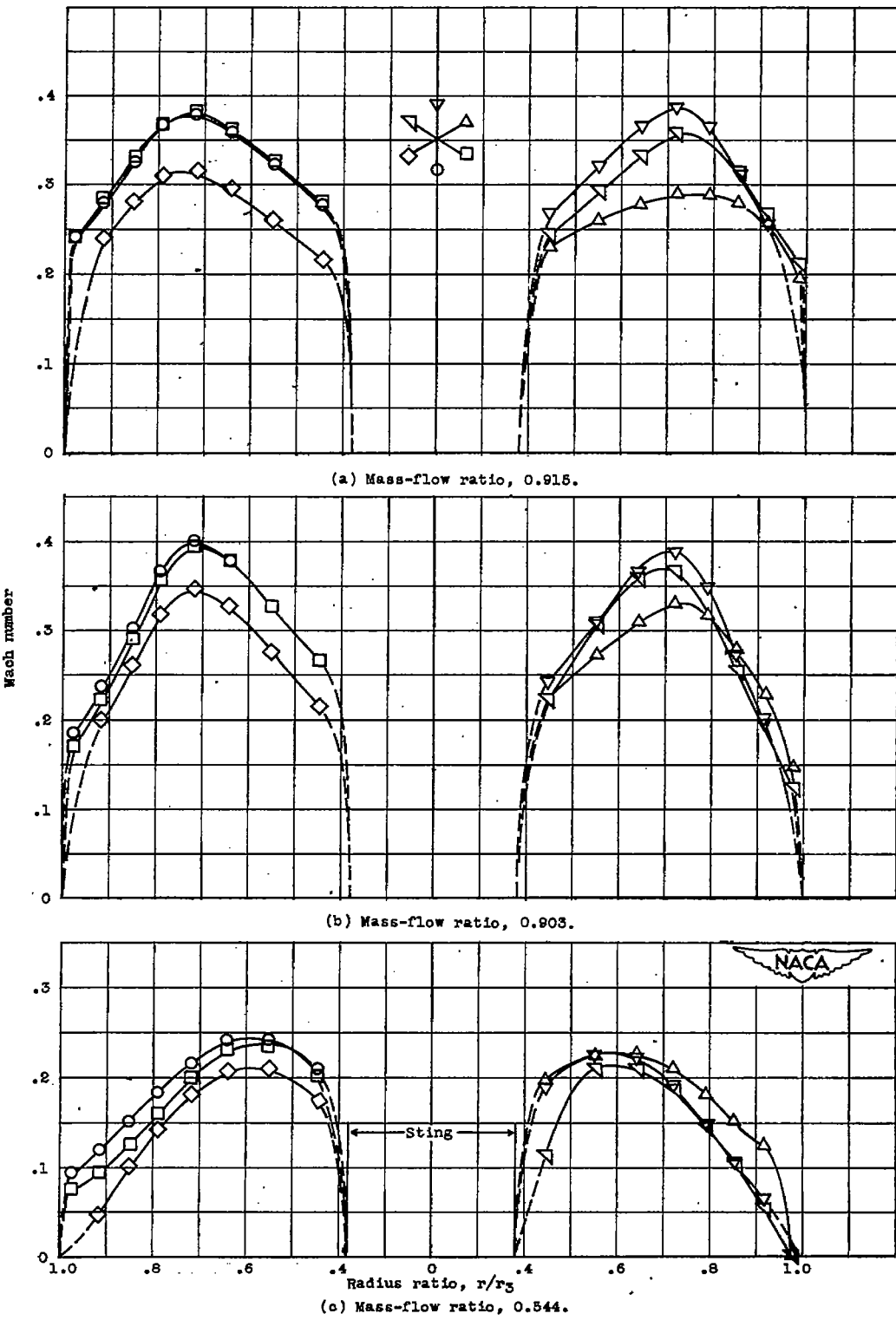
~~CONFIDENTIAL~~

Figure 27. - Variation of Mach number distribution at entrance to combustion chamber for several mass flows at zero angle of attack. Mach number, 1.79.

~~CONFIDENTIAL~~

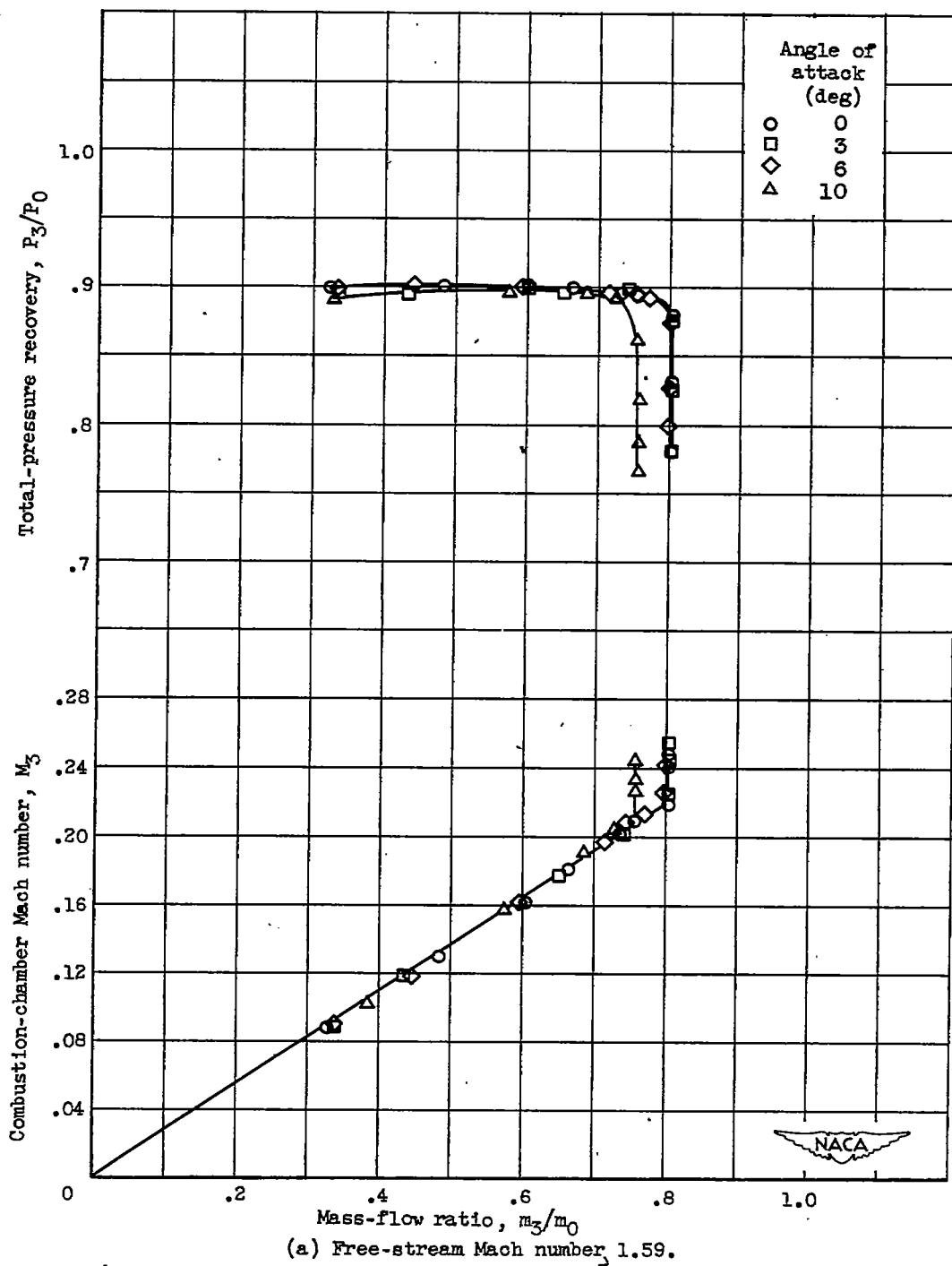
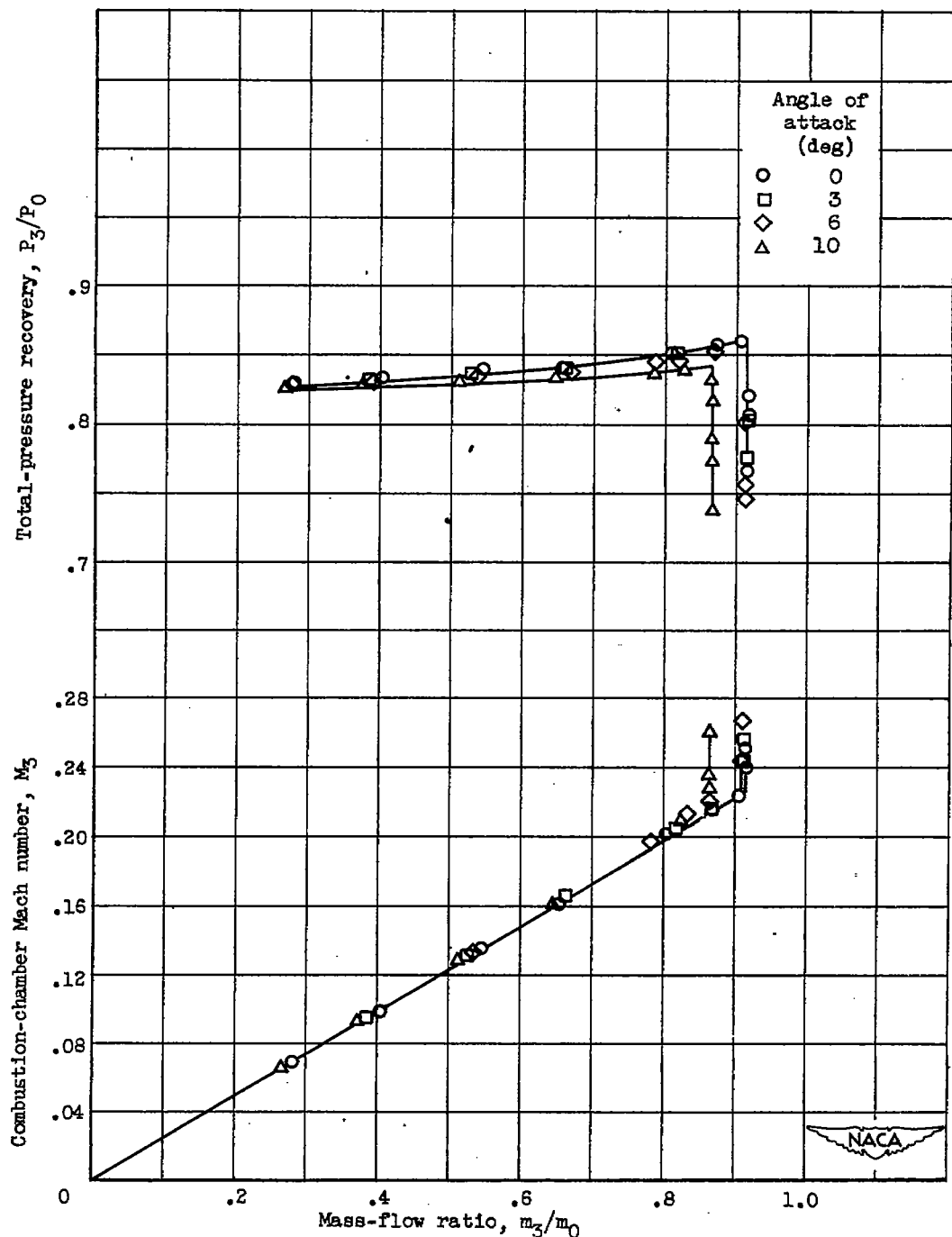


Figure 28. - Variation of total-pressure recovery and combustion-chamber Mach number with mass flow at four angles of attack for three Mach numbers.

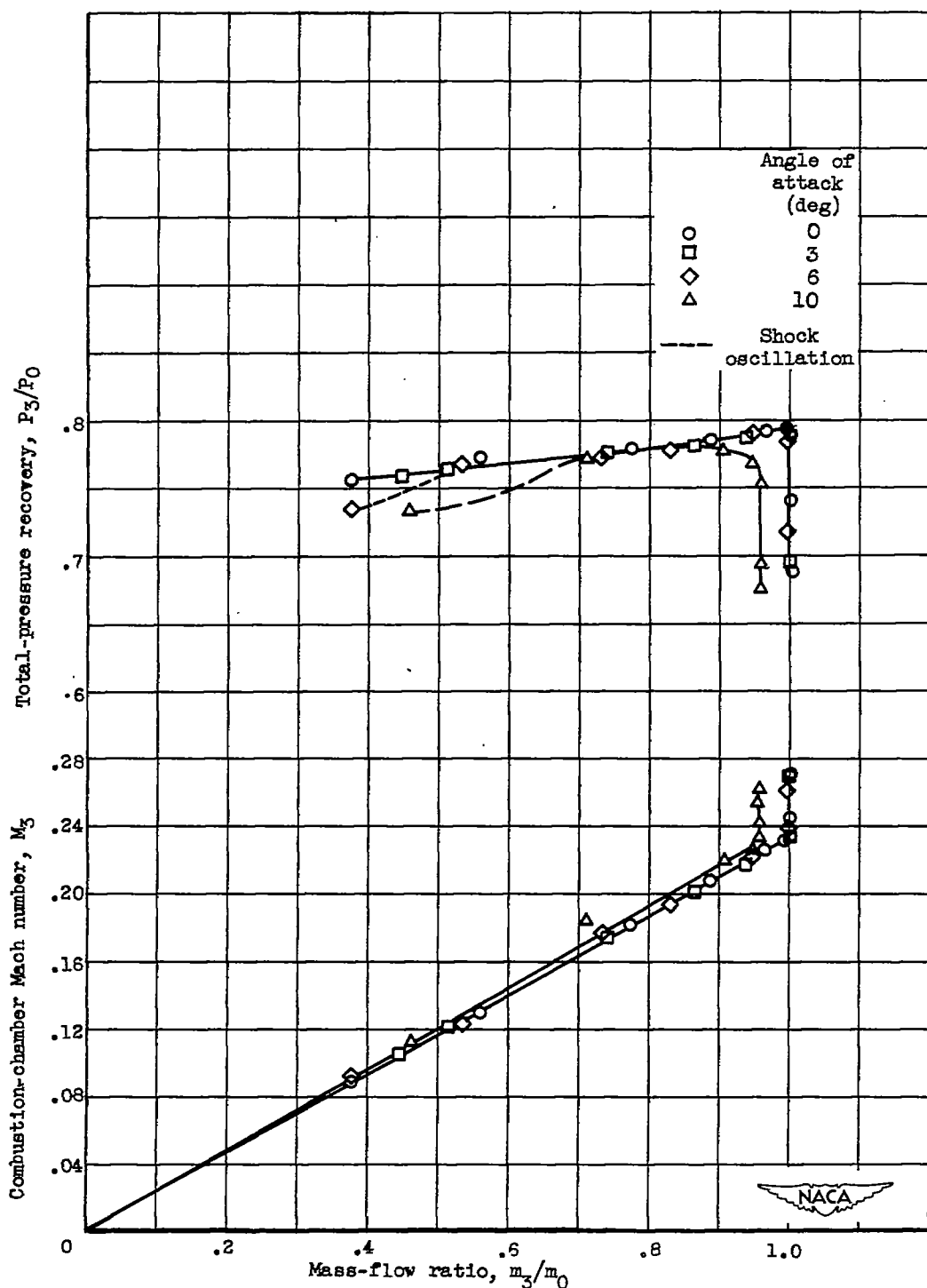
CONFIDENTIAL



(b) Free-stream Mach number 1.79.

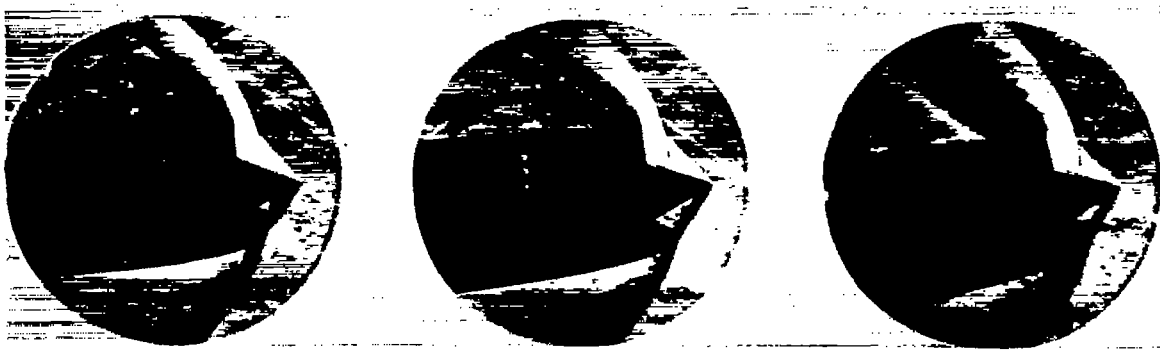
Figure 28. - Continued. Variation of total-pressure recovery and combustion-chamber Mach number with mass flow at four angles of attack for three Mach numbers.

CONFIDENTIAL



(c) Free-stream Mach number, 1.99.

Figure 28. - Concluded. Variation of total-pressure recovery and combustion-chamber Mach number with mass flow at four angles of attack for three Mach numbers.

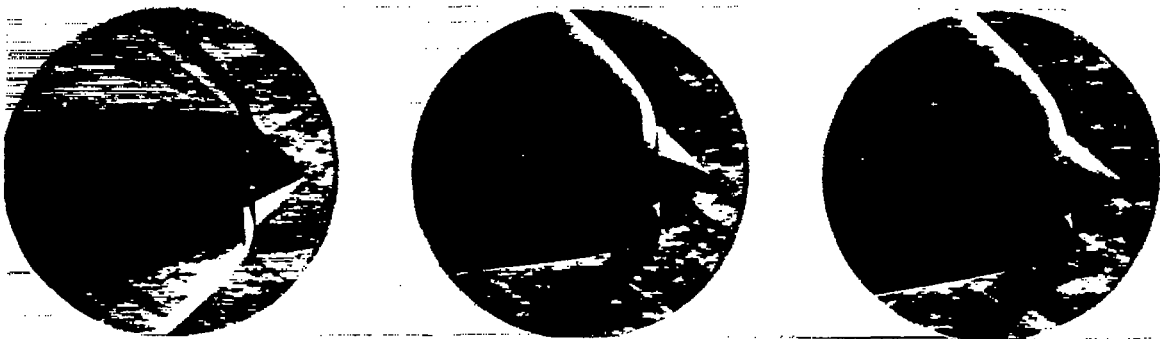


Angle of attack 3°
Mass-flow ratio 0.740

6°
0.754

10°
0.729

(a) Free-stream Mach number, 1.59

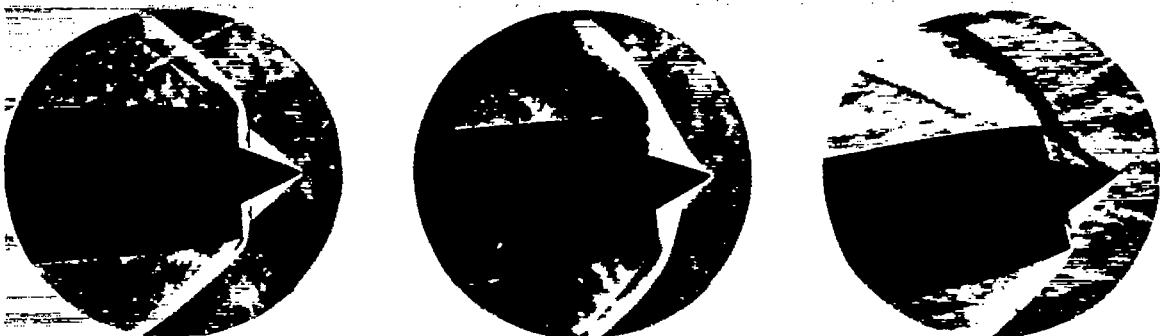


Angle of attack 3°
Mass-flow ratio 0.869

6°
0.869

10°
0.826

(b) Free-stream Mach number, 1.79



Angle of attack 3°
Mass-flow ratio 0.861

6°
0.733

10°
0.708

NACA
C-26040

(c) Free-stream Mach number, 1.99.

Figure 29. - Typical schlieren photographs at angles of attack for three Mach numbers.

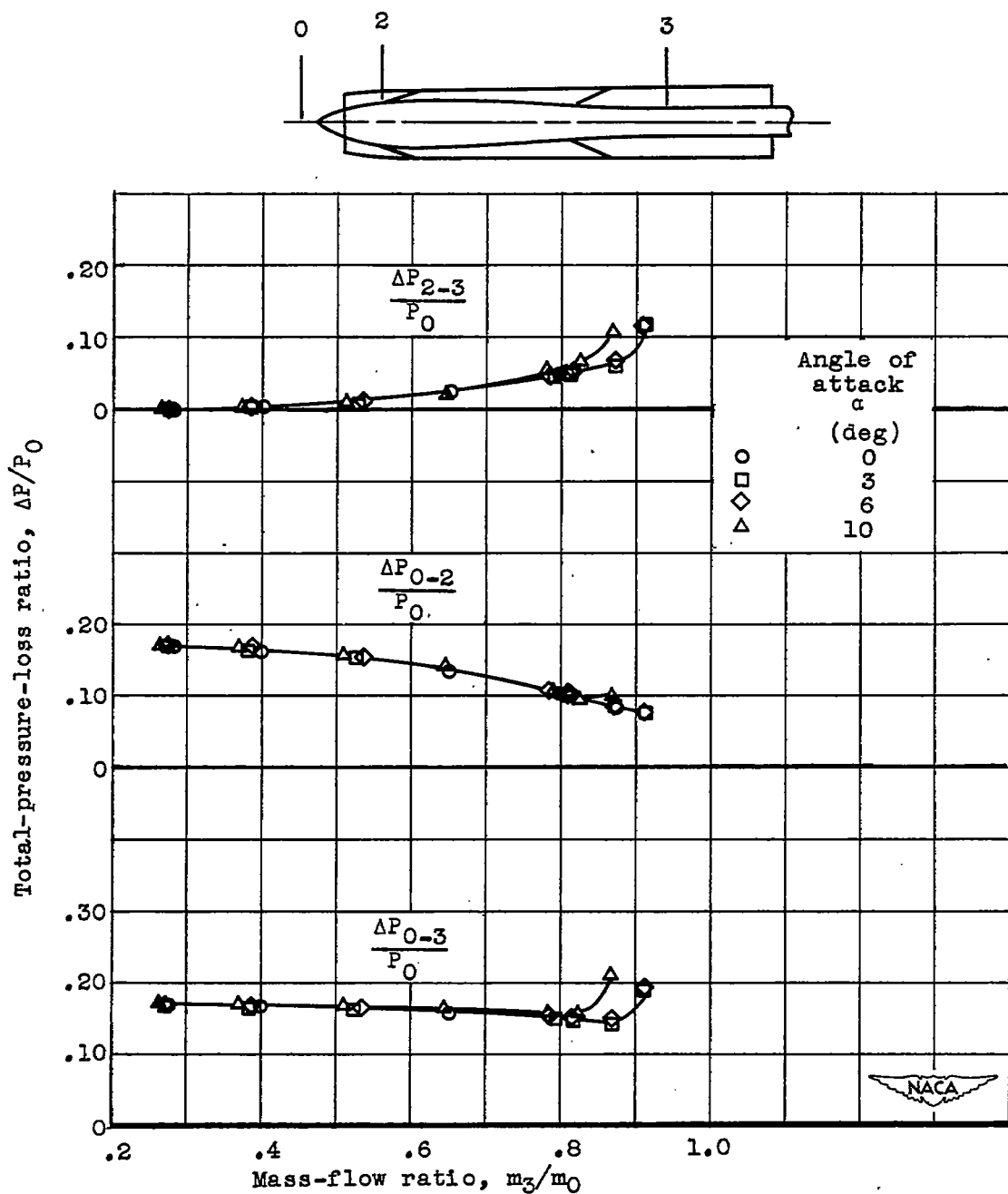


Figure 30. - Variation of inlet and subsonic diffuser losses with mass flow at four angles of attack. Mach number, 1.79.

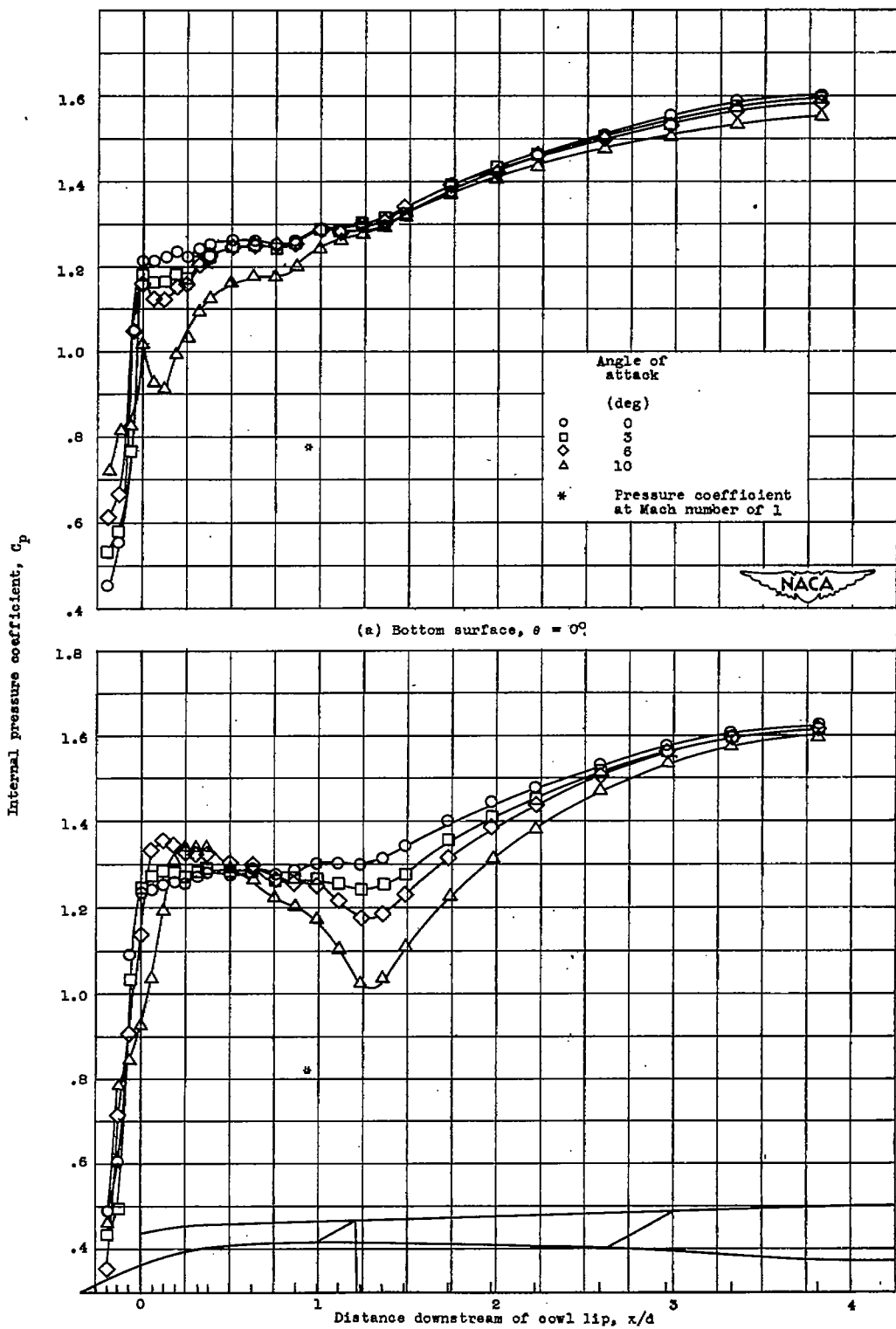


Figure 31. - Longitudinal variation of internal pressure coefficients at constant mass flow for four angles of attack. Mach number, 1.79; mass flow, 0.784.

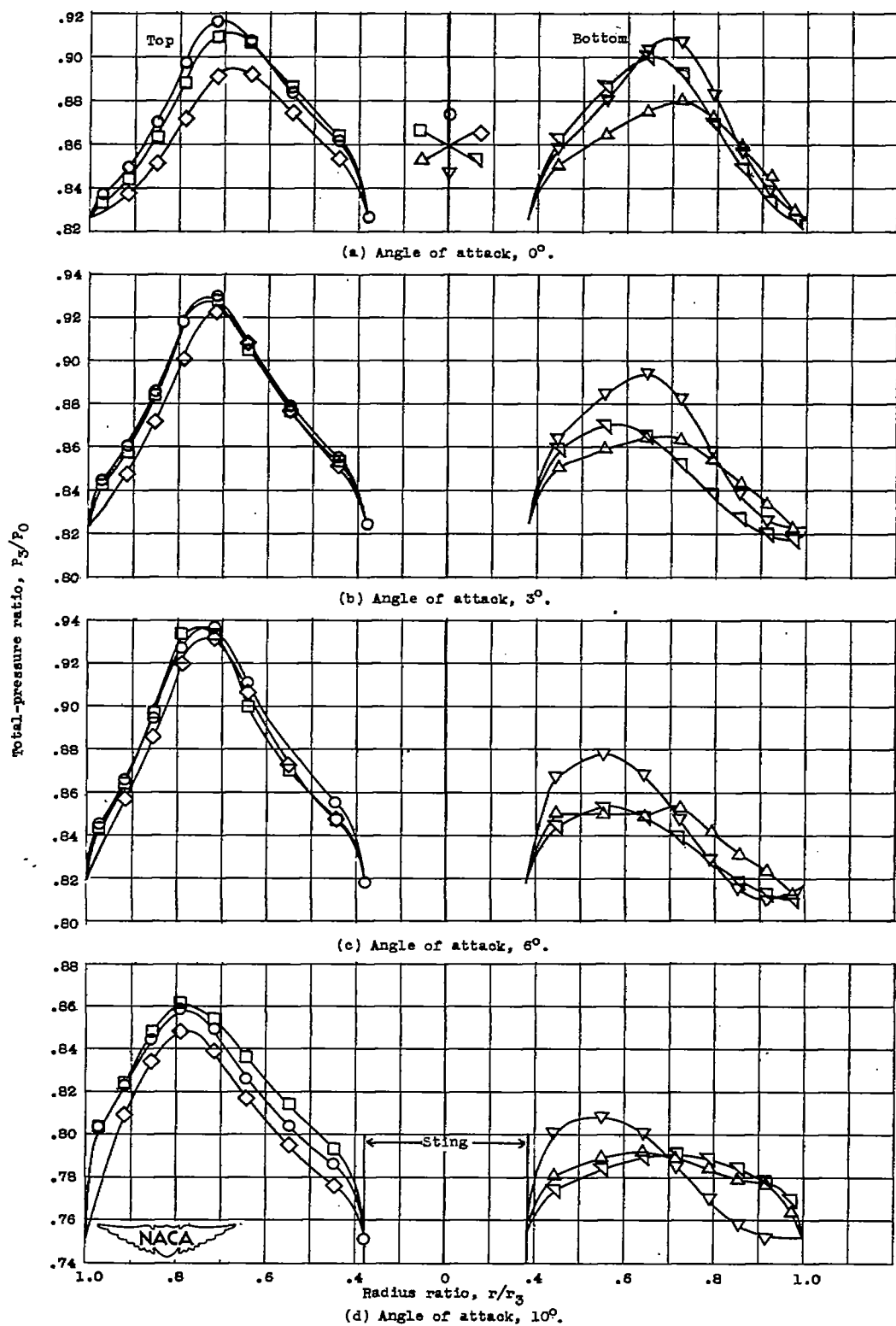


Figure 32. - Variation of total-pressure distribution at entrance to combustion chamber for constant mass flow at four angles of attack. Mach number, 1.79; mass-flow ratio, 0.869.